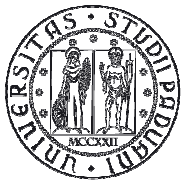

UNIVERSITY OF PADUA

FACULTY OF ENGINEERING

DEPARTEMENT OF MANAGMENT AND ENGINEERING

DOCTORAL SCHOOL OF INDUSTRIAL ENGINEERING
CURRICULUM IN MECHATRONICS AND INDUSTRIAL SYSTEMS
CYCLE XXIII

STRUCTURAL MODIFICATION APPROACHES TO MODAL DESIGN OPTIMISATION OF VIBRATING SYSTEMS

Ch.mo Prof. Paolo Bariani, Chair of the School

Ch.mo Prof. Alberto Trevisani, Curriculum Coordinator

Ch.mo Prof. Roberto Caracciolo, Candidate's Supervisor

Ph.D. candidate: Gabriele Zanardo

UNIVERSITÀ
DEGLI STUDI
DI PADOVA

Sede Amministrativa: Università degli Studi di Padova

Dipartimento di Tecnica e Gestione dei Sistemi Industriali

SCUOLA DI DOTTORATO DI RICERCA IN INGEGNERIA INDUSTRIALE
INDIRIZZO MECCATRONICA E SISTEMI INDUSTRIALI
CICLO XXIII

STRUCTURAL MODIFICATION APPROACHES TO MODAL DESIGN OPTIMISATION OF VIBRATING SYSTEMS

Direttore della Scuola : Ch.mo Prof. Paolo Bariani
Coordinatore d'indirizzo: Ch.mo Prof. Alberto Trevisani
Supervisore: Ch.mo Prof. Roberto Caracciolo

Dottorando: Gabriele Zanardo

To my family

Abstract

This dissertation addresses the problem of assigning the desired dynamic behaviour to vibrating systems, with particular attention on the generality of the approaches proposed. The main focus of this work is in developing structural modification approaches ensuring the feasibility and the optimality of the computed solution. The proposed approaches are suitable for both the design of new mechanical systems, and the performance optimisation of existing ones. Three formulations are proposed: in the first, the original system is modelled by means of mass and stiffness matrices, while in the second the Frequency Response Functions of the original system are employed. The final formulation allows for discrete structural modification, by casting the structural modification problem as a mixed-integer non-linear optimisation problem.

Compared with most of the approaches appearing in literature, one of the strengths of the approaches proposed is the capability to handle different design tasks. Also, the proposed approaches allow the modification of an arbitrary number of parameters (even in the presence of linear interrelated modifications) and of assigned vibration modes (regardless of their magnitude), as well as the possibility of dealing with mass and stiffness matrices with an arbitrary topology. To this purpose, the structural modification problem is formulated as a constrained inverse eigenvalue problem. The problem is constrained in the sense that a wide family of parameter constraints can be included in the formulations adopted in order to incorporate the physical constraints to the system modifications. Moreover, a regularization term biases the solution towards preferable modifications and assures good numerical conditioning. The problem is

then solved within the frame of constrained convex optimisation, which ensures that a unique, and hence global, optimal and feasible solution exists and that it can be efficiently computed by means of reliable numerical algorithms.

The effectiveness and the capabilities of the proposed approaches are demonstrated by firstly applying it to theoretical test cases and secondly through experiments on industrial and laboratory test cases. Such test cases involve lumped and distributed parameter modifications, as well as multimode and single mode assignments.

Sommario

In questa Tesi si affronta il problema di assegnare il comportamento dinamico desiderato a sistemi vibranti, e si dedica particolare attenzione alla generalità degli approcci proposti. Questo lavoro si concentra sullo sviluppo di approcci per il calcolo di modifiche strutturali che siano in grado di assicurare la realizzabilità fisica e l'ottimalità della soluzione calcolata. Gli approcci proposti sono adatti sia al progetto di nuovi sistemi meccanici, sia all'ottimizzazione delle performance di quelli esistenti. Vengono proposte tre formulazioni: nella prima il sistema originale é modellato per mezzo di matrici di massa e rigidezza, mentre nella seconda vengono impiegate le funzioni di risposta in frequenza (Frequency Response Functions). La terza formulazione prende in considerazione modifiche strutturali discrete, in quanto il problema delle modifiche strutturali viene formulato come un problema di ottimizzazione non-lineare mista-intera.

In confronto agli approcci presenti in letteratura, uno dei punti di forza degli approcci proposti risiede nella capacità di poter affrontare obiettivi di progetto diversificati tra loro. Degna di nota é la modifica di un numero arbitrario di parametri (anche in presenza di modifiche tra loro linearmente correlate) e di modi di vibrare (a prescindere dalla loro normalizzazione), cosi pure la possibilità di trattare matrici di massa e rigidezza con topologia arbitraria. A tale fine, il problema di modifica strutturale viene formulato come un problema agli autovalori inverso vincolato. Il problema é vincolato nel senso che una ampia famiglia di vincoli sui parametri può essere introdotta nelle formulazioni adottate, per includere nel problema i vincoli fisici sulle modifiche del sistema. Inoltre, un

termine di regolarizzazione permette di dirigere la soluzione verso modifiche preferenziali, ed assicura un buon condizionamento numerico. Il problema è risolto all'interno del contesto matematico dell'ottimizzazione convessa vincolata, che assicura l'esistenza di un'unica, e quindi globale, soluzione ottima realizzabile, e che tale soluzione sia calcolabile efficacemente per mezzo di algoritmi numerici consolidati ed affidabili.

L'efficacia degli approcci proposti, e la loro capacità di fornire soluzioni realizzabili è stata dapprima dimostrata applicandoli dapprima su esempi teorici, e successivamente su test case industriali e da laboratorio. Tali test case includono sia modifiche di parametri concentrati che parametri distribuiti, così come l'assegnazione di uno o più modi di vibrare.

Aknowledgments

I would like to express gratitude to my supervisors, Prof. Roberto Caracciolo and Prof. Alberto Trevisani, for their continuous encouragement and invaluable support from the very beginning of my PhD. They have always found the time to answer all my questions, providing me with reliable guidance. I am also grateful to the members of the Mechatronics Research Group for their kind suggestions and support, especially Dr. Dario Richiedei for the useful discussions and for patiently listening to my ideas before giving effective advice.

I would also like to thank Prof. Huajiang Ouyang for his availability to establish a very fruitful research collaboration, and for his help during my staying in Liverpool.

This research has been realized thanks to the support of FSU, "Fondazione Studi Universitari" Vicenza. I would like to express my gratitude to the Foundation for having funded my Doctoral course throughout the three years.

A special thanks goes to Rossella Rosa: she is a valid colleague and a good friend. I am also grateful to Eng. Robert Fullerton for checking the grammar and the spelling of this Thesis.

The most important thanks is deserved by my family for the faith they put in me: my parents and my schwesterlein Marina have been continuously supporting me with love and advice. All my uncles and aunts have been encouraging me, but a special thanks goes to my uncle Prof. Alberto Zanardo, who is still providing me with kind suggestions.

Finally, a thanks to my life-long friends Andrea, Massimiliano, Nicola, Filippo and all those playing in the band “I Derelitti”, as well as Pietro and Letizia and all those I was lucky enough to meet at the choir “I Trovatori”.

Contents

Introduction

Scope of the Thesis

The scope of this Thesis is to provide a collection of innovative methods for computing the physical parameters of mechanical systems ensuring the prescribed dynamic behaviour. Such computed physical parameters can be employed in the design phase of new devices or in the performance optimisation of existing ones. The problem of assigning prescribed dynamics through parameter modification is traditionally called “Inverse Structural Modification Problem”, and several approaches have been proposed in literature for the solution of some specific problem subclasses. The methods introduced in this Thesis address the problem of assigning dynamic behaviours prescribed by means of the system eigenstructure, and are based on the solution of inverse eigenvalue problems. In many applications it is in fact convenient to express the desired dynamic behaviour in terms of system eigenstructure. This is especially effective when only a small number of modes dominates in the system dynamic response at the frequencies of interest. Popular examples of such a condition are vibratory conveyors, linear feeders and sieves, which are actuated at a specific single-harmonic excitation frequency. Peculiar to the methods proposed is the interest towards the feasibility and the optimality of the computed solution. Noteworthy is also the method generality with respect to the data employed, to the parameters to be modified and to the dimension of the desired eigenstructure. These aims are achieved by formulating the mathematical problems in suitable work frames, allowing for the introduction of feasibility constraints and of penalty terms

reflecting the requirements of the designer. Finally, the solution of the mathematical problems within the frame of the convex optimisation provides useful mathematical and numerical tools, as well as algorithms which are very effective in the computation of the system modification. Noteworthy is the solution of structural modification problems in the mathematical frame of mixed-integer non linear programming, since it intrinsically reflects the industrial need of modularisation.

The Thesis is organised as follows: first, a literature review is proposed. Then, in the first Chapter, three formulations of methods for calculating structural modifications are developed. These formulations differ for the system model employed (spatial model or frequency response model) and for the mathematical frame of solution (real or mixed-integer non linear optimisation). Chapters 2, 3 and 4 are devoted to the application of the developed methods on simulated test cases: in the second Chapter the method employing the system spatial model is applied on lumped- and distributed-parameter systems, and a comparison is carried out with two state-of-the-art methods. In the third Chapter, a comparative application of the method employing the system frequency response is proposed. This section is focused on how to effectively exploit FRF data in order to compute structural modifications. The fourth Chapter contains a detailed explanation of the technique employed for computing effective structural modifications. Chapters 5, 6, 7 are devoted to the experimental validations of the methods developed: in chapter 5 the method employing the system spatial model is validated with reference to the optimisation of an industrial vibrating device. The validation of the method based on frequency response data is given in chapter 6, with reference

to a laboratory test rig. The same test rig has been used for providing experimental evidence of the effectiveness of the discrete modifications, as demonstrated in chapter 7.

Literature review

The optimisation of vibrating systems is aimed at improving the dynamic behaviour by properly choosing inertial, stiffness and damping parameters. This design problem is generally referred to as structural modification and two complementary approaches can be adopted: direct (forward) and inverse. In the direct structural modification problem the dynamic behaviour of a modified system is predicted, given known modifications. Conversely, in the inverse structural modification problem the suitable parameter modifications ensuring the desired change in the system dynamic behaviour are computed.

Several approaches for the solution of inverse structural modification problems have been developed, starting from the pioneering work [RAM 1991]. A wide collection of inverse problems in vibration can be found in [GLADWELL 2004]. Two main criteria can be adopted in order to group the approaches proposed in literature. The first grouping criterion is based on the dynamic properties to be assigned through structural modification: such properties usually are the system natural frequencies, the system vibration modes and the system point- and cross-receptances (in particular the system point- and cross-antiresonances). The second grouping criterion, used in the literature review proposed below, is the kind of description adopted for the original system model

and, hence, the original system data employed by the methods. According to this criterion, the works in literature can be grouped into three sets :

- the approaches based on physical models of the systems (e.g. [FARAHANI 2004A-B] and [LIANGSHENG 2003]), which employ inertial, stiffness and damping matrices;
- the approaches based on modal data (e.g. [BRAUN 2001], [BUCHER 1993]), which employ the system eigenstructures;
- the approaches directly based on the system receptances (Frequency Response Functions, FRF) (e.g. [MOTTERSHEAD 2001], [OUYANG 2009] and [PARK 2000]).

Approaches employing the original system spatial model

The early inverse structural modification techniques are based on the sensitivity analysis of the eigenstructure. These studies take advantage of the derivatives of the eigenvalues and of the eigenvectors of a dynamic system with respect to system parameter perturbations. Just to mention a few examples, in [FARAHANI 2004A-B] the modification in the system eigenstructure is approximated respectively thorough its first- and second-order derivatives with respect to the system physical modifications. The main problem associated with the perturbation approach is that it provides reliable and computationally efficient results as long as modifications are “small”. If the modifications are not small, numerical iterations are needed and the computational effort increases.

The method in [LIANGSHENG 2003] is targeted to the simultaneous modification of masses and stiffnesses for assigning a reduced subset of modes,

starting from the complete system model expressed in physical coordinates. Arbitrary matrix topologies are allowed for in this method. On the contrary, the number of assigned modes is not arbitrary since it is strictly related to the system model dimensions and to the number of design variables. Additionally, no constraints ensure the physical and technical feasibility of the solution.

The theory of the multi-degree-of-freedom dynamic absorber provided in [RAM 1996] is also based on system spatial models. The vibration absorption can be achieved for multiply-connected vibrating systems, but solutions are available only for the special case of absorbing the vibration in simply-connected systems through the addition of simply-connected systems.

The objective of the papers [WANG 2004] and [WANG 2006] is the maximisation of a system natural frequency, to be achieved by mean of proper placement of elastic supports. These studies are based on the derivatives of the system natural frequencies with respect to the support position.

A recent application of a procedure for maximizing the least eigenvalue of a constrained affine sum is exploited in [RAM 2009] in order to determine the mass distribution in vibrating system. The optimisation consists in maximising the lowest eigenvalue or in minimizing the highest. The method is based on the recursive solution of quadratic equations, and allows for a constraint on the total mass employed.

Approaches employing the original system modal model

In their pioneering work, Ram and Braun [RAM 1991] formulated the modification problem as an optimised inverse eigenvalue problem. In particular,

they dealt with the incompleteness of the original system model. They constrained the desired mode shapes to lie in the span of the known ones, and provided formulae for evaluating the family of all the mathematical solutions of the modification problem. The normalisation adopted for the desired mode shapes is crucial, since the solutions are dependent upon the magnitude of the desired mode shapes. The Authors also tackled the problem of attaining feasible and realistic mass and stiffness modifications, by defining a family of physically realizable solutions. Nevertheless, the Authors explicitly stated that there still remained the problem of developing an efficient algorithm for the evaluation of such a realizable solution. In addition, the number of assigned modes was limited by the dimension of the incomplete set of known modes and the computation of interrelated modifications (e.g. parameter modifications affecting both the mass and the stiffness matrices) was prevented.

Subsequently, Sivan and Ram [SIVAN 1999] improved the method in [RAM 1991] and focused on the feasibility problem. Under certain connectivity assumptions (lumped mass simply-connected systems) they extracted from the set of all the mathematical solutions those that can be realised by actual system modifications.

The method in [BUCHER 1993] takes advantage of the concept of left modal eigenvectors in order to overcome the truncated information of experimental FRFs. The Authors proved that if a structure is excited by a force vector that lies in the span of the truncated left modal vectors, then the steady-state response of the structure can be described exactly by the truncated modes. The basic equations for the extraction of the system left eigenvectors from

experimental FRFs are also proposed, and the exact solutions of the problems whose desired eigenvectors lie in the subspace of the extracted modes are also presented. Hence, at a maximum, the number of assigned modes is equal to the dimension of the incomplete set of known modes. Also, interrelated modifications are not considered, and no constraints ensure the feasibility of the computed modifications. A refined version of the method is proposed in [BRAUN 2001]: it is shown that solutions without truncation errors may be obtained if left eigenvectors are included in the modification procedure. However, the extraction of left eigenvectors from experimental FRFs implies ill-conditioned computations and hence is very sensitive to measurement noise, even if regularisation methods are suggested in [BUCHER 1997] in order to reduce such a sensitivity to measurement noise. In addition, such methods are tailored to the optimisation of simple connected systems, which can be modelled through diagonal mass matrices and tri-diagonal symmetric stiffness matrices. Moreover, the knowledge of the system mass matrix is implicitly required, since proper mass-related normalisation is required for the eigenvectors employed in the computations.

In [SIVAN 1996] the problems arising from the availability of truncated modal data has been dealt with in the assignment of natural frequencies. This paper is one of the few works which deals explicitly with interrelated mass and stiffness. Moreover, the explicit non-negativity constraints employed in the solution algorithm ensure obtaining feasible mass and stiffness modifications.

In [SIVAN 1997] Sivan and Ram proposed a method for constructing physically realizable multiple-connected mass-spring systems approximating prescribed eigenstructures. Non-negative constraints are imposed in the

computation, thus ensuring the system feasibility. In the method proposed, only the mass matrix is assumed to be diagonal. It is required to include all the system modes (i.e. the complete modal set) in the prescribed eigenstructure, and that the desired eigenvectors be mass-normalised, since the eigenvector magnitude considerably influences the method performance.

Approaches employing the original system Frequency Responses

Generally speaking, both the system physical models and the experimentally derived modal data suffer from the modal truncation arising from the finite dimensional models assumed and from the high amount of computations required for the model synthesis. In particular, the physical model experimental identification is often challenging when dealing with complex and uncertain systems, while the determination of complete modal models usually involves intrinsically ill-conditioned computations. These problems should therefore be properly tackled in the modification process.

In contrast with such models, the direct use of the measured receptances in structural modification problems overcomes both the incompleteness of the modal representation of large-scale systems and the need for accurate and updated modal or physical models. This simplifies significantly the numerical data analysis and increases the algorithm robustness with respect to parameter uncertainty, although receptances describe the system only in a finite frequency range.

The aforementioned appealing advantages have encouraged the development of FRF-based inverse structural modification approaches in recent years. In particular, FRF data have been directly employed in [MOTTERSHEAD

2001] in order to calculate structural modification for the assignment of antiresonances. In this paper, the concept of the adjoint system is employed in order to compute the system modifications assigning desired zeros to both the point- and cross-receptances of a structure. Such a result is attained by assigning the proper resonances to the adjoint system. The technique proposed requires a very small set of data from the unmodified structure: three and four frequency responses are required in the assignment of respectively point- and cross-receptances. In [KYPRIANOU 2004] the assignment of natural frequencies on the basis of the original system frequency responses is considered. The method is based on adding an oscillating mass connected to the original structure by mean of one or two springs, and hence implies the addition of a degree of freedom and a natural frequency. The conditions for computing realistic parameters are given, and the effect of the added mass and spring(s) on the system poles and zeros is explained. Furthermore, in [KYPRIANOU 2005] the solution of multivariate polynomial systems for the assignment of natural frequencies and antiresonances is proposed. Such systems arise when the modifications yield couplings between coordinates, e.g. the addition of beams. Important system modifications (e.g. addition of beams) may requires also the measurement of rotational receptances, which is usually difficult because of the practical problems of applying a pure moment. In [MOTTERSHEAD 2005] a method is proposed in order to estimate rotational receptances. The method is based on the attachment of a flexible substructure, and requires measurements of sole linear displacements and applied forces. However, the resulting equations are generally ill-conditioned (thus requiring regularisation techniques in the computations) and the natural

frequencies of the attached substructure may influence the measurements. The system frequency responses have been recently employed also in the prediction and in the assignment of the latent roots [OUYANG 2009] of asymmetric systems by means of mass, stiffness and damping modifications. The problem is not trivial since the major issue in asymmetric systems is the lack of stability. Therefore, the assignment of the real part of latent roots is much more important than the assignment of frequencies. Other FRF-based methods (e.g. [LI 1999], and [PARK 2000]) deal with the assignment of normal modes in vibrating systems. The former is based on the solution of linear equations. Nevertheless, as the Authors admit, it can usually be applied when either masses or stiffnesses are to be modified. Moreover, no condition assures the feasibility of the solutions. Furthermore, the number of modifiable parameters is dependent upon the number of equations translating the prescriptions of the assignment problem, since the method is based on solving a determined problem. The latter ([PARK 2000]) can handle also under-determined problems (i.e. problems with more modification parameters than equations), while an approximate procedure is only suggested for dealing with under-determination. In the selection of the best solution, however, no optimisation problem is explicitly defined and hence such a selection is not straightforward.

The journal papers [MOTTERSHEAD 1999-2000] describe the relationships between vibration nodes and the cancellation of poles and zeros. The former deals with the condition for creating a vibration node from zero-pole cancellation, while in the latter the special cases of multiple poles and zeros are discussed.

The analysis of the aforementioned works highlights that several issues are still open in this field since most of the approaches proposed so far lack flexibility and generality both in the formulation and in the solution of the problems. In such an open frame, the chief contribution of the work presented in this paper consists in formulating the modal optimisation problem so as to provide designers with the widest set of tools for coping with different design requirements. Starting from a dynamic model of the original (nominal) undamped system (either in spatial coordinates or made of frequency responses), the proposed formulations are targeted to the simultaneous modification of an arbitrary number of modes, through the assignment of both the frequencies and the mode shapes (without the need to meet the frequent requirement of a specific eigenvector normalization). The simultaneous modification of an arbitrary number of mass and stiffness parameters is also allowed, even when they are linearly interrelated, and regardless of the number of assignment requirements. These facts overcomes the limitations of most of the available methods where specific assumptions on both the number of assigned modes and on the class of modifiable parameters are stated. In particular, the method proposed in [LI 1999] allows the imposition of just a single mode while in [SIVAN 1997] all the modes must be simultaneously assigned. Alternatively, the number of assigned modes is limited by either the dimension of the system model and the number of modification parameters [LIANGSHENG 2003], or the dimension of the incomplete set of known modes ([RAM 1991] and [BRAUN 2001]). As far as the class of modifiable parameters is concerned, the simultaneous modification of mass and stiffness parameters [LI

1999] or the interrelated modifications (e.g. parameter modifications affecting both the mass and the stiffness matrices) are often prevented ([RAM 1991], [BRAUN 2001] and [SIVAN 1997]).

Besides being general with respect to the number of problem unknowns and requirements, the approaches proposed in this Thesis allow adopting non-diagonal mass matrices (both for the original and the modified systems) and non-tridiagonal symmetric stiffness matrices (e.g. those of finite elements). Such a possibility significantly enlarges the range of design problems to which the proposed design approach can be applied. It should be pointed out that in most of the works appearing in literature it is explicitly assumed that mass matrices are diagonal and stiffness matrices are tridiagonal symmetric (see e.g. [SIVAN 1997], [BRAUN 2001] and [RAM 2009]).

Another relevant feature of the proposed problem formulations is its capability to include in the problem solution physical constraints on the design variable values, translated into mathematical constraints. So far, the adoption of constraints in modal optimisation has instead been only partially exploited in a few other works, where only positivity constraints ([SIVAN 1997], [BRAUN 2001]), lower and upper bounds on single variables ([BRAUN 2001], [PARK 2000]), or constraint on the system total mass [RAM 2009] have been imposed. The formulations proposed in this work considerably improve the possibility of incorporating physical constraints by handling a wide family of complicated constraints in the form of arbitrary linear combinations of inhomogeneous design variables. The presence of these constraints on all the modification parameters together with the introduction of an additional term

penalizing large modifications, ensures the physical and technical feasibility of the solution, and also allows encouraging solutions which are small (in some norm sense), hence reducing the amount of parameter modifications required. This is usually desirable in practice. As a further aid to designers, some specific tools have been introduced in order to reflect differing levels of concern about both the modifications to be adopted (e.g. to penalize the modifications of some parameters) and the different requirements of the problem (e.g. different modes). Finally, it is noteworthy that the formulations proposed allow to easily compute optimal discrete modifications, which perfectly reflect the industrial need of modularisation. To the best of our knowledge, no study has ever been carried out on discretisation problems in inverse structural modification.

Besides the discussed generality and flexibility, a further relevant issue in inverse structural modification problems is the problem solvability, i.e. the capability to compute a reliable and optimal solution. Only some specific modal modification problems have analytical solutions ([BUCHER 1993], [LI 1999] and [LIANGSHENG 2003]), and hence numerical approaches generally need to be adopted, in particular when parameter constraints are to be taken into account. The main drawback of numerical solutions is that iterative algorithms usually find solutions depending on the chosen initial guess and that such solutions could be only one among the unknown number of local optima. A peculiar feature of all the approaches proposed in this paper is the convexity of the function to be optimised. The optimisation of convex functions on convex domains allows overcoming most limitations of general nonlinear optimisation, by ensuring that a globally optimal solution is found. In addition, efficient, highly robust and reliable

algorithms are available for solving convex optimisation problems [BOYD 2004]. These motivations have boosted the use of convex optimisation in a wide range of mechanical design problems [DEMEULENAERE 2006]. The chief challenge in adopting convex optimisation lies in the problem formulation, since recognizing its convexity is not straightforward [DEMEULENAERE 2006]. Once a problem is formulated within the frame of convex optimisation, it is quite straightforward to solve it. The capability of the proposed approaches to provide unique optima is further strengthened by its complete lack of dependence on eigenvector magnitude, i.e. on the normalization scheme adopted for the imposed eigenvectors. This is not the case with most of the reviewed works ([RAM 1991], [BUCHER 1993], [BRAUN 2001], [LIANGSHENG 2003] and [SIVAN 1997]), where eigenvector normalisation considerably affects the results (examples showing such a problem are proposed in this work).

Finally, problem numerical conditioning should also be tackled, both when analytical and numerical solutions are adopted. Numerical problems, for example, do not allow selecting eigenvectors with zero or close-to-zero components in one of the solutions proposed in [BUCHER 1993]. Numerical problems may also impose consistent modifications of the natural frequencies of the modes to be modified [LI 1999]. The approaches proposed in this work do not suffer from these limitations since the previously mentioned penalty term adopted for penalizing large modifications also plays a crucial role in the increase of both the numerical reliability of the solution, and of its robustness with respect to system model uncertainty.

Chapter 1. Modal design optimisation

1.1. Introductory theory

The aim of dynamic models is to describe the dynamic properties of real mechanical systems with the desired accuracy. This means that it is not necessary to model all the system interaction but that, in most cases, it is sufficient to consider the basic dynamic properties separated into simple discrete elements. Such system properties are mass, stiffness and damping which are responsible for inertial, elastic and dissipative forces respectively. Depending upon the number of degrees of freedom (DOF), models can be classified into single degree-of-freedom (SDOF) and multiple degree-of-freedom (MDOF) systems.

Good approximations of real structures are usually realized through models with finite number of elements representative of the most important features from a dynamic point of view: commonly used models consider discretised masses connected with springs and dashpots.

In such models of undamped systems composed by n masses and connected through springs, the equilibrium equation can be written in compact matrix form:

$$\mathbf{M}\ddot{\mathbf{x}}(t) + \mathbf{K}\mathbf{x}(t) = \mathbf{f}(t) \tag{1.1}$$

where $\mathbf{M} \in \mathbb{R}^{n\times n}$ is the system mass matrix, $\mathbf{K} \in \mathbb{R}^{n\times n}$ is the system stiffness matrix, vectors $\mathbf{x}(t) \in \mathbb{R}^{n\times 1}$ and $\ddot{\mathbf{x}}(t) \in \mathbb{R}^{n\times 1}$ represent respectively the system displacements and accelerations and $\mathbf{f}(t) \in \mathbb{R}^{n\times 1}$ is the vector of the external forces acting on the system. The number of degrees of freedom of such a system is n.

The solution of equation (1.1), when exciting the system with a harmonic force, is in the form:

$$\mathbf{x}(t) = \mathbf{u}\sin(\omega t) \tag{1.2}$$

where $\mathbf{u} \in \mathbb{R}^{n\times 1}$ is the vector of displacement amplitudes.

Considering the free motion, an eigenvalue problem is obtained:

$$\left(\mathbf{K} - \omega^2\mathbf{M}\right)\mathbf{u} = \mathbf{0} \tag{1.3}$$

whose solution vector **u** is non-trivial if:

$$\det\left(\mathbf{K} - \omega^2\mathbf{M}\right) = 0 \tag{1.4}$$

Eq. (1.4) yields *n* solutions $\omega_1^2, \omega_2^2, \ldots, \omega_n^2$ which are the system eigenvalues and whose square roots are the natural frequencies of the MDOF system. For each ω_i of the *n* natural frequencies, the solution of Eq. (1.3) is the non trivial vector $\mathbf{u}_i$. Such vectors are called the eigenvectors of the system.

The eigenvectors possess peculiar ortoghonality characteristics so that, if no particular normalisation is adopted, the following hold:

$$\mathbf{u}_j^{\mathrm{T}}\mathbf{K}\,\mathbf{u}_i = \begin{cases} \tilde{k} & if \quad i = j \\ 0 & if \quad i \neq j \end{cases} \tag{1.5}$$

$$\mathbf{u}_j^{\mathrm{T}}\mathbf{M}\,\mathbf{u}_i = \begin{cases} \tilde{m} & if \quad i = j \\ 0 & if \quad i \neq j \end{cases} \tag{1.6}$$

Also, by multiplying Eq. (1.3) at left by $\mathbf{u}^{\mathbf{T}}$ and subsequently dividing through $\mathbf{u}^{\mathbf{T}}\mathbf{M}\mathbf{u}$, it is possible to obtain an alternative expression for the eigenvalue in terms of its eigenvector, called the "Rayleigh Quotient" [MEIROVITCH 1980]:

$$\omega_i^2 = \frac{\mathbf{u}_i^{\mathbf{T}}\mathbf{K}\,\mathbf{u}_i}{\mathbf{u}_i^{\mathbf{T}}\mathbf{M}\,\mathbf{u}_i} \quad \forall i = 1,\ldots,n \tag{1.7}$$

1.2. Formulation of the method for system models in spatial coordinates

1.2.1. Multiple inverse eigenvalue problem

Let consider an undamped *N*-dof linear system to be modified in order to get a desired dynamic behaviour. Let assume that $\mathbf{M}$, $\mathbf{K} \in \mathbb{R}^{N\times N}$ are the mass and stiffness matrices of the system. The desired dynamic behaviour is assumed to be specified through an arbitrary number $n \le N$ of eigenpairs $\left(\omega_h^2, \mathbf{u}_h\right)$, $h = 1,\ldots,n$ where ω_h is the natural frequency of the mode with shape $\mathbf{u}_h$.

The allowed additive parameter modifications are described by the modification matrices $\Delta\mathbf{M}(\mathbf{x})$, $\Delta\mathbf{K}(\mathbf{x}) \in \mathbb{R}^{N\times N}$, where $\mathbf{x} \in \mathbb{R}^{N_x}$ collects the N_x problem unknowns, i.e. the design variables. The structures of $\Delta\mathbf{M}$ and $\Delta\mathbf{K}$ are a priori assumed and are coherent with the physically and technically feasible modifications of the system parameters.

For any desired eigenpair of the modified system $\left(\omega_h^2, \mathbf{u}_h\right)$, both the eigenvalue problem equation and the Rayleigh quotient associated with matrices $\mathbf{M}+\Delta\mathbf{M}(\mathbf{x})$ and $\mathbf{K}+\Delta\mathbf{K}(\mathbf{x})$ must hold:

$$\omega_h^2 \left(\mathbf{M} + \Delta\mathbf{M}\left(\mathbf{x}\right)\right)\mathbf{u}_h = \left(\mathbf{K} + \Delta\mathbf{K}\left(\mathbf{x}\right)\right)\mathbf{u}_h \quad \forall h = 1,\ldots,n \tag{1.8}$$

$$\omega_h^2 = \frac{\mathbf{u}_h^{\mathbf{T}}\left(\mathbf{K} + \Delta\mathbf{K}\left(\mathbf{x}\right)\right)\mathbf{u}_h}{\mathbf{u}_h^{\mathbf{T}}\left(\mathbf{M} + \Delta\mathbf{M}\left(\mathbf{x}\right)\right)\mathbf{u}_h} \quad \forall h = 1,\ldots,n \tag{1.9}$$

Let the modification parameters be only those linearly affecting the entries Δm_{ij} and Δk_{ij}. For each $h = 1,\ldots,n$ the real matrix $\tilde{\mathbf{U}}_h \in \mathbb{R}^{N\times N_x}$ allows expressing the following equality:

$$\omega^2\Delta\mathbf{M}\left(\mathbf{x}\right)\mathbf{u}_h - \Delta\mathbf{K}\left(\mathbf{x}\right)\mathbf{u}_h = \tilde{\mathbf{U}}_h\mathbf{x} \tag{1.10}$$

where, using the vector differentiation operator $\partial/\partial\mathbf{x} = \left[\partial/\partial x_1,\ldots,\partial/\partial x_{N_x}\right]$

$$\tilde{\mathbf{U}}_h = \frac{\partial\left(\left[\omega_h^2\Delta\mathbf{M} - \Delta\mathbf{K}\right]\mathbf{u}_h\right)}{\partial\mathbf{x}} \tag{1.11}$$

The matrix $\tilde{\mathbf{U}}_h$ only depends on the desired eigenpair $\left(\omega_h^2, \mathbf{u}_h\right)$ and on the parameters selected for modification.

On the basis of Eq. (1.10) the h^{th} inverse eigenvalue problem stated through Eqs. (1.8) and (1.9) can be reformulated as the linear system

$$\mathbf{U}_h\mathbf{x} = \mathbf{b}_h \tag{1.12}$$

where both the matrix $\mathbf{U}_h \in \mathbb{R}^{(N+1)\times N_x}$

$$\mathbf{U}_h = \begin{bmatrix} \tilde{\mathbf{U}}_h \\ \beta_h\mathbf{u}^{\mathbf{T}}\tilde{\mathbf{U}}_h \end{bmatrix} \tag{1.13}$$

and the vector $\mathbf{b}_h \in \mathbb{R}^{(N+1)}$

$$\mathbf{b}_h = \begin{Bmatrix} \left(-\omega_h^2\mathbf{M} + \mathbf{K}\right)\mathbf{u}_h \\ \beta_h\mathbf{u}_h^{\mathbf{T}}\left(-\omega_h^2\mathbf{M} + \mathbf{K}\right)\mathbf{u}_h \end{Bmatrix} \tag{1.14}$$

depend on the original system characteristics and on the desired h^{th} vibration mode. The positive scalar coefficient β_h has been introduced to suitably weigh the Rayleigh equation (1.9) in the linear system (1.12), in order to boost the natural frequency achievement in the inverse eigenvalue problem.

Since no assumption has been made on the number of modification parameters and hence on the dimensions and on the rank of $\mathbf{U}_h$, an exact solution of the linear system (1.12) is not ensured for the general case. A least-squares solution of the linear system, must therefore be computed:

$$\min_{\mathbf{x}} \left\{ f_h(\mathbf{x}) := \left\| \mathbf{U}_h \mathbf{x} - \mathbf{b}_h \right\|_2^2 \right\} \tag{1.15}$$

Subsequently, in order to explicitly state the modification problem for the n eigenpairs, the h^{th} single mode eigenvalue problem (1.15) is weighed by means of the positive scalar α_h. The multimode inverse eigenvalue problem can therefore be written as:

$$\min_{\mathbf{x}} \left\{ f(\mathbf{x}) = \sum_{h=1}^{n} \alpha_h f_h(\mathbf{x}) := \left\| \mathbf{U}\mathbf{x} - \mathbf{b} \right\|_2^2 \right\} \tag{1.16}$$

where $\mathbf{U} := \left[\sqrt{\alpha_1}\mathbf{U}_1^{\mathrm{T}}, \ldots, \sqrt{\alpha_n}\mathbf{U}_n^{\mathrm{T}} \right]^{\mathrm{T}}$ and $\mathbf{b} := \left[\sqrt{\alpha_1}\mathbf{b}_1^{\mathrm{T}}, \ldots, \sqrt{\alpha_n}\mathbf{b}_n^{\mathrm{T}} \right]^{\mathrm{T}}$. The different values of the weights α_h are chosen so as to reflect differing levels of concern about the sizes of the h^{th} residual $\mathbf{U}_h\mathbf{x} - \mathbf{b}_h$.

1.2.2. Regularised multiple inverse eigenvalue problem

The solution of the quadratic optimisation problem can be improved by including in Eq. (1.20) an extra term penalizing large mass and stiffness modifications. As a matter of fact, not only may large structural modification

cause spillover phenomena on the neglected modes, but also small parameter modifications are highly desirable from a technical and economical point of view. Additionally, robustness issues may arise in calculating the numerical value of the solution of the quadratic optimisation problem in Eq. (1.20). Robust solutions of the inverse eigenvalue problem are those exhibiting small variations with respect to the problem parameter variations (e.g. $\mathbf{U}$ and $\mathbf{b}$). Such variations are mainly caused by the unavoidable system model uncertainties. The robustness issue is tightly related to the ill-posed nature of the least-squares solutions. This problem arises even when dealing with the unconstrained problem in Eq. (1.16), since the numerical value of the analytical solution $\mathbf{x} = \mathbf{U}^{+}\mathbf{b}$ (where $\mathbf{U}^{+}$ is the pseudo-inverse of $\mathbf{U}$) generally overestimates the actual solution and is very sensitive to the problem parameter uncertainties [CALVETTI 2005]. Similar ill-posed nature and robustness issues obviously need to be coped with when solving the constrained problem in Eq. (1.20).

Both the robustness issue and the technical requirement of small modifications can be tackled by adding a Tikhonov's regularising term to the formulation of the problem. Such a term allows stating the multiple inverse eigenvalue problem as a Tikhonov-regularised bi-criterion quadratic optimisation of the convex objective function $g(\mathbf{x})$:

$$\min_{\mathbf{x}} \left\{ g(\mathbf{x}) := f(\mathbf{x}) + \lambda \left\| \mathbf{\Omega}_{\mathbf{x}} \mathbf{x} \right\|_2^2 \right\} \tag{1.17}$$

The scalar positive value λ is the regularisation parameter, trading between the cost of missing the target specifications ($f(\mathbf{x})$) and the cost of using large values of the design variables ($\left\| \mathbf{\Omega}_{\mathbf{x}} \mathbf{x} \right\|_2^2$). The positive-definite diagonal matrix

$\mathbf{\Omega}_\mathbf{x} \in \mathbb{R}^{N_x \times N_x}$ is the regularisation operator, and defines a scalar product which induces a norm on $\mathbb{R}^{N_x}$. $\mathbf{\Omega}_\mathbf{x}$ is employed in order to suitably weigh the components of **x**, i.e. to selectively penalize the modifications of the design variables, in accordance to their technological feasibility and economic outcome.

1.2.3. Constrained Regularised multiple inverse eigenvalue problem

In order to avoid physically and technologically infeasible modifications (e.g. negative masses or too large modifications), the solution must be constrained within a feasible domain Γ. Peculiar are the constraints expressed through

$$\Gamma = \left\{ \mathbf{x} : \mathbf{A}\mathbf{x} \le \mathbf{c},\ \mathbf{A} \in \mathbb{R}^{N_\gamma \times N_x},\ \mathbf{c} \in \mathbb{R}^{N_\gamma} \right\} \tag{1.18}$$

The polyhedron Γ allows simultaneously dealing with an arbitrary number of N_γ constraints and is a convex set, because for any $\mathbf{x}_1, \mathbf{x}_2 \in \Gamma$ and any real θ ($0 \le \theta \le 1$), the following holds [BOYD 2004]:

$$\theta \mathbf{x}_1 + (1-\theta)\mathbf{x}_2 \in \Gamma \tag{1.19}$$

By means of a proper selection of **A** and **c**, the adopted definition of Γ allows imposing lower and upper bounds both on each variable and on linear combinations of the variables (e.g. constraints on the total mass modification can be set, as well as constraints on the ratios of unknowns).

The inverse eigenvalue problem is therefore expressed as a constrained quadratic optimisation problem

$$\min_{\mathbf{x}} \left\{ g(\mathbf{x}), \mathbf{x} \in \Gamma \right\} \tag{1.20}$$

in which the residual of the linear system (1.17) is minimized over the feasible domain Γ.

1.2.4. Convexity of the formulated problem

It is worth noticing that the formulation of the inverse structural modification problem proposed in Eq. (1.20) represents a convex optimisation problem, since it consists in minimizing the convex function $g:\Gamma\to\mathbb{R}$ on the polyhedron Γ, which is itself a convex domain [BOYD 2004]. The function $g(\mathbf{x})=\|\mathbf{U}\mathbf{x}-\mathbf{b}\|_2^2+\lambda\|\mathbf{\Omega}_\mathbf{x}\mathbf{x}\|_2^2=\left\|\begin{bmatrix}\mathbf{U}\\ \sqrt{\lambda}\mathbf{\Omega}_\mathbf{x}\end{bmatrix}\mathbf{x}-\begin{bmatrix}\mathbf{b}\\ \mathbf{0}\end{bmatrix}\right\|_2^2$ is also convex, because it is defined on a convex set Γ and satisfies the inequality below for any real σ ($0\le\sigma\le1$), for any $\mathbf{x}_1,\ \mathbf{x}_2\in\Gamma$, and for any rank or dimension of matrix $\mathbf{U}$:

$$\left\|\begin{bmatrix}\mathbf{U}\\ \sqrt{\lambda}\mathbf{\Omega}_\mathbf{x}\end{bmatrix}\left(\sigma\mathbf{x}_1+(1-\sigma)\mathbf{x}_2\right)-\begin{bmatrix}\mathbf{b}\\ \mathbf{0}\end{bmatrix}\right\|_2^2\le \sigma\left\|\begin{bmatrix}\mathbf{U}\\ \sqrt{\lambda}\mathbf{\Omega}_\mathbf{x}\end{bmatrix}\mathbf{x}_1-\begin{bmatrix}\mathbf{b}\\ \mathbf{0}\end{bmatrix}\right\|_2^2+(1-\sigma)\left\|\begin{bmatrix}\mathbf{U}\\ \sqrt{\lambda}\mathbf{\Omega}_\mathbf{x}\end{bmatrix}\mathbf{x}_2-\begin{bmatrix}\mathbf{b}\\ \mathbf{0}\end{bmatrix}\right\|_2^2 \tag{1.21}$$

The convexity of the problem stated in Eq. (1.20) ensures that an unique global optimum exists and can be computed numerically regardless of the initial solution guess. Additionally, since $\left(\mathbf{U}^\mathbf{T}\mathbf{U}+\lambda\mathbf{\Omega}_\mathbf{x}{}^\mathbf{T}\mathbf{\Omega}_\mathbf{x}\right)>0$ for any rank or dimension of matrix $\mathbf{U}$ and for any $\lambda>0$, and the rank of $\mathbf{U}^\mathbf{T}\mathbf{U}+\lambda\mathbf{\Omega}_\mathbf{x}{}^\mathbf{T}\mathbf{\Omega}_\mathbf{x}$ is maximum, the regularised problem in Eq. (1.17) has an analytical solution for the unconstrained problem ($\Gamma=\mathbb{R}^{N_x}$):

$$\mathbf{x}=\left(\mathbf{U}^\mathbf{T}\mathbf{U}+\lambda\mathbf{\Omega}_\mathbf{x}{}^\mathbf{T}\mathbf{\Omega}_\mathbf{x}\right)^{-1}\mathbf{U}^\mathbf{T}\mathbf{b} \tag{1.22}$$

When dealing with the constrained problem, if the unconstrained solution in Eq. (1.22) does not lie in the feasible set Γ, the constrained optimal solution must be computed numerically by exploiting the convex optimisation algorithms.

Equation (1.22) clearly proves the effectiveness of the regularisation term in improving the numerical conditioning and the robustness of the solution: the condition number of the matrix $\mathbf{U}^{\mathrm{T}}\mathbf{U}+\lambda\boldsymbol{\Omega}_{\mathbf{x}}{}^{\mathrm{T}}\boldsymbol{\Omega}_{\mathbf{x}}$, i.e. $\left\|\left(\mathbf{U}^{\mathrm{T}}\mathbf{U}+\lambda\boldsymbol{\Omega}_{\mathbf{x}}{}^{\mathrm{T}}\boldsymbol{\Omega}_{\mathbf{x}}\right)\right\|\left\|\left(\mathbf{U}^{\mathrm{T}}\mathbf{U}+\lambda\boldsymbol{\Omega}_{\mathbf{x}}{}^{\mathrm{T}}\boldsymbol{\Omega}_{\mathbf{x}}\right)^{-1}\right\|$, is a decreasing function of λ [CALVETTI 2004]. The bigger λ is, the more reliable and the less sensitive the solution is.

The selection of an optimal value of λ clearly depends on the acceptability of missing the target specifications and of using large parameter modifications, which are often conflicting requirements. Among the methods presented in literature for a proper choice of the regularisation parameter λ, one should recall the *L*-curve method [CHOI 2007], the *L*-ribbon and the curvature-ribbon [CALVETTI 2004], the discrepancy principle and the crossvalidation principle [HANSEN 2002]. In particular the *L*-curve method suggests choosing λ on the basis of the curve:

$$L := \left\{\left(\log\left\|\boldsymbol{\Omega}_{\mathbf{x}}\mathbf{x}_{\lambda}\right\|_2^2, \log f\left(\mathbf{x}_{\lambda}\right)\right) : \lambda > 0\right\} \tag{1.23}$$

where $\mathbf{x}_{\lambda}$ is the problem solution for a given λ. Such a curve is usually called the *L*-curve, since its graph looks like a letter "L", when plotted with a log-log scale. In [CHOI 2007] it is proposed to choose the value of λ that corresponds to the point at the "vertex" of the "L", where the vertex is defined to be the point on the *L*-curve with the largest magnitude curvature.

Examples of the method application on simulated test case are provided in Chapter 2.

1.3. Formulation of the method employing FRF system models

1.3.1. Definition of the modification problem

Let consider that the dynamics of the system to be modified can be adequately described through an *N*-dof undamped linear model. The problem of assigning the desired eigenstructure is aimed at computing the matrices $\mathbf{\Delta M}$ and $\mathbf{\Delta K}$ satisfying the eigenvalue problem:

$$\omega_h^2 \left(\mathbf{M}+\mathbf{\Delta M}\right)\mathbf{u}_h = \left(\mathbf{K}+\mathbf{\Delta K}\right)\mathbf{u}_h \qquad h=1,\ldots,n\le N \tag{1.24}$$

In Eq. (1.24) $\mathbf{M},\mathbf{K}\in\mathbb{R}^{N\times N}$ are the mass and stiffness matrices of the original (unmodified) system, $\left(\omega_h^2,\mathbf{u}_h\right)$ is the h^{th} eigenpair to be assigned ($h=1,\ldots,n$) and $\mathbf{\Delta M},\mathbf{\Delta K}\in\mathbb{R}^{N\times N}$ are the additive modification mass and stiffness matrices representing the modifiable parameters and their locations. Since $\mathbf{H}\left(\omega_h\right)=\left(\mathbf{K}-\omega_h^2\mathbf{M}\right)^{-1}=\sum_{i=1}^{N}\frac{\mathbf{u}_i\mathbf{u}_i^{\mathbf{T}}}{\omega_i^2-\omega_h^2}$ is the frequency response function matrix (the receptance matrix) of the original system at the frequency ω_h, Eq. (1.24) can be rewritten as:

$$\mathbf{H}(\omega_h)(\omega_h^2\mathbf{\Delta M}-\mathbf{\Delta K})\mathbf{u}_h=\mathbf{u}_h \qquad h=1,\ldots,n \tag{1.25}$$

Equation (1.25) is a system of linear equations whose unknowns are the N_m entries of matrix $\mathbf{\Delta M}$ and the N_k entries of matrix $\mathbf{\Delta K}$. By collecting all the N_x ($N_x=N_m+N_k$) unknowns into vector $\mathbf{x}$, it is possible to rearrange the single eigenpair assignment problem in Eq. (1.25) as:

$$\mathbf{H}(\omega_h)\mathbf{U}_h\mathbf{x} = \mathbf{u}_h \tag{1.26}$$

where, using the vector differentiation operator $\partial/\partial\mathbf{x} = \left[\partial/\partial x_1, \ldots, \partial/\partial x_{N_x}\right]$,

$$\mathbf{U}_h = \frac{\partial\left(\left[\omega_h^2\boldsymbol{\Delta}\mathbf{M} - \boldsymbol{\Delta}\mathbf{K}\right]\mathbf{u}_h\right)}{\partial\mathbf{x}} \tag{1.27}$$

The matrix $\mathbf{U}_h$ only depends on the desired eigenpair $\left(\omega_h^2, \mathbf{u}_h\right)$ and on the parameters selected for modification, which impose the structure of the modification matrices.

It should be stressed that the single eigenpair assignment problem stated in Eq. (1.26) does not admit an exact solution for general cases, since no assumption has been made on the rank of the real matrix $\mathbf{G}_h(\omega_h) := \mathbf{H}(\omega_h)\mathbf{U}_h$ ($\mathbf{G}_h(\omega_h) \in \mathbb{R}^{N\times N_x}$). As a consequence it is necessary to compute a least-square solution, by minimizing the square of the Euclidean norm of the residual $\left\|\mathbf{G}_h\left(\omega_h\right)\mathbf{x} - \mathbf{u}_h\right\|_2^2$. In order to formulate the generalized multi-mode modification problem, each h^{th} single eigenpair assignment problem is weighed through the positive scalars α_h, which reflect the level of concern on the minimization of the h^{th} residual. The multiple eigenstructure assignment problem can therefore be cast as:

$$\min_{\mathbf{x}}\left\{\sum_{h=1}^{n}\alpha_h\left\|\mathbf{G}_h\left(\omega_h\right)\mathbf{x} - \mathbf{u}_h\right\|_2^2\right\} \tag{1.28}$$

Problem (5) can be rewritten in the more compact matrix form

$$\min_{\mathbf{x}}\left\{\left\|\mathbf{G}\left(\omega_1, \ldots, \omega_n\right)\mathbf{x} - \mathbf{u}\right\|_2^2\right\} \tag{1.29}$$

where

$$\mathbf{G} := \left[\sqrt{\alpha_1}\mathbf{G}_1^{\mathrm{T}}(\omega_1), \ldots, \sqrt{\alpha_n}\mathbf{G}_n^{\mathrm{T}}(\omega_n) \right]^{\mathrm{T}}, \ \mathbf{u} := \left[\sqrt{\alpha_1}\mathbf{u}_1^{\mathrm{T}}, \ldots, \sqrt{\alpha_n}\mathbf{u}_n^{\mathrm{T}} \right]^{\mathrm{T}}. \tag{1.30}$$

Such a receptance-based problem formulation does not require the knowledge of the nominal values of mass and stiffness matrices, which makes the proposed approach suitable for the modification of systems whose masses and stiffnesses are either unknown or difficult to estimate.

1.3.2. Problem constraints and solution

The straightforward minimization of problem (1.28), which admits an analytical solution, does not prevent theoretical modifications from being physically and technically infeasible (e.g. with negative masses or too large modifications) and/or not robust and numerically unreliable.

Firstly, the feasibility requirement imposes both lower and upper bounds on the values of the design variables. In addition, constraints on linear combinations of the design variables (e.g. constraints on the total mass or stiffness modifications) are often required. These problem specifications may be translated into the structural modification problem through a feasible domain Γ constraining the set of allowed modifications:

$$\Gamma = \left\{ \mathbf{x} : \mathbf{A}\mathbf{x} \le \mathbf{c}, \ \mathbf{A} \in \mathbb{R}^{N_\gamma \times N_x}, \ \mathbf{c} \in \mathbb{R}^{N_\gamma} \right\} \tag{1.31}$$

where N_γ is the number of constraints to be simultaneously satisfied. The inverse eigenvalue problem can therefore be expressed as a constrained quadratic optimisation problem, minimizing the square Euclidean norm of the linear system residual over the feasible domain Γ:

$$\min_{\mathbf{x}} \left\{ \left\| \mathbf{G}(\omega_1,\ldots,\omega_n)\mathbf{x}-\mathbf{u} \right\|_2^2, \mathbf{x}\in\Gamma \right\} \tag{1.32}$$

Secondly, the robustness and numerical issues are tackled by properly regularising the problem to be minimized. Robust solutions are those exhibiting small changes in response to small parameter variations, which are caused by the uncertainty affecting the measured FRFs. In particular, unmodeled dynamics (e.g. damping), measurement disturbances and errors, may considerably affect the numerical results. The robustness issue is strictly related to the numerical ill-posed nature of the problem stated in Eq. (1.32), whose computed solution generally overestimates the actual solution and is very sensitive to the parameter uncertainties [CALVETTI 2005]. Both issues can be simultaneously tackled by adding the Tikhonov regularisation term [BOYD 2004]. The regularised inverse eigenvalue problem finally becomes the following bi-criterion optimisation problem:

$$\min_{\mathbf{x}} \left\{ f(\mathbf{x}) := \left\| \mathbf{G}(\omega_1,\ldots,\omega_n)\mathbf{x}-\mathbf{u} \right\|_2^2 + \lambda \left\| \mathbf{\Omega}_{\mathbf{x}}\mathbf{x} \right\|_2^2, \mathbf{x}\in\Gamma \right\} \tag{1.33}$$

The positive definite matrix $\mathbf{\Omega}_{\mathbf{x}} \in \mathbb{R}^{N_x \times N_x}$, is the regularisation operator and is adopted to suitably weigh the components of $\mathbf{x}$. The scalar $\lambda > 0$ is the regularisation parameter and is selected to trade between the cost of using "large" values of $\left\| \mathbf{\Omega}_{\mathbf{x}}\mathbf{x} \right\|_2^2$ and the cost of missing the target specification $\left\| \mathbf{G}(\omega_1,\ldots,\omega_n)\mathbf{x}-\mathbf{u} \right\|_2^2$. The bigger λ, the more reliable and the less sensitive the solution [CALVETTI 2005]. The regularisation parameter λ is often chosen as the vertex of the so called L-curve, which is obtained by plotting the couple $\left\{ \log\left(\left\| \mathbf{\Omega}_{\mathbf{x}}\mathbf{x}_\lambda \right\|_2^2 \right), \log\left(\left\| \mathbf{G}(\omega_1,\ldots,\omega_n)\mathbf{x}_\lambda-\mathbf{u} \right\|_2^2 \right) \right\}$ for every λ, where $\mathbf{x}_\lambda$ is the

solution for a given λ. The L-curve approach is successfully adopted also in model updating providing reliable and robust results [AHMADIAN 1998].

It should be noticed that the polyhedron Γ is a convex set [BOYD 2004], since for any $\mathbf{x}_1, \mathbf{x}_2 \in \Gamma$ and any $\theta \in \mathbb{R}, 0 \le \theta \le 1$, it holds $\theta \mathbf{x}_1 + (1-\theta)\mathbf{x}_2 \in \Gamma$. In addition, the function $f(\mathbf{x}) : \Gamma \to \mathbb{R}$ in (1.33) is itself a convex function for any $\lambda > 0$, since for any $\mathbf{x}_1, \mathbf{x}_2 \in \Gamma$, and any real α, $0 \le \alpha \le 1$, it holds $f(\alpha \mathbf{x}_1 + (1-\alpha)\mathbf{x}_2) \le \alpha f(\mathbf{x}_1) + (1-\alpha) f(\mathbf{x}_2)$. Hence, the optimisation problem in Eq. (1.33) is a convex optimisation problem [BOYD 2004]. This ensures that a global optimum exists, and can be computed regardless of the initial guess. In addition, since **G**, **u**, $\mathbf{\Omega_x}$ are real, the problem solution is also real. Since $\left(\mathbf{G}^{\mathrm{T}}\mathbf{G} + \lambda \mathbf{\Omega_x}^{\mathrm{T}} \mathbf{\Omega_x}\right) > 0$, an analytical solution of the regularised problem (1.33) is available for the specific case $\Gamma \equiv \mathbb{R}^{N_x}$ (unconstrained problem):

$$\mathbf{x} = \left(\mathbf{G}^{\mathrm{T}}\mathbf{G} + \lambda \mathbf{\Omega_x}^{\mathrm{T}} \mathbf{\Omega_x}\right)^{-1} \mathbf{G}^{\mathrm{T}}\mathbf{u} \tag{1.34}$$

If such a solution does not lie inside the feasible domain Γ, the constrained optimum must be computed numerically by exploiting convex optimisation algorithms. Once a problem is formulated within such a frame of convex optimisation, it is straightforward to solve it since numerous effective and reliable numerical techniques are available in literature (e.g. [BOYD 2004], [GRANT 2008]

As a final advantage, besides increasing robustness and numerical reliability, the Tikhonov regularisation adopted allows penalizing large mass and stiffness modifications, which are often undesirable from a technical and economical point of view and may lead to spillover phenomenon. In particular,

through a proper selection of $\mathbf{\Omega}_\mathbf{x}$, it is possible to influence the solution, i.e. to selectively penalize the modification of the design variables, in accordance with their technological feasibility and economic outcome.

Examples of the method application on simulated test case are provided in Chapter 3.

1.4. Formulation of the method allowing for discrete modification

1.4.1. Inverse Eigenvalue Problem as a mixed-integer non linear optimisation

When dealing with a generic structural optimisation problem, both continuous and discrete design variables may simultaneously exist. In order to keep the problem formulation as general as possible, vector **x** is partitioned into a discrete N_z-dimensional vector $\mathbf{z_d}$, collecting the discrete design variable, and the N_r-dimensional real vector **r**, collecting the continuous design variable (N_z+ N_r = N_x):

$$\mathbf{x} = \left\{ \mathbf{z_d}^{\mathrm{T}} \quad \mathbf{r}^{\mathrm{T}} \right\}^{\mathrm{T}} \tag{1.35}$$

The discrete design variables are those admitting only values which are integer multiple of a discretization value d_i:

$$\mathrm{z}_{\mathrm{d}_i} = \mathrm{z}_i \cdot d_i, \quad \mathrm{z}_i \in \mathbb{Z} \tag{1.36}$$

Equation (1.36) allows defining the integer vector $\mathbf{z} \in \mathbb{Z}^{N_z}$, and therefore translating the problem stated by Eq. (1.20) into a mixed-integer non linear optimisation (MINLP),

$$\min_{\substack{\mathbf{z}\in\mathbb{Z}^{N_z}\\ \mathbf{r}\in\mathbb{R}^{N_r}}}\left\{ g(\boldsymbol{\chi}) := \left\| \mathbf{U}_d \begin{Bmatrix}\mathbf{z}\\ \mathbf{r}\end{Bmatrix} - \mathbf{b} \right\|_2^2 + \delta \left\| \boldsymbol{\Omega}_\chi \begin{Bmatrix}\mathbf{z}\\ \mathbf{r}\end{Bmatrix} \right\|_2^2, \boldsymbol{\chi} := \left\{ \mathbf{z}^{\mathrm{T}} \quad \mathbf{r}^{\mathrm{T}} \right\}^{\mathrm{T}}, \mathbf{z}\in\Psi, \mathbf{r}\in\Upsilon \right\} \tag{1.37}$$

where $\mathbf{U}_d \in \mathbb{R}^{N\times N_x}$ is attained by multiplying the *i-th* column of $\mathbf{U}$ (i=1: N_z) with the discretisation value d_i. The feasible domain Γ is introduced in order to ensure strictly feasible modifications:

$$\Gamma = \left\{ \mathbf{z}, \mathbf{r} : \mathbf{z}\in\Psi\subset\mathbb{Z}^{N_z}, \mathbf{r}\in\Upsilon\subset\mathbb{R}^{N_r} \right\} \tag{1.38}$$

where:

$$\begin{aligned} \Psi &= \left\{ \mathbf{z}\in\mathbb{Z}^{N_z} : \mathbf{A}_\mathbf{z}\mathbf{z} \le \mathbf{c}_\mathbf{z},\ \mathbf{A}_\mathbf{z}\in\mathbb{R}^{N_\psi\times N_z},\ \mathbf{c}_\mathbf{z}\in\mathbb{R}^{N_\psi} \right\} \\ \Upsilon &= \left\{ \mathbf{r}\in\mathbb{R}^{N_r} : \mathbf{A}_\mathbf{r}\mathbf{r} \le \mathbf{c}_\mathbf{r},\ \mathbf{A}_\mathbf{r}\in\mathbb{R}^{N_\gamma\times N_r},\ \mathbf{c}_\mathbf{r}\in\mathbb{R}^{N_\gamma} \right\} \end{aligned} \tag{1.39}$$

The sets Υ and Ψ allow defining N_γ and N_ψ constraints on, respectively, the integer and on the continuous variable. For example, lower and upper bounds can be imposed both on each variable and on linear combinations of the variables. The polyhedron Υ is a convex set, since for any $\mathbf{r}_1, \mathbf{r}_2 \in \Upsilon$ and any real θ ($0 \le \theta \le 1$), it holds $\theta\mathbf{r}_1 + (1-\theta)\mathbf{r}_2 \in \Upsilon$ [BOYD 2004]. On the other hand, the constraint of the integer variables, Ψ, is not convex since it contains a discrete number of points. Nevertheless, the definition assumed by Eq. (1.39) ensures that the continuous relaxation of Ψ, i.e. the polyhedron $\Psi_\mathbb{R} = \left\{ \mathbf{z}\in\mathbb{R}^{N_z} : \mathbf{A}_\mathbf{z}\mathbf{z} \le \mathbf{c}_\mathbf{z},\ \mathbf{A}_\mathbf{z}\in\mathbb{R}^{N_\psi\times N_z},\ \mathbf{c}_\mathbf{z}\in\mathbb{R}^{N_\psi} \right\}$ is convex and it is equal to the convex hull of Ψ.

The proposed formulation of the MINLP inverse structural modification problem, given by (1.37), (1.38) and (1.39) leads to a convex integer programming problem, since it consists in minimizing the convex function

$g:\Gamma \to \mathbb{R}$ on the set Γ, whose continuous relaxation $\Gamma_{\mathbf{R}}$ is convex. The function $g(\chi)$ is convex since for any real θ $(0 \le \theta \le 1)$, for any χ_1, χ_2, and for any rank or dimension of matrix **U** the following inequality holds:

$$g(\theta\chi_1 + (1-\theta)\chi_2) \le \theta g(\chi_1) + (1-\theta) g(\chi_2) \tag{1.40}$$

The convexity of the problem ensures that a global optimal solution of the continuous relaxation of problem (1.37) exists and that such a global optimal solution can be computed numerically regardless of the initial solution guess. This feature allows overcoming the lack of an analytical solution for the constrained mixed-integer problem.

1.4.2. Solution of the mixed-integer non linear optimisation problem

1.4.2.a. Proximity between the continuous solution and the integer solution

The computation of the mixed-integer solution of the inverse structural modification problem, stated by the non-separable function $g(\chi)$, cannot be performed by simply rounding the continuous optimal solution to the nearest integer, since rounded solutions can be significantly far from the optimality and might also be infeasible. A useful result for the estimation of an upper bound of the Euclidean norm of the distance between the mixed-integer minimiser of $g(\chi)$, $\chi_{\mathbf{opt}}$, and the continuous one $\chi_{\mathbf{R}}$, arises from [LI 2006].

Let consider the continuous relaxation of $g(\chi)$, i.e. $g(\chi): \mathbb{R}^{N_x} \to \mathbb{R}$. It is a twice differentiable convex function, which satisfies the strong convexity condition for any $\delta > 0$ [BOYD 2004]:

$$0 < \lambda_L \le \lambda_{\min}\left(\nabla^2 \boldsymbol{g}(\boldsymbol{\chi})\right) \le \lambda_{\max}\left(\nabla^2 \boldsymbol{g}(\boldsymbol{\chi})\right) \le \lambda_U \quad \forall \boldsymbol{\chi} \in \mathbb{R}^{N_x} \tag{1.41}$$

where $\lambda_{\min}, \lambda_{\max}$ denote respectively the minimum and the maximum eigenvalues, while λ_L, λ_U are two real positive scalar, representing respectively the lower and the upper bound on the eigenvalues.

If the unconstrained problem is considered, it holds that:

$$\left\|\boldsymbol{\chi}_{\mathbf{opt}} - \boldsymbol{\chi}_{\mathbf{R}}\right\|_2 \le \frac{1}{2}\sqrt{\frac{\lambda_U}{\lambda_L} N_x} \tag{1.42}$$

It should be pointed out that, beside increasing the robustness and the numerical reliability of the solution, the regularisation adopted allows reducing the distance between the continuous and the mixed-integer solutions. In fact, since $\nabla^2 \boldsymbol{g}(\boldsymbol{\chi}) = 2\left(\mathbf{U}_d{}^T \mathbf{U}_d + \delta \boldsymbol{\Omega}_{\chi}\right)$, the ratio $\dfrac{\lambda_{\max}\left(\nabla^2 \boldsymbol{g}(\boldsymbol{\chi})\right)}{\lambda_{\min}\left(\nabla^2 \boldsymbol{g}(\boldsymbol{\chi})\right)}$, i.e. the condition number of matrix $\mathbf{U}_d{}^T \mathbf{U}_d + \delta \boldsymbol{\Omega}_{\chi}$, is a decreasing function of δ [CALVETTI 2004]. In particular, if $\boldsymbol{\Omega}_{\chi} = \mathbf{I}$, then $\dfrac{\lambda_{\max}\left(\nabla^2 \boldsymbol{g}(\boldsymbol{\chi})\right)}{\lambda_{\min}\left(\nabla^2 \boldsymbol{g}(\boldsymbol{\chi})\right)} = \dfrac{\lambda_{\max}\left(\mathbf{U}_d{}^T \mathbf{U}_d\right) + \delta^2}{\lambda_{\min}\left(\mathbf{U}_d{}^T \mathbf{U}_d\right) + \delta^2}$ [HOLDER 2004].

As a corollary of Eq. (1.42), when the constrained problem is considered, $\boldsymbol{\chi}_{\mathbf{opt}}$ must lie in the intersection of the Euclidean ball in $\mathbb{R}^{N_x}$ given by Eq. (1.42), and the feasible domain Γ (1.38):

$$\boldsymbol{\chi}_{\mathbf{opt}} \in \left\{\left(\left\|\boldsymbol{\chi} - \boldsymbol{\chi}_{\mathbf{R}}\right\|_2 \le \frac{1}{2}\sqrt{\frac{\lambda_U}{\lambda_L} N_x}\right) \cap \Gamma\right\} := \boldsymbol{\Phi} \tag{1.43}$$

where $\boldsymbol{\Phi}$ denotes the set to be investigated for the computation of the mixed-integer solution.

1.4.2.b. The Branch and Bound method

Equation (1.42) and (1.43) clearly highlight that the higher the number of design variables, the larger is the set $\mathbf{\Phi}$. When solving large scale problems, this implies that the full solution enumeration, i.e. the explicit analysis of all the feasible combinations of the design variables within $\mathbf{\Phi}$, is practically infeasible. It follows that the partial enumeration of the solution is an attractive approach in case the formulation adopted for the inverse structural modification problem ensures the computation of the exact optimal solution $\boldsymbol{\chi}_{\mathbf{opt}}$. In particular, in this work the non-linear Branch and Bound technique has been applied to perform the partial enumeration of the convex MINLP inverse structural modification problem described by (1.37), (1.38) and (1.39). The Branch and Bound idea was originally developed for the solution of Mixed-Integer Linear Problems [LAND 1960] and then extended to the solution of MINLP by Gupta [GUPTA 1985].

The basic idea behind the Branch and Bound method is to branch the initial problem (1.37), denoted with $\boldsymbol{P}$, into a set of subproblems $\boldsymbol{P_i}$, by attaining a node-tree structure where each node represents a subproblem. The method is based on computing the optimal solution of the continuous relaxation of each subproblems, and therefore leads to the solution of a NLP at each node. Clearly, the solution of the continuous relaxation of problem $\boldsymbol{P_i}$ will provide a minimum not greater than the value provided by the integer solution.

The branching phase is usually performed by selecting a fractional (non-integer) variable χ_j (the branching variable) of the solution of the continuous relaxation of $\boldsymbol{P_i}$ within the respective feasible domain ${}^{i}\Gamma_{\mathbf{R}}$, and by splitting

problem $\boldsymbol{P_i}$ into two sub-problems. The two sub-problems defined at node *i* are attained by adding further closed half-space constraints to ${}^{i}\Gamma_{\mathbf{R}}$:

$$ {}^{i}_{right}\Gamma_{\mathbf{R}} = \left\{ {}^{i}\Gamma_{\mathbf{R}} \cap \chi_j \geq ceil({}^{i}\chi_j^{*}) \right\} \qquad (1.44) $$

$$ {}^{i}_{left}\Gamma_{\mathbf{R}} \left\{ {}^{i}\Gamma_{\mathbf{R}} \cap \chi_j \leq floor({}^{i}\chi_j^{*}) \right\} $$

where ${}^{i}_{right}\Gamma_{\mathbf{R}}$ and ${}^{i}_{left}\Gamma_{\mathbf{R}}$ denote the feasible domain of respectively, the "right hand" and "left hand" sub-problems of problem $\boldsymbol{P_i}$, and the scalar ${}^{i}\chi_j^{*}$ denotes the value of the *j*-th variable of the solution of the *i*-th node. The functions *ceil* and *floor* round the function argument to the nearest integer towards, respectively, plus and minus infinity. The addition of the closed half-space constraints given by Eq. (1.44) to the existing constraints preserves the convexity of the feasible domain, and therefore a global optimal solution is still computed for any sub-problem.

The current best integer feasible solution found is called the incumbent. The incumbent is updated whenever a better integer feasible solution is found.

A node, and the corresponding problem $\boldsymbol{P_i}$, is said to be fully investigated, and therefore it has no sub-problems deserving investigation, when one among the following conditions holds:

1. $\boldsymbol{P_i}$ has an integer feasible solution, which becomes the current incumbent;
2. the constraints defining $\boldsymbol{P_i}$ make it infeasible;
3. the lower bound on the minimum of $\boldsymbol{P_i}$ is greater than the minimum provided by the current incumbent, and therefore the addition of further constraints would not allow reducing the cost. This condition is called bounding.

This procedures ensures systematically discarding non-promising sub-problems, hopeless in achieving optimality for $\boldsymbol{P}$. The last two conditions are typically implemented by computing the lower bound on the $\boldsymbol{Pi}$ minimum as the minimum of the continuous relaxation of problem $\boldsymbol{P_i}$. The branching is performed until all the nodes have been fully investigated, and therefore no more new sub-problems can be generated.

A key issue in the development of an efficient branch-and-bound method, ensuring the computation of the actual optimum, is to provide the lower bound on the problem $\boldsymbol{P_i}$ minimum. The more reliable the lower bound, the higher the number of analysed sub-problems and the faster the algorithm convergence rate.

When applied to the minimization of nonlinear convex problem, such as the one stated in Eq. (1.37), such a technique ensures the convergence to the exact optimal global solution within a finite and reduced number of steps [LI 2006]. Other algorithms have been proposed to solve convex MINLP, such as Extended Cutting Plane method, Outer Approximation, Generalized Benders Decomposition, Branch-and-Cut [LI 2006]. Nevertheless the analysis of the most suitable approach goes beyond the scope of this thesis.

A first method application demonstrating the method effectiveness is proposed in Chapter 4 with reference to a simulated lumped parameter system. Further experimental evidence is provided in Chapter 7, where effective discrete modifications of a laboratory test-rig are computed and applied. Also, in Chapter 7, different rules for the selection of the branching variable are applied and discussed.

Chapter 2. Comparative applications of the method based on the system mass and stiffness matrices on simulated test cases

In order to prove the effectiveness of the method proposed in the first Section of Chapter 1, it is applied to two examples of mechanical systems. The first one is a lumped parameter three-mass system, while the second one comprises both distributed and lumped parameter components. Beam finite elements are adopted to model such a second system. The two systems are sketched in Figs. 2.1 and 2.2.

In addition, in order to highlight the features of the proposed method and to asses its performances, a comparison is proposed with the outcomes of the methods described in [LIANGSHENG 2003] and in [SIVAN 1997], applied to achieve identical modifications target of the first mechanical system.

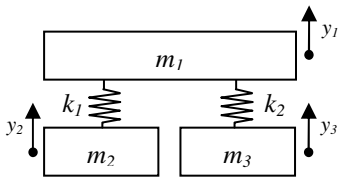

Fig. 2.1 Lumped parameter system.

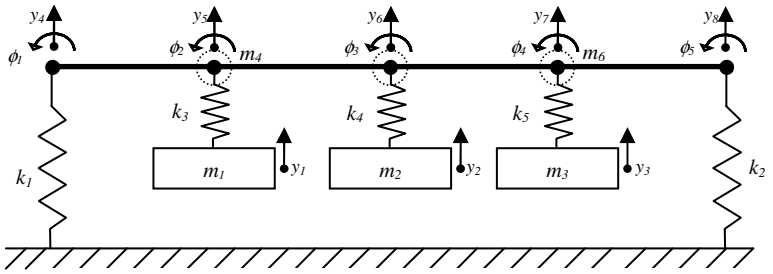

Fig. 2.2 Distributed-and-lumped parameter system.

The convex problem stated in Eq. 1.20 has been solved by means of the efficient numerical algorithm proposed in [GRANT 2008] and [GRANT 2010], which is suitable for solving large scale convex problems.

2.1. Lumped parameter system

The lumped parameter system is a three-dof system with three masses and two springs. The inertial and elastic parameters of the system, which are the modifiable parameters, are listed in the third column of Table 2.1, while the original system eigenstructure is shown in Table 2.2.

Two investigations are carried out to demonstrate the effectiveness of the proposed method: in the first investigation one vibration mode is assigned to the system, while in the second investigation the target is to assign the complete three-mode eigenstructure. For the sake of comparison, the well established methods presented in [LIANGSHENG 2003] and in [SIVAN 1997] have been applied. Henceforth, they will be referred to as respectively “method B1”, and “method B2”.

Thanks to its general nature, the proposed method can be applied to both the investigations. On the contrary, method B2 cannot be applied to the first investigation (single mode assignment), since it imposes the complete three-mode eigenstructure to be defined for the assignment. Method B1 cannot instead be employed in the second investigation, since it requires an equal number of modifiable parameters and system equations.

Nonetheless, these benchmark methods have been chosen being probably the most relevant appearing in literature, among those making use of system

complete models, showing promising results in their original papers. In particular, method B2 is the sole approach specifically aimed at the simultaneous assignment of the complete eigenstructure. It also ensures the system physical feasibility, by applying non negative constraints on masses and stiffnesses.

As far as method B1 is concerned, it is targeted to the simultaneous modification of masses and stiffnesses for assigning a reduced subset of modes, starting from the complete system model expressed in physical coordinates. Nonetheless, the number of assigned modes is not arbitrary since it is strictly related to the system model dimensions and to the number of design variables. Additionally, no constraints ensure the physical and technical feasibility of the solution.

Table 2.1
Lumped parameter system properties.

	Original values	Constraints
m_1 [kg]	$m_{1,0}$=45	[-45,∞)
m_2 [kg]	$m_{2,0}$=25	[-25,∞)
m_3 [kg]	$m_{3,0}$=25	[-25,∞)
k_1 [kN/m]	$k_{1,0}$=2.50e3	[-2.5e3,∞)
k_2 [kN/m]	$k_{2,0}$=2.50e3	[-2.5e3,∞)

Table 2.2
Original system eigenstructure.

Mode number (i)	1	2	3
$u_i(1)$	1.0	0	-1.1
$u_i(2)$	1.0	1.0	1.0
$u_i(3)$	1.0	-1.0	1.0
f_i [Hz]	0	50.33	73.13

2.1.1. Single mode assignment

The goal is to assign a vibration mode with the mode shape $\mathbf{u} = \{-2, 1.5, 1.0\}^{\mathrm{T}}$ at f_1=50 Hz ($\omega_1=2\pi f_1$). The eigenvector of the original system

whose natural frequency is closest to 50 Hz is reported in the second column of Table 2.2: the cosine of the angle between such an eigenvector and the desired one is 0.1313.

In order to properly apply method B1, four modification parameters have to be chosen among the five available, since four problem equations can be written. The parameters selected for modification are the values of the masses m_1, m_2 and the stiffnesses of the springs k_1 and k_2: $\mathbf{x} = \{\Delta m_1, \Delta m_2, \Delta k_1, \Delta k_2\}^{\mathrm{T}}$. Coherently, the same parameters are assumed modifiable when applying the method proposed in this paper. Additionally, for the proposed method, the regularisation operator $\mathbf{\Omega}_{\mathbf{x}} = diag(m_{1,0}^{-1}, m_{2,0}^{-1}, k_{1,0}^{-1}, k_{2,0}^{-1})$ has been chosen in order to equally weigh parameter percentage modifications with respect to their original values. Finally, it has been taken $\lambda = 1e8$ and $\beta = 3$ (see Eqs. 1.13, 1.14 and 1.17) and the feasible solution set Γ has been constrained by only posing lower bounds coinciding with the initial values of the variables. Such a choice prevents getting physically meaningless solutions (see second column of Table 2.1).

Method B1 yields the modification shown in the first row of Table 2.3, while the proposed method generates the results shown in the second row of Table 2.3. It immediately arises that method B1 leads to a physically meaningless solution. Other solutions might be achieved through a different normalization of the eigenvector (e.g. setting $\mathbf{u}^* = 0.05\mathbf{u}$ yields $m_1 = 58.93$, $m_2 = 61.90$, $k_1 = 2.62e6$, $k_2 = 0.82e6$). Nonetheless such an influence of the eigenvector normalization on the result is a major drawback of method B1.

The proposed method leads instead to modifications which are concurrently feasible and very effective, since the cosine between the desired eigenvector and the one of the modified system is 1.0000, and the natural frequency differs from the desired one by just 7.08*e*-3 Hz.

Table 2.3
Parameter modifications for the single mode assignment.

	m_1 [kg]	m_2 [kg]	k_1 [kN/m]	k_2 [kN/m]
Method B1	45 – 43.1	25 - 39.10	2.5*e*3 - 3.096*e*3	2.5*e*3 - 1.678*e*3
Proposed Method	45 - 8.32	25 + 6.79	2.5*e*3 - 1.151*e*3	2.5*e*3 - 1.667*e*3

2.1.2. Complete eigenstructure assignment

In this investigation, a complete eigenstructure (see Table 2.4) is assigned. It is also assumed that all the system parameters can be modified, which leads to five problem unknowns collected in the unknown vector $\mathbf{x} \in \mathbb{R}^5$, $\mathbf{x} = \{\Delta m_1, \Delta m_2, \Delta m_3, \Delta k_1, \Delta k_2\}^{\mathbf{T}}$.

A comparison is carried out with the method B2. A proper comparison makes it necessary to choose a feasible solution set overlapping the solution set of method B2 (non-negative modifiable parameters). To this purpose it has been set $\Gamma=[\mathbf{x_{min}},+\infty)$, where $\mathbf{x_{min}} = -\{m_{1,0}, m_{2,0}, m_{3,0}, k_{1,0}, k_{2,0}\}^{\mathrm{T}}$. Additionally, it has been taken $\mathbf{\Omega_x} = diag(m_{1,0}^{-1}, m_{2,0}^{-1}, m_{3,0}^{-1}, k_{1,0}^{-1}, k_{2,0}^{-1})$, $\lambda = 1e9$ and each Rayleigh equation in the problem formulation has been weighed with $\beta = 2$.

The first two rows in Table 2.5 summarize the results achieved by applying the two methods. Similarly, the rows 1, 2, 4 and 5 in Table 2.6 show the differences between the desired eigenstructure and the eigenstructures computed

through the two methods. The discrepancies are shown in terms of both natural frequencies and cosines between mode shapes. Clearly, both methods lead to physically realizable systems: the masses and the stiffnesses of the modified systems are all positive. Nonetheless, the inertial and stiffness parameters computed through method B2 appear quite undersized and hence unconvincing. Additionally even in terms of cosines and natural frequencies method B2 appears less effective.

A different choice of the norm of the mode shape can considerably improve method B2 performances. As an example, by applying method B2 after normalizing the desired eigenvectors with respect to the mass matrix of the original system, the results shown in Table 2.5 (third row, referred to as method B2') and in Table 2.6 (third and sixth row) can be achieved. The interested reader should refer to the next section to check the values taken by the matrices $\mathbf{\Phi}$ and $\mathbf{\Phi}''$ (defined according to [SIVAN 1997]) in both investigations made using method B2.

It should be noticed that, contrary to method B2, the method proposed in this paper is not affected by the desired mode shape normalization, and therefore it does not require a priori knowledge of the goal system inertial characteristics, which is an important advantage.

Table 2.4
Desired eigenstructure.

Mode number	*1*	*2*	*3*
$u_i(1)$	1.0	1.0	-2.0
$u_i(2)$	1.0	6.5	1.5
$u_i(3)$	1.0	-8.0	1.0
f_i [Hz]	0	32	50

Table 2.5
System modifications for the complete eigenstructure assignment.

	m_1 [kg]	m_2 [kg]	m_3 [kg]	k_1 [kN/m]	k_2 [kN/m]
Method B2	45 - 44.78	25 - 24.96	25 - 24.98	2.5*e*3 - 2.497*e*3	2.5*e*3 - 2.499*e*3
Proposed Method (PM)	45 - 4.23	25 + 5.74	25 + 3.89	2.5*e*3 - 1.149*e*3	2.5*e*3 - 1.459*e*3
Method B2'	45 - 6.81	25 + 3.82	25 + 1.32	2.5*e*3 - 1.217*e*3	2.5*e*3 - 1.564*e*3

Table 2.6
Eigenstructure comparison.

Mode number, i	*1*	*2*	*3*
$\cos(\mathbf{u}_i, \mathbf{u}_i^{B2})$	1	0.8849	0.7866
$\cos(\mathbf{u}_i, \mathbf{u}_i^{PM})$	1	0.9996	0.9990
$\cos(\mathbf{u}_i, \mathbf{u}_i^{B2'})$	1	0.9996	0.9989
$f_i - f_i^{B2}$ (Hz)	0	-4.459*e*0	4.594*e*0
$f_i - f_i^{PM}$ (Hz)	0	4.741*e*-1	-1.942*e*-1
$f_i - f_i^{B2'}$ (Hz)	0	5.612*e*-1	-1.235*e*-1

2.1.3. Method B2 relevant matrices

By applying method B2 to the investigation described in Section 2.1.2, without the normalisation of the desired eigenstructure with respect to the original system mass matrix, the following holds:

$$\mathbf{\Phi} = \begin{bmatrix} 1.5361 & 0.0922 & 1.5101 \\ 2.8608 & 2.5979 & 3.0687 \\ 2.9803 & 6.4012 & 2.6407 \end{bmatrix} \qquad \mathbf{\Phi}'' = \begin{bmatrix} 1.9112 & -0.3078 & -0.9494 \\ 1.9112 & -1.4423 & 4.3148 \\ 1.9112 & 7.1286 & 1.5364 \end{bmatrix}$$

With desired eigenstructure normalisation with respect to the original system mass matrix, it holds:

$$\mathbf{\Phi} = \begin{bmatrix} 0.1026 & 0.0192 & -0.1237 \\ 0.1026 & 0.1251 & 0.0928 \\ 0.1026 & -0.1539 & 0.0619 \end{bmatrix} \qquad \mathbf{\Phi}'' = \begin{bmatrix} 0.1035 & 0.0145 & -0.1235 \\ 0.1035 & 0.1178 & 0.1006 \\ 0.1035 & -0.1500 & 0.0691 \end{bmatrix}$$

2.2. Distributed-and-lumped parameter system

The aim of this test is to validate the proposed modal optimisation method on the design of a complicated system, which includes finite elements (and therefore a non-diagonal mass matrix and non-triangular stiffness matrix), an arbitrary number of design variables (also including interrelated modifications)

and different kinds of constraints (also relating non-homogeneous variables). It should be noticed that none of the previously adopted benchmark methods can be employed in this test case.

The distributed-and-lumped parameter system considered is shown in Fig. 2.2. It consists of a beam and three concentrated masses (m_1, m_2, m_3) connected to the beam through three linear springs (k_3, k_4, k_5). The beam is modeled through four Euler-Bernoulli beam finite elements. Two linear springs k_1 and k_2 also connect the external tips of the first and fourth beams to the frame. The adopted system model leads to thirteen dofs. The inertial and elastic characteristics of the system are summarized in the third column of Table 2.7. Such a system may be thought of as a simplified representation of a linear vibratory feeder, similar to those typically employed in the food industry. As a matter of fact, the beam represents the feeder tray, while the concentrated masses represent the external electromagnetic actuator masses.

In this test case it is assumed that system modifications also include distributed parameters (i.e. the beam bending stiffness EJ and the beam linear mass density ρA). In addition, all the lumped masses and all the springs are modifiable and it is assumed that three further nodal masses (m_4, m_5, m_6) can be added (they are represented in Fig. 2.2 by the circles in dotted lines). The relative distances between the springs are instead set constant and equal to 0.5 m.

Both box constraints on each modifiable variable and a constraint on two interrelated modifications are employed. In other words, lower and upper bounds are imposed in the optimisation problem for each variable modification $\Gamma_1 = \{\mathbf{x}:\ \mathbf{x}_{\min} \le \mathbf{x} \le \mathbf{x}_{\max}\}$, as well as limits on the ratio between ρA and EJ

$\left(\frac{\rho A}{EJ}\right)_{\min} \le \frac{\rho A}{EJ} \le \left(\frac{\rho A}{EJ}\right)_{\max}$, which should be typically bounded by realistic values.

Hence, the feasible domain is $\Gamma_2 = \left\{\Gamma_1 \cap \left\{\left(\frac{\rho A}{EJ}\right)_{\min} \le \frac{\rho A}{EJ} \le \left(\frac{\rho A}{EJ}\right)_{\max}\right\}\right\}$. The values of the bounds for the mass and stiffness modifications and for the $\frac{\rho A}{EJ}$ ratio are stated in the fourth column of Table 2.7.

The regularisation operator has been selected to penalize the modifications of the beam properties more than the modifications of the other parameters, and, at the same time, to favour modifications of the masses m_1, m_2, m_3. In order to account for the different magnitude of the components of **x**, the weights of the modifications (i.e. the entries of $\mathbf{\Omega}_\mathbf{x}$) have been normalized with respect to their original value (e.g. $k_{i,0}$, i=1,...,5, or $m_{j,0}$, j=1,...,3, $(\rho A)_0$, $(EJ)_0$) or to their largest allowed modification when the original value was equal to zero ($m_{j,max}$, j=4,...,6). There follows that $\mathbf{\Omega}_\mathbf{x} = diag(\frac{\mathbf{w}}{\|\mathbf{w}\|_2})$, where vector **w** has been chosen as follows:

$$\mathbf{w} = \left\{k_{1,0}^{-1}, k_{2,0}^{-1}, k_{3,0}^{-1}, k_{4,0}^{-1}, k_{5,0}^{-1}, 0.01m_{1,0}^{-1}, 0.01m_{2,0}^{-1}, 0.01m_{3,0}^{-1}, m_{4,max}^{-1}, m_{5,max}^{-1}, m_{6,max}^{-1}, (\rho A)_0^{-1}, (EJ)_0^{-1}\right\}.$$

The regularisation parameter selected is λ=1e3.

The structural modification goal is to assign to the system a vibration mode at 50 Hz with the mode shape reported in the third column of Table 2.8. Basically, only identical translations of the nodes of the beams (*u(1)*, *u(3)*, *u(5)*, *u(7)*, *u(9)*) are desired, while the rotations of the nodes (*u(2)*, *u(4)*, *u(6)*, *u(8)*, *u(10)*) should be prevented, and the opposite movements of the concentrated masses m_1, m_2, m_3 (*u(11)*, *u(12)*, *u(13)*) should be kept lower than the node displacements. The uniform translation of the beam at the excitation frequency

ensures a uniform product flow along the tray. Such a goal is coherent with the typical design specifications of linear vibratory feeders, which are operated under a single-harmonic oscillatory forced motion whose excitation frequency is constant and is usually close to 50 or 60 Hz [VAN DEN BERG 2004].

The choice of this assignment test, together with the definition of the design parameters, leads to fourteen equations and thirteen unknowns, which are listed in the second column of Table 2.8. Clearly, it might be possible to apply the method proposed with a different choice of system parameters subjected to redesign: the method can be applied regardless of the number of modifiable parameters.

The mode shape of the original system eigenvector with the highest participation factor at 50 Hz is shown in the second column of Table 2.8, together with its natural frequency. It is also depicted in Fig. 2.3, where the relative displacements between the concentrated masses m_1, m_2, m_3 have been magnified ten times in order to provide a clearer representation, and the thin lines are employed to show the system undeformed configuration.

The parameter modification obtained through the method proposed are listed in the fifth column of Table 2.7: as requested, each modification is feasible, as well as the $\frac{\rho A}{EJ}$ ratio. As one could expect, the solution provided is on the lower bound of the $\frac{\rho A}{EJ}$ ratio, i.e., a very stiff and light beam is needed. What it is worth noticing is the not trivial way to achieve the best $\frac{\rho A}{EJ}$ ratio: the computed

solution suggests boosting the reduction of the beam linear density (so as to reach its lower bound), rather than increasing the beam bending stiffness.

The fourth column of Table 2.8 reports the vibration mode of the system computed through the method proposed in this paper. The mode shape is also depicted in Fig. 2.4. Three criteria are adopted to assess the effectiveness of the method proposed: the comparison among the modes of the original, modified and desired systems, the cosines of the angles δ between eigenvectors, and the difference between the natural frequencies. These data are collected in Table 2.9. It can be noticed that both the eigenvector and the eigenvalue specifications are considerably missed in the original system, while the mode of the modified system almost coincides with the desired one. Implementative details are provided in the next subsection.

Table 2.7
Properties and modifications of the distributed-and-lumped parameter system.

	Unknowns	Original values	Constraints	Modified values
k_1 [kN/m]	x(1)	1.0	[-0.8,1.0*e*4]	1.0 + 311
k_2 [kN/m]	x(2)	1.0	[-0.8,1.0*e*4]	1.0 + 311
k_3 [kN/m]	x(3)	8.7*e*2	[-7.0*e*2,8.7*e*2]	8.7*e*2 – 2.65*e*2
k_4 [kN/m]	x(4)	8.7*e*2	[-7.0*e*2,8.7*e*2]	8.7*e*2 – 2.65*e*2
k_5 [kN/m]	x(5)	8.7*e*2	[-7.0*e*2,8.7*e*2]	8.7*e*2 – 2.65*e*2
m_1 [kg]	x(6)	25	[0,5]	25 + 0.00
m_2 [kg]	x(7)	25	[0,5]	25 + 0.00
m_3 [kg]	x(8)	25	[0,5]	25 + 0.00
m_4 [kg]	x(9)	-	[0,2]	1.80
m_5 [kg]	x(10)	-	[0,2]	1.80
m_6 [kg]	x(11)	-	[0,2]	1.80
EJ [Nm^2]	x(12)	4.5*e*5	[-0.9*e*5,0.9*e*5]	4.5e5 - 0.29*e*5
ρA [kg/m]	x(13)	15.8	[-3.16,3.16]	15.8 - 3.16
$\rho A/EJ$ [kg/(Nm^3)]		3.51*e*-5	[3.0*e*-5,2.5*e*-3]	3.0*e*-5

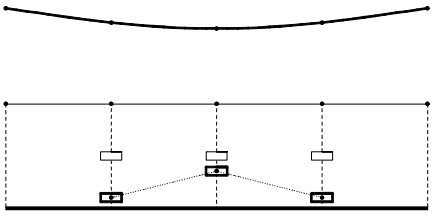

Fig. 2.3 Original mode shape at 53.74 Hz.

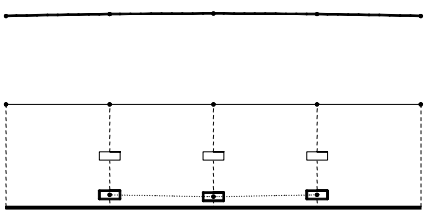

Fig. 2.4 Modified mode shape at 49.98 Hz.

Table 2.8
Eigenstructure comparison.

	Original	Desired	Modified
u(1)	0.4572	0.4337	0.4266
u(2)	-0.1461	0	0.0258
u(3)	0.3887	0.4337	0.4362
u(4)	-0.1097	0	0.0128
u(5)	0.3599	0.4337	0.4394
u(6)	0	0	0
u(7)	0.3887	0.4337	0.4362
u(8)	0.1097	0	-0.0128
u(9)	0.4572	0.4337	0.4266
u(10)	0.1461	0	-0.0258
u(11)	-0.1709	- 0.1408	-0.1418
u(12)	-0.1582	- 0.1408	-0.1429
u(13)	-0.1709	- 0.1408	-0.1429
f_1 [Hz]	53.74	50.00	49.98

Table 2.9
Aggregated evaluation parameters.

	Original system	Modified system
cos(δ)	0.9618	0.9991
Δf_1 [Hz]	3.74	0.02

2.2.1 Implementative details on the application of the method proposed to the distributed-and-lumped parameter system

The system mass and stiffness matrices are obtained by assembling the mass and stiffness matrices of the four beam finite elements ($\mathbf{M}^{FE}$ and $\mathbf{K}^{FE}$) and those of the lumped masses and stiffnesses ($\mathbf{M}^{L}$ and $\mathbf{K}^{L}$):

$$\mathbf{M} = \mathbf{M}^{L} + \mathbf{M}^{FE}$$
$$\mathbf{K} = \mathbf{K}^{L} + \mathbf{K}^{FE} \tag{2.1}$$

As far as the contributions of the lumped masses and stiffnesses is concerned, the following matrices have been adopted:

$$\mathbf{M}^L = \sum_{s\in\psi} m_s \mathbf{C}_s^M \quad \text{where} \quad \mathbf{C}_s^M = \left[c_{ij}^M \right] = \begin{cases} c_{ss}^M = 1 \\ c_{ij}^M = 0 \quad elsewhere \end{cases} \tag{2.2}$$

and

$$\mathbf{K}^L = \sum_{\substack{d,r\in\phi \\ r\neq d}} k_{dr} \mathbf{C}_{dr}^K \quad \text{where}$$

$$\mathbf{C}_{dr}^K = \left[c_{ij}^K \right] = \begin{cases} c_{dd}^K = c_{rr}^K = 1 \\ c_{dr}^K = c_{rd}^K = -1 \\ c_{ij}^K = 0 \qquad elsewhere \end{cases} \tag{2.3}$$

In (2.2) ψ denotes the set of six concentrated masses and the index *s* refers to the related degrees of freedom. Similarly, in (2.3) ϕ denotes the set of degrees of freedom *r* and *d* connected through the five concentrated springs.

As far as the distributed masses and stiffnesses is concerned:

$$\begin{aligned} \mathbf{M}^{FE} &= \sum_{e\in\zeta} (\mathbf{M}_{Aug}^{Beam})_e \\ \mathbf{K}^{FE} &= \sum_{e\in\zeta} (\mathbf{K}_{Aug}^{Beam})_e \end{aligned} \tag{2.4}$$

where ζ denotes the set of beam finite elements adopted, while $\mathbf{M}_{Aug}^{Beam}$ and $\mathbf{K}_{Aug}^{Beam}$ are the augmented mass and stiffness matrices of each beam element. Such matrices are attained by augmenting the element matrices with a suitable number of null entries.

Similarly, the modification matrices can be expressed as the sum of two contributions:

$$\Delta\mathbf{M} = \Delta\mathbf{M}^{L} + \Delta\mathbf{M}^{FE}$$
$$\Delta\mathbf{K} = \Delta\mathbf{K}^{L} + \Delta\mathbf{K}^{FE} \tag{2.5}$$

Which leads to the following decomposition of matrix $\tilde{\mathbf{U}} = \left[\tilde{\mathbf{U}}^{L}, \tilde{\mathbf{U}}^{FE}\right]$ (see Eq. 1.10). The contribution of the lumped mass and stiffness, $\tilde{\mathbf{U}}^{L}$, can be written as follows:

$$\tilde{\mathbf{U}}^{L} = \left[\tilde{U}_{ij}^{L}\right] = \begin{cases} u(r) - u(i) & x(j) = \Delta k_s^{ir} \\ \omega^2 u(i) & x(j) = \Delta m_s^{i} \\ 0 & elsewhere \end{cases} \tag{2.6}$$

where the scalars Δm and Δk are the parameter modification $\left(\Delta m, \Delta k \in \mathbf{x}\right)$ adopted in the formulation of $\Delta\mathbf{M}^{L}$ and $\Delta\mathbf{K}^{L}$:

$$\Delta\mathbf{M}^{L} = \sum_{s\in\psi} \Delta m_s \mathbf{C}_s^{M}$$
$$\Delta\mathbf{K}^{L} = \sum_{\substack{d,r\in\phi \\ d\neq r}} \Delta k_{dr} \mathbf{C}_{dr}^{K} \tag{2.7}$$

The contribution of the modification of the finite elements, $\tilde{\mathbf{U}}^{FE}$, can in turn be separated into the terms due to the modification of ρA and those related to the modification of EJ, $\tilde{\mathbf{U}}^{FE} := \left[\tilde{\mathbf{U}}^{\rho A}, \tilde{\mathbf{U}}^{EJ}\right]$, where

$$\tilde{\mathbf{U}}^{\rho A} = \omega^2 \sum_{e=1}^{4} \frac{\partial\left(\Delta\mathbf{M}_{Aug}^{Beam}\right)_e}{\partial\left(\rho A\right)}\mathbf{u} \in \mathbb{R}^{10\times 1} \tag{2.8}$$

$$\tilde{\mathbf{U}}^{EJ} = -\sum_{b=1}^{4} \frac{\partial(\Delta\mathbf{K}_{Aug}^{Beam})_e}{\partial\left(EJ\right)}\mathbf{u} \in \mathbb{R}^{10\times 1} \tag{2.9}$$

Similarly with Eq. (2.4), the matrices $\Delta\mathbf{M}_{Aug}^{Beam}$ and $\Delta\mathbf{K}_{Aug}^{Beam}$ are attained by augmenting the mass and stiffness modification matrices of each beam element ($\Delta\mathbf{M}^{Beam}$ and $\Delta\mathbf{K}^{Beam}$) with a suitable number of null entries. In particular, in this

example the Euler-Bernoulli formulation has been adopted, and the axial flexibility has been neglected. Which leads to the following derivatives:

$$\frac{\partial(\Delta \mathbf{M}^{Beam})}{\partial(\rho A)} = \frac{L_e}{420}\begin{bmatrix} 156 & 22L_e & 54 & -13L_e \\ 22L_e & 4L_e^2 & 13L_e & -3L_e^2 \\ 54 & 13L_e & 156 & -22L_e \\ -13L & -3L_e^2 & -22L_e & 4L_e^2 \end{bmatrix} \tag{2.10}$$

$$\frac{\partial(\Delta \mathbf{K}^{Beam})}{\partial(EJ)} = \begin{bmatrix} \frac{12}{L_e^3} & \frac{6}{L_e^2} & -\frac{12}{L_e^3} & \frac{6}{L_e^2} \\ \frac{6}{L_e^2} & \frac{4}{L_e} & -\frac{6}{L_e^2} & \frac{2}{L_e} \\ -\frac{12}{L_e^3} & -\frac{6}{L_e^2} & \frac{12}{L_e^3} & -\frac{6}{L_e^2} \\ \frac{6}{L_e^2} & \frac{2}{L_e} & -\frac{6}{L_e^2} & \frac{4}{L_e} \end{bmatrix} \tag{2.11}$$

where L_e is the length of the finite element considered.

Chapter 3. Application of the method based on the system Frequency Responses on simulated test cases

3.1. Simulated test-case

In order to assess numerically the effectiveness of the method proposed in the second Section of Chapter 1, it has been firstly applied to the modification of the vibrating system sketched in Figure 3.1. It is a five-degree-of-freedom system with five lumped masses (m_i, i=1,…,5), each one connected to the rigid ground through springs k_{gi} (i=1,…,5) and to the contiguous masses through springs k_{ij} ($i \neq j$). The values of the original system parameters are listed in the first row of Table 3.1, where the same stiffness value k_g has been assumed for all the ground springs k_{gi}.

Table 3.1: System parameter nominal values and modification bounds

	k_{12} [N/m]	k_{23} [N/m]	k_{34} [N/m]	k_{45} [N/m]	k_g [N/m]	m_1 [kg]	m_2 [kg]	m_3 [kg]	m_4 [kg]	m_5 [kg]
Nominal	7.36e4	6.82e4	7.35e4	8.21e4	9.89e4	1.73	5.12	8.21	2.61	1.34
Modification lower bound	-	-	-	-	0	0	0	0	0	0
Modification upper bound	-	-	-	-	4.83e5	2	2	2	2	2

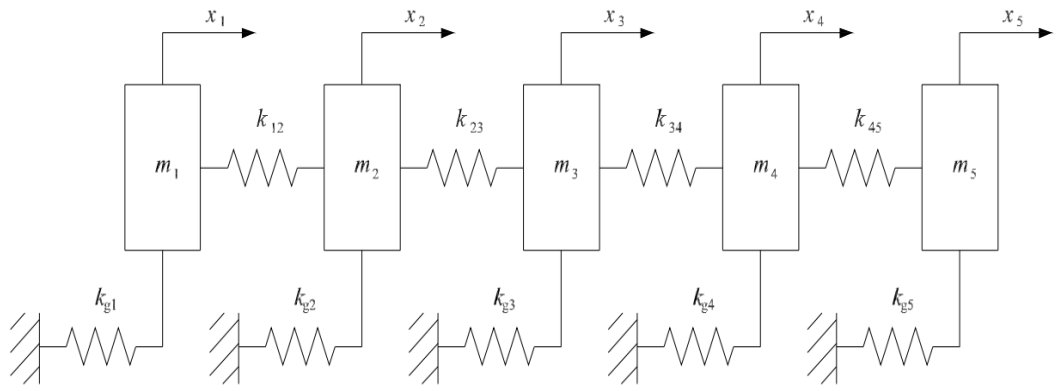

Figure 3.1: Simulated 5-dof system

3.2. Benchmark method description

In order to highlight the effectiveness and the ease of implementation of the proposed approach, also in the presence of uncertainty affecting the system parameters, a comparison is made with the results of the well established technique proposed by Braun and Ram in [BRAUN 2001]. Such a method, henceforth referred to as "method BR", has been chosen being the one showing the most promising results among those reported in literature making use of incomplete experimental data. In addition, it can also account for inequality constraints, so as to ensure the physical feasibility of the solution. All these features meet those of the method proposed in this work, and therefore make it suitable for comparison. As it has been quoted in the introductive literature review, method BR takes advantage of the left and right eigenvectors extracted from the measured frequency responses for attaining general results of the structural modification problem. In the comparison proposed, the left and right eigenvector extraction has been performed through the technique proposed in [BUCHER 1997] by Braun and Bucher, as it is suggested in [BRAUN 2001].

Though very effective, the chosen benchmark method has some drawbacks. On the one hand, the extraction of the system left eigenvectors requires acquiring FRFs over a wider spectrum and is intrinsically ill-conditioned [BUCHER 1997]. On the other hand, in order to calculate reliable eigenvectors, regularisation techniques need to be employed, which in general are based on the knowledge of the system mass matrix. However, the system mass may be often only approximately known or may be even unknown. In method BR the knowledge of the mass matrix is implicitly required also in the computation of

parameter modifications, since the approach is based on mass normalized eigenvectors. In contrast, the method proposed in this paper relies only on the frequency responses of the original system, without requiring the estimation of the mass matrix.

3.3. Modification objectives and constraints

The goal of this investigation is to assign the two vibration modes listed in Table 3.2 at frequencies f_1 and f_2 (with $\omega_h = 2\pi f_h$). All the masses and the five grounded springs are assumed to be modifiable. This leads to ten problem unknowns. The feasible domain Γ has been set by defining lower and upper bounds on each modifiable parameter, as listed in the third and the fourth rows of Table 3.1. Since the masses and the stiffnesses of the original system may not be known in the application of the proposed method, the lowest bounds of the parameter modifications ensuring a physically realizable system could be unknown. In this numerical investigation this is simply tackled by not allowing negative modifications, i.e. reduction of the original masses and stiffnesses. Indeed, allowing only positive modifications of the system parameters ensures that the modified system makes sense from a physical point of view. The same bounds have been adopted also in the application of method BR. Finally, the original system eigenstructure is presented in Table 3.3. It should be noticed that both the eigenvector and the eigenvalue to be assigned are considerably different from those of the original system dynamics.

Table 3.2: Desired igenstructure

Mode number, h	1	2
f_h [Hz]	39.00	55.00
$u_h(1)$	1.00	0
$u_h(2)$	-0.55	0.01
$u_h(3)$	0.2	-0.10
$u_h(4)$	0	0.80
$u_h(5)$	0.05	1.00

Table 3.3: Original system eigenstructure

Mode number, i	1	2	3	4	5
f_i [Hz]	22.28	32.61	42.94	52.74	64.59
$u_i(1)$	0.357	0.736	0.094	1.000	0.003
$u_i(2)$	0.673	1.000	0.060	-0.234	-0.004
$u_i(3)$	1.000	-0.418	-0.217	0.025	0.032
$u_i(4)$	0.460	-0.337	1.000	-0.008	-0.482
$u_i(5)$	0.244	-0.222	0.983	-0.019	1.000

3.4. Application of the methods: results and discussion

For the numerical application of the proposed method, the system FRFs have been computed by inverting matrix $\left[\omega_h^2\mathbf{M}-\mathbf{K}\right]$ at the natural frequencies of the desired modes ω_1 and ω_2.

The parameters α_1 and α_2 in Eq. (1.30) have been set equal to 1 in order to impose the two vibration modes with the same level of concern. Such a choice allows reproducing the same operating conditions of method BR. For the same reason, $\mathbf{\Omega_x}$ has been selected so as to equally weigh the percentage modifications of all the modifiable parameters: $\mathbf{\Omega_x} = diag(\mathbf{w}/\|\mathbf{w}\|_2)$, where $\mathbf{w} = \left\{m_1^{-1}, m_2^{-1}, m_3^{-1}, m_4^{-1}, m_5^{-1}, k_{g1}^{-1}, k_{g2}^{-1}, k_{g3}^{-1}, k_{g4}^{-1}, k_{g5}^{-1}\right\}$. Finally, it has been set $\lambda = 1e-3$. With such choices, the proposed method yields the modifications listed in the second column of Table 3.4.

Table 3.4: System modifications

	Proposed method	Method BR
m_1 [kg]	1.723 + 1.816	1.723 + 1.907
m_2 [kg]	5.123 + 1.495	5.123 + 2.000
m_3 [kg]	8.214 + 0.808	8.214 + 0.000
m_4 [kg]	2.609 + 0.000	2.609 + 0.953
m_5 [kg]	1.334 + 0.878	1.334 + 0.000
k_{g1} [kN/m]	98.94 + 0	98.94 + 5.294
k_{g2} [kN/m]	98.94 + 11.94	98.94 + 28.43
k_{g3} [kN/m]	98.94 + 0.00	98.94 + 78.16
k_{g4} [kN/m]	98.94 + 153.20	98.94 + 264.22
k_{g5} [kN/m]	98.94 + 149.69	98.94 + 44.13
$\left\|\boldsymbol{\Omega}_x\mathbf{x}\right\|_2^2$	5.79	8.74

Table 3.5: Modified mode shapes and eigenstructure comparison

Modified system mode number, i	Proposed method					Method BR				
	1	2	**3**	**4**	5	1	2	**3**	**4**	5
f_i [Hz]	21.62	28.89	**39.07**	**55.02**	68.97	24.47	31.82	**38.99**	**54.93**	70.55
$u_i(1)$	0.585	1.000	**1.000**	**-0.003**	-0.001	0.801	-0.848	**1.000**	**-0.003**	0.000
$u_i(2)$	0.853	0.759	**-0.558**	**0.009**	0.004	1.000	-0.375	**-0.547**	**0.011**	-0.002
$u_i(3)$	1.000	-0.693	**0.116**	**-0.071**	-0.051	0.614	1.000	**0.192**	**-0.090**	0.026
$u_i(4)$	0.219	-0.172	**0.039**	**0.801**	1.000	0.113	0.218	**0.055**	**0.799**	-0.463
$u_i(5)$	0.002	-0.055	**0.016**	**1.000**	-0.957	0.048	0.104	**0.031**	**1.000**	1.000
Desired mode number, h	-	-	**1**	**2**	-	-	-	**1**	**2**	-
$\lvert f_h - f_i \rvert$ [Hz]	-	-	**0.068**	**0.020**	-	-	-	**0.014**	**0.066**	-
$\cos(u_i, u_h)$	-	-	**0.9964**	**0.9997**	-	-	-	**0.9987**	**1.0000**	-

For the application of method BR the unmodified system eigenstructure has to be extracted from the system FRFs. In this work, such frequency responses are computed numerically by inverting matrix $\left[\omega^2\mathbf{M}-\mathbf{K}\right]$ at five selected frequencies, and therefore the effect of noise and disturbances is only marginal. As a consequence, the application of the method proposed in [BUCHER 1997] leads to an exact eigenvector computation regardless of the frequencies at which the FRFs are evaluated. On the other hand, the selection of the evaluation frequencies has great importance when dealing with experimental, and hence noisy, receptances: it may cause a wrong eigenvector extraction. The solution

computed through the application of method BR is listed in the third column of Table 3.4.

The eigenstructures of the systems obtained by applying the modifications in Table 3.4 are collected in Table 3.5.

A set of indexes is useful to compare the performances of the two methods:

- the solution $\mathbf{\Omega}_x$-norm, shown in the last row of Table 3.4;
- the difference between the desired and the attained natural frequency of each assigned mode, shown in the second last row of Table 3.5;
- the cosine between the desired eigenvector and the attained one of each assigned mode, shown in the last row of Table 3.5.

It is apparent that the proposed method provides effective results, comparable with those of method BR. It should be noticed that the $\mathbf{\Omega}_x$-norm of the solution calculated through the proposed method is smaller, as a consequence of the regularisation term included in the problem. Small values of the solution $\mathbf{\Omega}_x$-norm indicate that a minor amount of modifications is required, which is usually important from a technical and economic point of view. Other remarkable advantages of the proposed method are that it is not affected by the ill-conditioning of the eigenstructure extraction [BUCHER 1997], and that no knowledge of the original physical model is needed. On the contrary, since method BR requires knowing the system mass matrix, the solution computed through method BR is quite sensitive to the uncertainty affecting the knowledge of the system mass matrix. In order to assess such sensitivity, a statistical analysis has been carried out by perturbing all the mass matrix entries with an uncertainty

term. In particular, uniform-distributed random values have been added to the mass elements. Each value ranges independently from -5% to 5% of the nominal value. Then 500,000 system modification attempts with the identical task have been carried out. The effectiveness of method BR considerably decreases with such a level of uncertainty. On average, the uncertainty impact on the method performance is mainly reflected by the natural frequency mismatches: their mean absolute values are 0.165 Hz and 0.143 Hz respectively for the first and the second desired natural frequencies. It is worth highlighting that mass matrix uncertainty has no impact on the performance of the method proposed in this Thesis, since the method is based solely on the system receptances.

As a further proof of the results attained, Figure 3.2 shows the absolute values of the frequency responses $\mathbf{H}_{i,5}(\omega)$ (i=1,…,5) of the original system (dotted line) and of the systems modified according to both the proposed method (solid line) and the BR method (dashed line). It is evident that both methods can modify the system so as to attain natural frequencies which are very close to those of the desired modes.

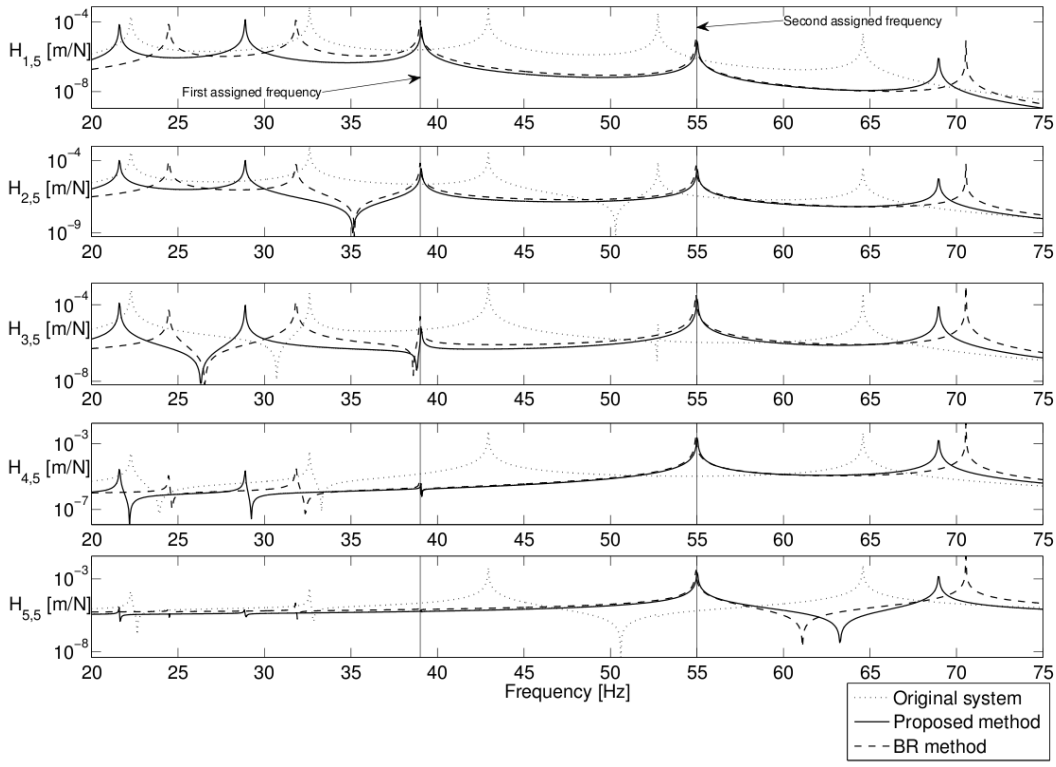

Figure 3.2: Frequency response comparison

Chapter 4. Comparative application of the method allowing for discrete modifications

In this chapter the method described in the fourth section of Chapter 1 is applied to a three degree-of-freedom system. Such method is based on the system spatial model and allows for discrete modifications. A comparison is carried out with the results provided by the method based on the same model data (i.e. the system spatial model) but yielding real modifications. This chapter is organised as follows: a brief description of the simulated system and of the modification objective are firstly given. Then, the solution of the modification problem is sought for in the mathematical set of real numbers. Finally, the solution of the modification problem is sought for in the integer field by means of the Branch and Bound technique. Each step of the Branch and Bound techniques is illustrated.

4.1 System description and modification problem

The mechanical system consists in three vibrating masses connected through two springs, and is shown in Figure 4.1. The values of the system parameters are listed in the second column of Table 4.1.

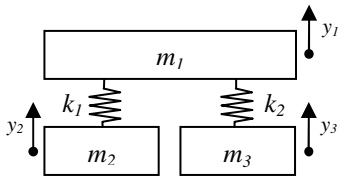

Figure 4.1: Simulated vibrating system

Table 4.1: system properties and constraints.

	Original value	Lower bound	Upper bound
m_1 [kg]	45	-10	10
m_2[kg]	32	0	10
m_3[kg]	32	0	10
k_1[N/m]	2.5*e*6	-2.25*e*6	1.25*e*6
k_2[N/m]	2.5*e*6	-2.25*e*6	1.25*e*6

In this example, it is desired to assign to the system the eigenvector $\mathbf{u} = \{-1.5, 1, 0.5\}^{\mathrm{T}}$ at the natural frequency of 60 Hz. All the system parameters are assumed modifiable, and the modification values are constrained by the lower and upper bound listed respectively in the third and in the fourth column of Table 4.1. In order to prove the effectiveness of the proposed method, the system masses are also constrained to assume only integer values.

4.2 Solution of the problem within the field of real numbers

A set of effective modifications are firstly computed by means of the method described in the second section of Chapter 1. With reference to objective function $g(\chi) = \left\| \mathbf{U}\chi - \mathbf{b} \right\|_2^2 + \lambda \left\| \mathbf{\Omega}_\chi \chi \right\|_2^2$, it has been set $\lambda = 1$ and $\mathbf{\Omega}_\chi = \left\{ m_1^{-1}, m_2^{-1}, m_3^{-1}, k_1^{-1}, k_2^{-1} \right\}$. Such a choice allows equally weighing the percentage modification of the parameters. The solution provided is listed in the penultimate row of Table 4.2.

The effectiveness of such a solution can be evaluated by means of the following parameters:

- The value of the function $g(\chi)$ at the computed solution;
- The difference δf between the achieved and the desired natural frequencies;

- The cosine cos(φ) of the angle φ between the achieved and desired eigenvectors.

For the computed modifications, such indexes are listed in the penultimate row of Table 4.3.

Clearly, the computed solution is very effective, since both the natural frequency and the eigenvector shape perfectly match the desired ones. However, the computed modifications are real values which do not respect the integer constraints on the masses, and therefore may be impossible to realize in an industrial context. An integer solution must be therefore sought for.

4.3 Integer solution of the problem

4.3.1 Complete solution enumeration

The optimal integer solution of the problem described in section 4.1 cannot be obtained by simply rounding the continuous optimal modification of each discrete variable to the nearest integer, since rounded solutions can be significantly far from the optimality [LI 2006]. The complete solution enumeration ensures computing the optimal integer solution. Nevertheless, such an approach becomes infeasible as the number of unknowns increases. In this modification problem, the complete solution enumeration consists in solving 2541 optimisation problems, and subsequently in choosing the solution providing the smallest among the minima of the objective function. In each of the 2541 optimisation problems the integer values of the mass modifications are set and the stiffness modifications are unknown. The computed optimum is listed in the last row of Table 4.2, and its effectiveness, though lower, is comparable with that of

the real solution, as proved by the set of indexes provided in the last row of Table 4.3. It is evident that such a solution cannot be obtained by simply rounding the variables of the optimal solution to the nearest integer, even in such a low-scale problem.

Table 4.2: Optimal solutions

	δm_1 [kg]	δm_2 [kg]	δm_3 [kg]	δk_1 [kN/m]	δk_2 [kN/m]
Real	-6.755	5.612	7.509	-3.61e2	-1.096e3
Integer	-7	5	8	-3.97e2	-1.079e3

Table 4.3: Solution effectiveness

	$\boldsymbol{g(\chi)}$	$cos(\varphi)$	δf [Hz]
Real	0.3208	1.000	0.000
Integer	0.3223	1.000	0.000

4.3.2 Partial solution enumeration

As pointed out in the previous section, the complete solution enumeration becomes infeasible in usual problems. Thanks to the convexity of continuous relaxation of the modification problem, the partial solution enumeration allows providing the integer optimum with a lower number of function evaluation. In this section, such partial solution enumeration is performed by means of the Branch and Bound algorithm. As far as the branching rule adopted, the selection of the branching variable has been done on the basis of the variable index: the branching variable is the one with the lowest index among those not having an integer value (Lowest-Index-First). Also, in each bounding phase, the lower bound on the optimum of the discrete function has been set equal to the optimum of the continuous relaxation of the respective constrained problem. Of course, it is expected that the application of the Branch and Bound technique yields the same result of the complete enumeration in a lower number of evaluated solutions.

The application of the Branch and Bound technique for the partial solution enumeration yields the solution listed in the last row of Table 4.2, whose effectiveness can be evaluated by means of the indexes in the last row of Table 4.3. As expected, the optimal integer modifications are those provided also through the complete solution enumerations. On the contrary, the solution computation required only seven steps (and hence, the solution of only seven optimisation problems). Details about each step of the Branch and Bound technique are listed in Table 4.4. The complete tree of the technique application is shown in Figure 4.2. It is noteworthy that, even if at the node $\boldsymbol{P_5}$ an integer solution was provided, the algorithm proceeded by branching node $\boldsymbol{P_4}$, according to the Branch and Bound rules, since $\boldsymbol{P_4}$ Objective Function (O.F.) was lower.

Table 4.4: Branch and bound application

Node	δm_1 [kg]	δm_2 [kg]	δm_3 [kg]	δk_1 [kN/m]	δk_2 [kN/m]	O.F.
$\boldsymbol{P_1}$	-6.755	5.612	7.509	-3.62*e*2	-1.096*e*3	0.3208
$\boldsymbol{P_2}$	-7	5.346	7.309	-3.77*e*2	-1.103*e*3	0.3213
$\boldsymbol{P_3}$	-6	6.475	8.051	-3.13*e*2	-1.077*e*3	0.3228
$\boldsymbol{P_4}$	-7.149	5	7.554	-3.97 *e*2	-1.095*e*3	0.3213
$\boldsymbol{P_5}$	-7	6	6	-3.40*e*2	-1.150*e*3	0.3247
$\boldsymbol{P_6}$	-7.333	5	7	-3.97*e*2	-1.114*e*3	0.3228
$\boldsymbol{P_7}$	**-7**	**5**	**8**	**-3.97*e*2**	**-1.079*e*3**	**0.3223**

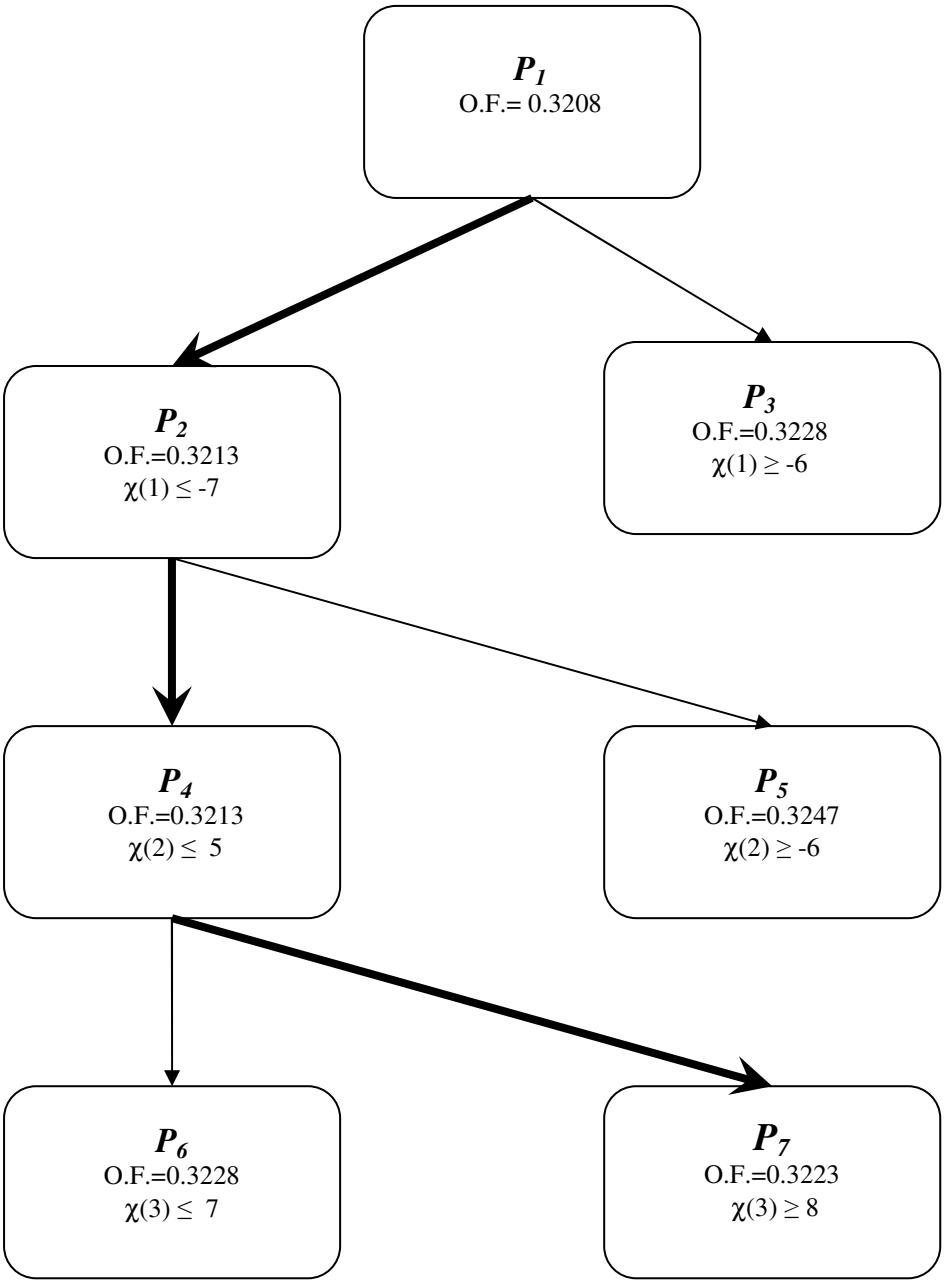

Figure 4.2: Branch and Boud tree

Chapter 5. Design of an industrial linear feeder by means of a spatial model based structural modification method

5.1 Device description

The theory developed in the second section of Chapter 1 has been applied to an industrial device similar to the one shown in Figure 5.1. Such a device is a linear feeder commonly employed in the food packaging industry. It consists of a steel tray which is actuated by inertial electromagnetic exciters. This type of device exploits the vibrations of the feeder tray to make the transported items continuously impact with the tray itself, and hence carried from the back tip to the front tip of the tray, in conformity with the tray vibration direction.

The steel tray is strengthened with an aluminium beam, which is connected to each of the actuators by means of leaf springs. The stiffness of the leaf springs can be varied by choosing the number of plastic plates of each leaf spring stack. The tray is also connected to a steel U-beam through a variable number of suspension units allowing movement in both the horizontal and the vertical directions. Finally, the U-beam is mounted on two steel legs, in order to set the device at the proper working height.

The device configuration can be changed by adding or removing electromagnetic exciters and suspension units, and by altering the inertial properties of the exciters and the stiffness of the leaf springs employed in the electromagnetic exciters.

Figure 5.1: Example of short length linear feeder

A frequency response survey has been carried out on the system in a configuration employing three exciters. The acceleration of twelve points along the tray has been measured in working condition. Subsequently, the system frequency responses, with reference to the same aforementioned twelve points along the tray, have been acquired through a series of impact tests. Such frequency response functions permitted the extraction of the system vibration modes. In particular, truncated vibration modes, with reference to the sole twelve measurements points, have been extracted by peak picking [EWINS 1994].

Experimental evidence shows that the dynamic behaviour of such devices is dominated by just one of the system vibration modes. Figure 5.2, in fact, perfect overlapping between the system vibration mode at 39.37 Hz (pictured in solid line) and the tray oscillation (pictured in dashed line) in working condition at 38.76 Hz. Both the eigenvector and the vector collecting the forced vibration amplitudes have been normalised so that their norm is unitary. As a matter of fact, the cosine between the two vectors is 0.9998.

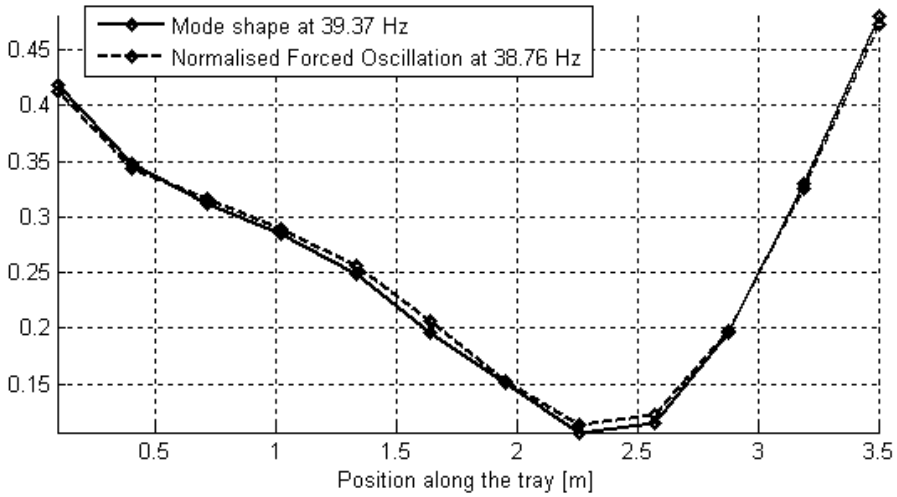

Figure 5.2: Mode shape and forced vibration distribution along the tray

5.2 Single-mode excitation

The reason for this peculiar behaviour is the shape of the forcing vector **f** in the system dynamic equilibrium equation $\mathbf{M}\ddot{\mathbf{x}} + \mathbf{K}\mathbf{x} = \mathbf{f}$. Since such a forcing vector is nearly parallel to one of the system modes, it follows that generally speaking the system dynamic behaviour is dominated by a single mode, which will be called "the dominating mode". In fact, the response **x** can be written as:

$$\mathbf{x} = \left(\mathbf{K} - \omega^2\mathbf{M}\right)^{-1}\mathbf{f} \tag{5.1}$$

where

$$\left(\mathbf{K} - \omega^2\mathbf{M}\right)^{-1} = \mathbf{\Phi} diag\left(\frac{1}{\omega_i^2 - \omega^2}\right)\mathbf{\Phi}^{\mathbf{T}}, \quad i = 1..n \tag{5.2}$$

Clearly, if **f** is parallel to any of the left eigenvectors of the system $\mathbf{l}_j$, ($\mathbf{f} = \alpha\mathbf{l}_j$), the following holds

$$\mathbf{x} = \mathbf{\Phi} diag\left(\frac{1}{\omega_i^2 - \omega^2}\right)\mathbf{\Phi}^{\mathbf{T}}\alpha\mathbf{l}_j = \frac{\boldsymbol{\varphi}_j\alpha}{\omega_j^2 - \omega^2} \tag{5.3}$$

thanks to the orthonormality relationship between the left and the right system eigenvectors

$$\mathbf{l}_j^T \boldsymbol{\varphi}_i = \delta_{ij} \tag{5.4}$$

Eq. (5.3) shows that the system dynamic response is participated by only one vibration mode, regardless of the excitation frequency, if the excitation force vector **f** is parallel to any of the system left eigenvectors.

Such a parallelism condition is hard to attain in systems in which only a limited number of degrees of freedom is actuated, nonetheless it is possible to achieve very similar conditions when the forcing term is nearly parallel to a system right eigenvector. In this case, the closer the excitation frequency to the vibration mode natural frequency, the higher the participation factor of the mode with respect to the participation factor of the remaining modes.

Numerical simulations on lumped- and distributed- parameter systems recalling linear feeders confirm that not only for excitation frequencies close to the natural frequency of the dominating mode, but also quite far from it (but still avoiding other natural frequencies) the system response is dominated by the working mode.

As a first example, let us consider the lumped parameter system in Figure 5.3. The system parameters and the system eigenstructure are listed respectively in Table 5.1 and Table 5.2. Figure 5.4 shows the ratio between the modal participation factors of the highest frequency mode and the most excited among the other modes, with the excitation vector $\mathbf{f} = \{3, -1, -1, -1\}^T$. Such a forcing vector recalls the typical excitation vector in linear feeders and, as a matter of fact, is mainly spanned by the highest frequency mode shape, as is evident from the cosines (listed in Table 5.3) between the forcing vector f and the system eigenvectors.

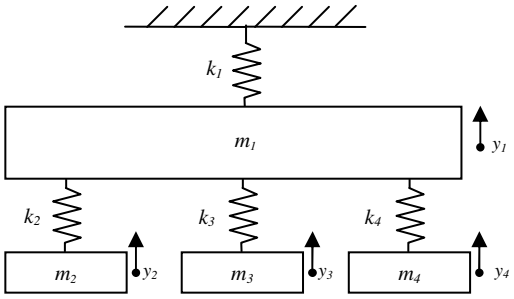

Figure 5.3: Lumped parameter system

Table 5.1: Lumped system parameters	
m_1 [kg]	10
m_2 [kg]	3
m_3 [kg]	3
m_4 [kg]	3
k_1 [kN/m]	10
k_2 [kN/m]	100
k_3[kN/m]	100
k_4 [kN/m]	100

Table 5.2: Lumped paramete system eigenstructure.

Mode number	1	2	3	4
u(1)	0.4941	0.0000	0.0000	-0.4668
u(2)	0.5020	-0.5774	-0.5026	0.5106
u(3)	0.5020	0.7887	-0.3059	0.5106
u(4)	0.5020	-0.2113	0.8086	0.5106
f [Hz]	3.6376	29.058	29.058	40.207

Table 5.3: Force vector projections

Eigenvector, i	cos(**f**,**u**$_i$)
1	0.0068
2	4.2e-17
3	1.1e-16
4	0.8465

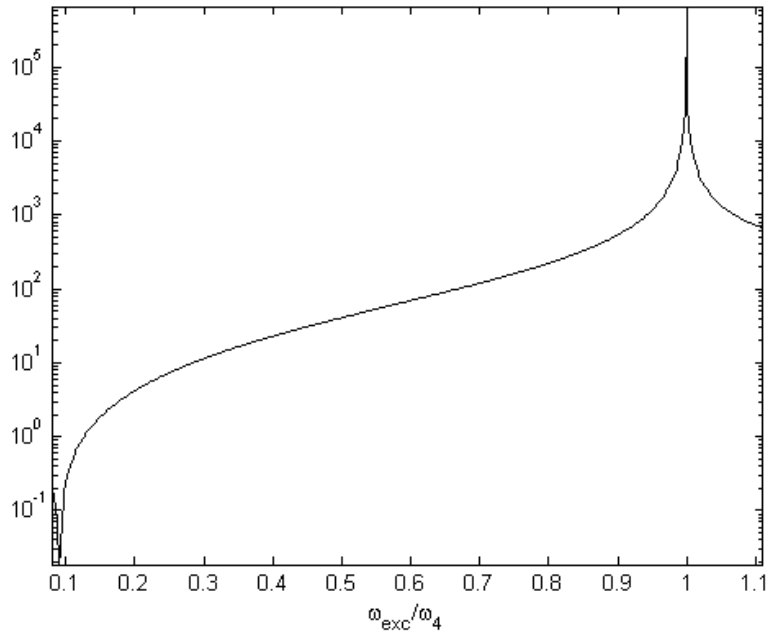

Figure 5.4: Ratio between modal participation factors

Clearly, at the fourth system natural frequency ($\omega_{exc}/\omega_4 = 1$) the dominant mode is the fourth. Also, as one could expect, at the other system natural frequencies the contribution of the fourth vibration mode is usually negligible with respect to the most participated mode. It is also significant that in a very wide range of frequencies the most excited mode is the fourth, even when other natural frequencies are much closer to the excitation frequency than the fourth system natural frequency. It must be highlighted that, for this peculiar case of perfectly symmetric system and under such excitation conditions, the contributions of the second and of the third vibration modes is always null, as a consequence of the cosines listed in Table 5.3. Nonetheless, such a perfectly symmetric system can represent very well systems with up to 5% uncertainty on each system parameter.

As a second example, the system in Figure 5.5 is considered. Its characteristics and its natural frequencies are shown respectively in Table 5.4 and in the second column of Table 5.5. Let us assume the excitation vector to be

$\mathbf{f} = \{0,0,1,0,1,0,1,0,0,0,-1,-1,-1\}^{\mathrm{T}}$ (i.e., electromagnetic forces are exchanged at the connecting points). Also in this case vector **f** is mainly spanned by a sole eigenvector, namely the fifth system eigenvector (cosines between vector f and the eigenvectors are listed in the third column of Table 5.5). As a consequence, the fifth vibration mode is the dominating mode in a very wide range of frequencies, as is it evident in Figure 5.6, which shows the ratio between the modal participation vectors of the fifth vibration mode and the most participating among the other system modes.

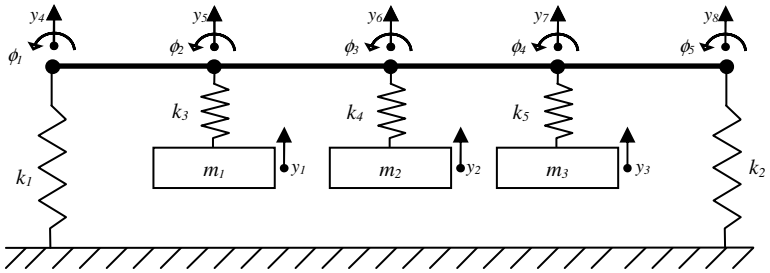

Figure 5.5: Distributed-and-lumped parameter system

Table 5.4: Properties of the distributed-and-lumped parameter system.

k_1 [kN/m]	1.0
k_2 [kN/m]	1.0
k_3 [kN/m]	8.7*e*2
k_4 [kN/m]	8.7*e*2
k_5 [kN/m]	8.7*e*2
m_1 [kg]	25
m_2 [kg]	25
m_3 [kg]	25
EJ [Nm^2]	4.5*e*5
ρA [kg/m]	15.8

Table 5.5: Force vector projections

Mode number, i	Natural frequency [Hz]	cos(**f**,**u**$_i$)
1	0.6891	0.0002
2	1.4820	0.0000
3	29.2840	0.0064
4	43.6799	0.0000
5	53.7383	0.6684
6	154.3357	0.0839
7	419.0886	0.0000
8	820.5652	0.0023

All these facts suggest that the optimal design of the device can be attained by imposing the shape of the most participated eigenvector in working condition. Such a shape must reflect the design requirements typical of linear feeders in industrial context.

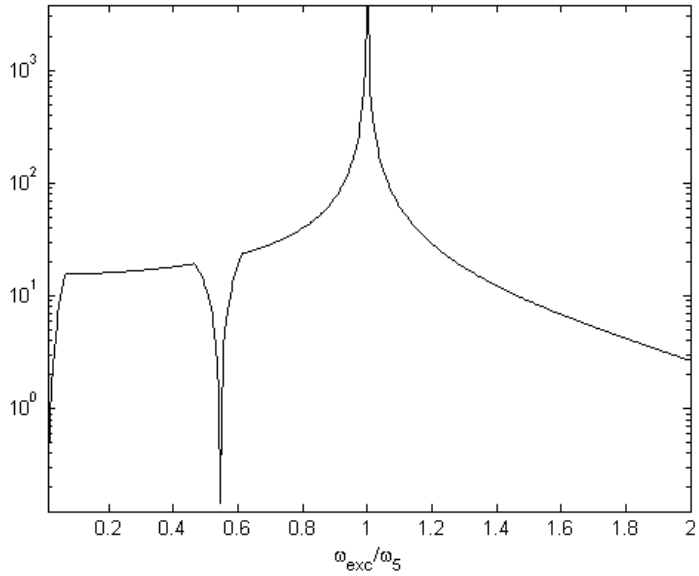

Figure 5.6: Ratio between modal participation factors

5.3 Linear feeder dynamic model

In modelling the vibrating feeder, it has been assumed that the tray can perform a planar motion only in the x-y plane and that the tray is horizontal at rest. Furthermore, it has been assumed that the natural frequencies of the tray longitudinal modes are much higher than the frequency range of interest. Consequently, the dynamic behaviour of the steel tray-strengthening beam has been modelled using both Euler-Bernoulli beam finite elements (as far as the vertical displacements are concerned) and a rigid-body model (as far as the horizontal displacement is concerned). The suspension units have been modelled through both two linear springs acting respectively along the horizontal and the

vertical axes, and a torsion spring. The nodes of the finite element mesh on the tray have been chosen so as to properly collocate the forces acting between the tray, the actuators and the suspension units. The bending stiffness of the finite elements and the stiffness of the springs representing the suspension units have been deduced by means of a comparison between the modelled natural frequencies and those measured through modal testing on a suspended tray in absence of the actuators; the natural frequencies listed in Table 5.6 demonstrate close agreement between the experimental data and the model prediction, and hence, good tuning of the model parameters.

Table 5.6: Tuning of model parameters: natural frequency comparison

Measured Frequency [Hz]	*Modeled Frequency [Hz]*
8.62	8.85
13.12	13.5
29.07	28.02
68.21	68.31
108.87	111.13

As far as the electromagnetic actuators are concerned, preliminary considerations on the axial stiffness of the leaf springs led to the assumption that at the frequency range of interest no relative rotation occurs between each actuator and its connecting points with the tray. As a consequence, each actuator has been given a single degree of freedom with respect to the node on the tray to which it is connected. The degree of freedom considered is the relative displacement of the actuator in the direction of the normal to the leaf spring stacks (Figure 5.7). Hence, the stiffness properties of the leaf springs have been modelled through a linear spring connecting the node on the tray with the actuator centre of mass, which takes account of the inertial properties of the actuator. Therefore, the

motion of the each actuator in the plane x-y is fully described by the set of coordinates (x_1, y_1, ϕ_1, n):

$$\begin{Bmatrix} x_2 \\ y_2 \\ \phi_2 \end{Bmatrix} = \begin{bmatrix} 1 & 0 & \cos(\alpha) & -l\sin(\gamma) \\ 0 & 1 & \sin(\alpha) & l\cos(\gamma) \\ 0 & 0 & 0 & 1 \end{bmatrix} \begin{Bmatrix} x_1 \\ y_1 \\ n \\ \phi_1 \end{Bmatrix} \tag{5.5}$$

where x_1 and y_1 are respectively the horizontal and vertical displacement of the node on the tray, ϕ_1 is the rotation of both the tray node and the actuator and n is the linear spring extension (i.e. the relative displacement), as in Figure 5.8.

Electromagnetic actuators

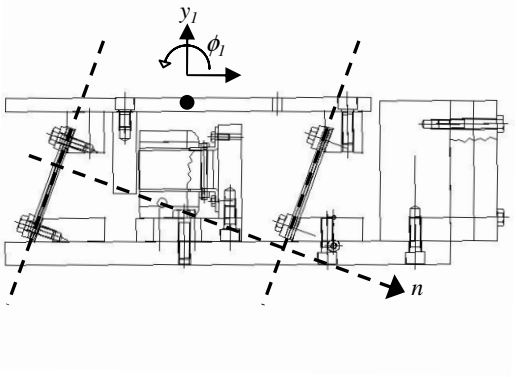

Figure 5.7: Schematic drawing

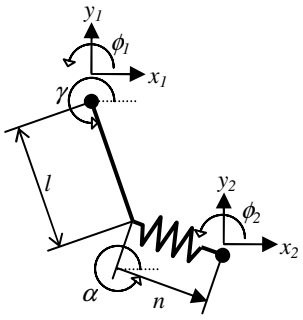

Figure 5.8: Lumped parameter model

With the purpose of a modular implementation in a numerical simulation environment, the following stiffness and mass matrices have been calculated for each electromagnetic actuator, by mean of expression (5.5):

$$\mathbf{K}_{act} = k \begin{bmatrix} 0 & 0 & 0 & 0 \\ 0 & 0 & 0 & 0 \\ 0 & 0 & 1 & 0 \\ 0 & 0 & 0 & 0 \end{bmatrix} \tag{5.6}$$

$$\mathbf{M}_{act} = m\begin{bmatrix} 1 & 0 & \cos(\alpha) & -l\sin(\gamma) \\ 0 & 1 & \sin(\alpha) & l\cos(\gamma) \\ \cos(\alpha) & \sin(\alpha) & 1 & -l\sin(\gamma-\alpha) \\ -l\sin(\gamma) & l\cos(\gamma) & -l\sin(\gamma-\alpha) & l^2 \end{bmatrix} \tag{5.7}$$

where k is the stiffness equivalent to that of the leaf spring stacks and m is the total mass of the electromagnetic actuator. Also, since no relative rotation is assumed to take place between the electromagnetic actuators and their connecting points on the tray, actuator rotational inertia J is added to the rotational inertia of the connecting point on the tray.

Finally, the tray front tip deserves some considerations: its shape is different from the rest of the tray (see the examples in Figure 5.9) and, moreover, it is not strengthened through the aluminium beam. Therefore, the tip inertial and stiffness characteristics have been considered at the end of the aluminium beam. Clearly, a finite element node has been set on such a point.

Figure 5.9: Examples of feeder tips

The implementation of a modular simulator of vibrating feeders in the Matlab programming environment allows to easily evaluate different set up configurations. For the case of a linear feeder with two electromagnetic actuators

and four suspension units, a 23 degree-of-freedom model is provided. Such a model is pictured in Figure 5.10. With reference to Figure 5.10, $y_{1,}\ldots,y_{10}$ are the beam vertical displacements, $\phi_{1,}\ldots,\ \phi_{10}$ are the beam nodal rotation, x_1 is the beam horizontal displacement and n_1 and n_2 are the electromagnetic actuator relative displacements with respect to the connecting point on the tray.

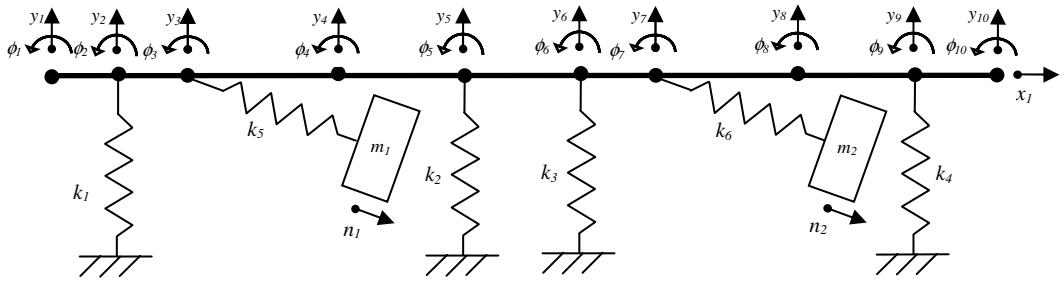

Figure 5.10: Linear feeder simplified model

5.4 Modification calculation

The model described in Section 5.3 has been used to optimally design the vibrating linear feeder by means of the method in the second Section of Chapter 1. The design requirement is to make the transported items advance with a constant speed along most of the tray. In the remaining part, which is the back tip of the tray, transported items are required to advance with a higher speed than the rest of the tray, in order avoid jams between the material feeder and the vibrating tray. Such design requirements are reflected by the desired tray shape shown in dotted line in Figure 5.11, where the desired vibrating amplitude is constant between x = -0.07 and x = 2.85, and is a linear increasing function of the position along the tray between x = 2.85 and x = 3.6. The highest vibrating amplitude is desired on the back tip of the tray, and is 2 times the value of the desired constant amplitude.

The horizontal displacement of the tray has been set on the basis of an optimal value of 20° for the angle between the horizontal and the vertical tray displacements.

In order to achieve the desired dynamic behaviour, the shape in Figure 5.11 has been itself selected as desired mode shape, and coherent values for the relative displacement between the tray and the electromagnetic exciters have been chosen. The natural frequency of the desired mode has been set to 35 Hz, coherently with an excitation frequency possibly used in an industrial context. The desired vibrating mode is listed in the third column of Table 5.9, with reference to the model in Figure 5.10. For the sake of clarity, a different normalisation for the shape of the desired vibrating mode is listed in brackets in the third column of Table 5.9.

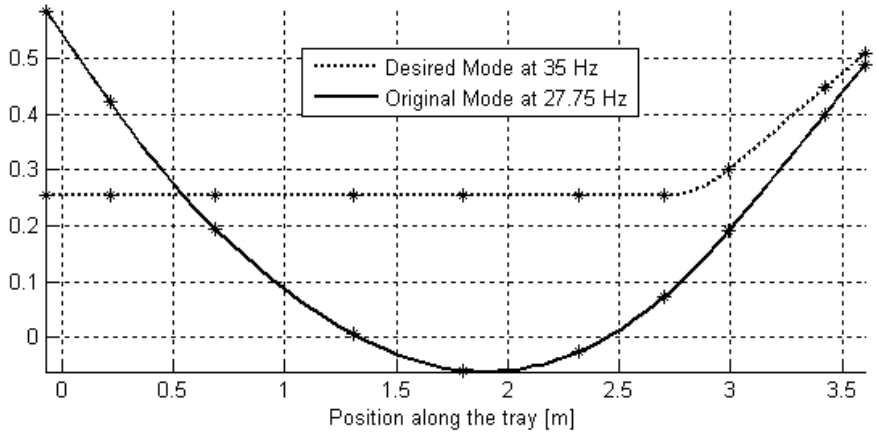

Figure 5.11: Mode shape comparison: desired and first design guess system

In order to demonstrate the capability of the method described in the second section of Chapter 1 in handling both lumped and distributed parameters modifications, the following system parameters have been chosen as modifiable, and collected in the unknown vector **x**:

- the tray equivalent bending stiffness $(EJ)_{Eq}$;
- the tray linear density ρ;
- the stiffness of the suspension units $k_1 \ldots k_4$;
- the mass of the electromagnetic actuators m_1, m_2;
- the stiffness of the leaf springs connecting the tray with the electromagnetic actuators k_5, k_6.

In order to apply the method in the second section of Chapter 1, a first design guess is needed. The first design guess values of the modifiable parameter are listed in the third column of Table 5.7. The tray bending stiffness and the tray linear density at the first design guess are those corresponding to a conventional steel tray strengthened through an aluminium beam of rectangular cross section. Only two suspension units are employed in the first design guess, but a further two more can be connected. Therefore, four suspension units are totally accounted for, but the stiffness of two among them is set to zero. The two electromagnetic actuators are in their base form, i.e. at the minimum weight and their stiffness corresponds to three leaf springs, each provided with a stack of nine plastic plates. Such first guess values yield to a vibrating system whose natural frequencies are partially shown in Table 5.8. The working mode, i.e. the mode with the highest participation factor in the design working condition, is the sixth (listed in the second column of Table 5.9), though its natural frequency lies quite far from the desired natural frequency.

The upper and lower bounds constraining each single parameter and combinations of parameters are shown in the fourth column of Table 5.7. In

particular, the bounds on the distributed parameters (EJ) and (ρA), as well as those on the ratio $\frac{\rho A}{EJ}$, constrain the beam cross section to realistic values.

As to the optimisation parameters, it has been chosen $\mathbf{\Omega}_{\mathbf{x}} = diag(20m_{1,0}^{-1}, 20m_{2,0}^{-1}, 0.1k_{1,0}^{-1}, 0.1k_{2,0}^{-1}, 0.1k_{3,0}^{-1}, 0.1k_{4,0}^{-1}, 2k_{5,0}^{-1}, 2k_{6,0}^{-1}, (EI)_0^{-1}, (\rho A)_0^{-1})$ and $\lambda = 1e9$, where the subscript "0" indicates the first design values of the system parameters, as listed in the third column of Table 5.7. The Rayleigh quotient equation in the problem formulation has been weighed with $\beta = 10$.

Table 5.7: Properties and modifications of the first design guess system.

	Unknowns	Original values	Constraints	Modified values
k_1 [kN/m]	x(1)	1.80*e*2	[-1.80*e*2,0]	1.80*e*2 + 0
k_2 [kN/m]	x(2)	0	[0,1.80*e*2]	0 + 1.80*e*2
k_3 [kN/m]	x(3)	0	[0,1.80*e*2]	0 + 1.80*e*2
k_4 [kN/m]	x(4)	1.80*e*2	[-1.80*e*2,0]	1.80*e*2 + 0
k_5 [kN/m]	x(5)	4.59*e*2	[-3.06*e*2,6.12*e*2]	4.59*e*2 + 0.43*e*2
k_6 [kN/m]	x(6)	4.59*e*2	[-3.06*e*2,6.12*e*2]	4.59*e*2 + 1.86*e*2
m_1 [kg]	x(7)	23	[0,6.05]	23 + 0.85
m_2 [kg]	x(8)	23	[0,6.05]	23 + 1.70
EJ [Nm^2]	x(9)	1.93*e*5	[-6.19*e*4,0]	1.93*e*5 - 6.19*e*4
ρA [kg/m]	x(10)	22.87	[-11.77,0]	22.87 - 11.77
$\rho A/EJ$ [kg/(Nm^3)]		1.18*e*-4	[8.45*e*-5,1.18*e*-4]	8.45*e*-5

Table 5.8: Natural frequencies comparison

Mode number, i	First design system [Hz]	Modified system [Hz]
1	5.5186	8.9584
2	7.0008	13.0692
3	11.1248	13.5709
4	22.1164	24.2713
5	24.4751	28.7661
6	27.7528	34.8396
7	52.3809	54.2614
8	99.2722	102.7709

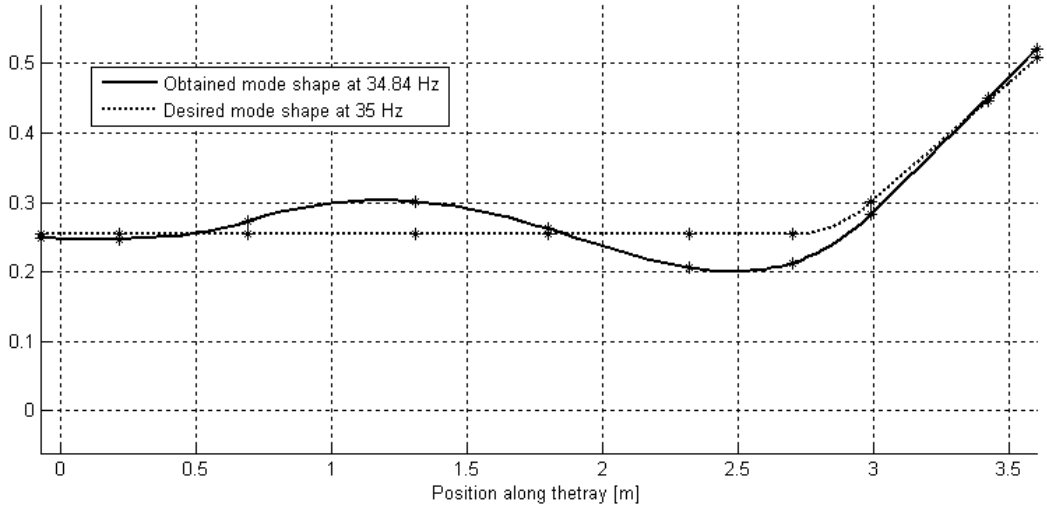

Figure 5.12: Mode shape comparison: desired and obtained

Table 5.9: Working mode comparison.

		First design	Desired	Modified
u(1)	y_1	0.2354	0.1058 (1.000)	0.1003
u(2)	ϕ_1	-0.2319	0	-0.0036
u(3)	y_2	0.1693	0.1058 (1.000)	0.0998
u(4)	ϕ_2	-0.2202	0	0.0032
u(5)	y_3	0.0779	0.1058 (1.000)	0.1102
u(6)	ϕ_3	-0.1534	0	0.0485
u(7)	y_4	0.0024	0.1058 (1.000)	0.1216
u(8)	ϕ_4	-0.0868	0	-0.0127
u(9)	y_5	-0.0236	0.1058 (1.000)	0.1058
u(10)	ϕ_5	-0.0166	0	-0.0472
u(11)	y_6	-0.0099	0.1058 (1.000)	0.0831
u(12)	ϕ_6	-0.0705	0	-0.0257
u(13)	y_7	0.0295	0.1058 (1.000)	0.0861
u(14)	ϕ_7	0.1371	0	0.0510
u(15)	y_8	0.0768	0.1255 (1.1867)	0.1145
u(16)	ϕ_8	0.1901	0.1410 (1.333)	0.1519
u(17)	y_9	0.1609	0.1862 (1.7600)	0.1817
u(18)	ϕ_9	0.1984	0.1410 (1.333)	0.1583
u(19)	y_{10}	0.1967	0.2115 (2.000)	0.2102
u(20)	ϕ_{10}	0.1990	0.1410 (1.333)	0.1591
u(21)	n_1	0.5694	0.5288 (5.000)	0.5283
u(22)	n_2	0.4634	0.6346 (6.000)	0.6309
u(23)	x_1	-0.1626	-0.2906 (-2.748)	-0.2804
f [Hz]		27.75	35.00	34.84
cos(**u**,**u***)		0.8574	1.0000	0.9949
|δf| [Hz]		7.25	0.00	0.16

Application of the optimisation procedure yields the values listed in fifth column of Table 5.7. The system modified according to the computed solution displays the dynamic behaviour whose natural frequencies are listed in the third

column of Table 5.8. The working mode of such a system is listed in the fifth column of Table 5.9. The last two rows of Table 5.9 also collects a set of useful indexes for the evaluation of the results attained. It is noteworthy that the computed solution results in a very close approximation of the desired eigenproperties. The mode shape obtained for the modified system at 34.84 Hz is shown in solid line in Figure 5.12, together with the desired mode shape in dotted line.

5.5 Results and discussion

The physical implementation of the modifications causes some approximations of the computed theoretical solution, in order to conform to the commercial availability of masses and springs. The values applied are listed in the third column of Table 5.10. In particular, the stiffness modifications of the electromagnetic actuators leaf springs have been realized by adding or removing the integer number of standard plastic plates which allows the closest approximation of the theoretical stiffness modification. The same procedure has been followed to calculate the number of mass modules to add to the electromagnetic actuators. The nominal stiffness of each plastic plate spring is 5.10*e*4 kN/m, while the mass of each mass module is 0.165 kg. As far as the stiffness of the suspension units is concerned, the alterations computed are perfectly reflected by the addition two further suspension units. No investigation of the best integer approximation of the continuous solution has been performed, since it is beyond the scope of this experimental validation.

Table 5.10: Computed and applied system modification values

	Computed modifications	Applied modifications
k_1 [kN/m]	0	0
k_2 [kN/m]	1.80e2	1.80e2
k_3 [kN/m]	1.80e2	1.80e2
k_4 [kN/m]	0	0
k_5 [kN/m]	0.43e2	0.51e2
k_6 [kN/m]	1.86e2	2.04e2
m_1 [kg]	0.85	0.78
m_2 [kg]	1.70	1.72
EJ [Nm^2]	6.19e4	6.19e4
ρA [kg/m]	11.77	11.77

The same peak-picking procedure described in the first section of this chapter has been adopted for the partial identification of the modified system eigenstructure. In Table 5.11 a comparison between a choice of some of the measured natural frequencies and the expected ones (computed by means of the system simplified model on the basis of the system values in the third column of Table 5.10) is proposed. Four system vibration modes have been also extracted, and their shapes are shown in dotted line in Figure 5.13. They match almost perfectly the modeled ones, pictured in solid line in Figure 5.13. As far as the desired mode shape at 35 Hz, it is shown in the bottom-left hand side picture of Figure 5.13 in dashed line. With reference to the first design guess, the clear improvement, in the indexes introduced in section 5.3 and listed in the last rows of Table 5.9 (cosine between mode shapes and natural frequency mismatch) confirms that a very good achievement of the goal vibration mode has been attained. In fact, the cosines between the measured mode shape at 35.28 Hz, and the modeled and the desired ones are respectively 0.9964 and 0.9861. Furthermore, the mismatch between the measured natural frequency and the

modeled and the desired ones are only 0.08 Hz and 0.28 Hz, thus confirming the method effectiveness in the design of vibrating devices.

Table 5.11: Natural frequency comparison

Measured Frequency [Hz]	*Modeled Frequency [Hz]*
24.78	24.46
29.42	28.83
35.28	35.20
54.93	54.23

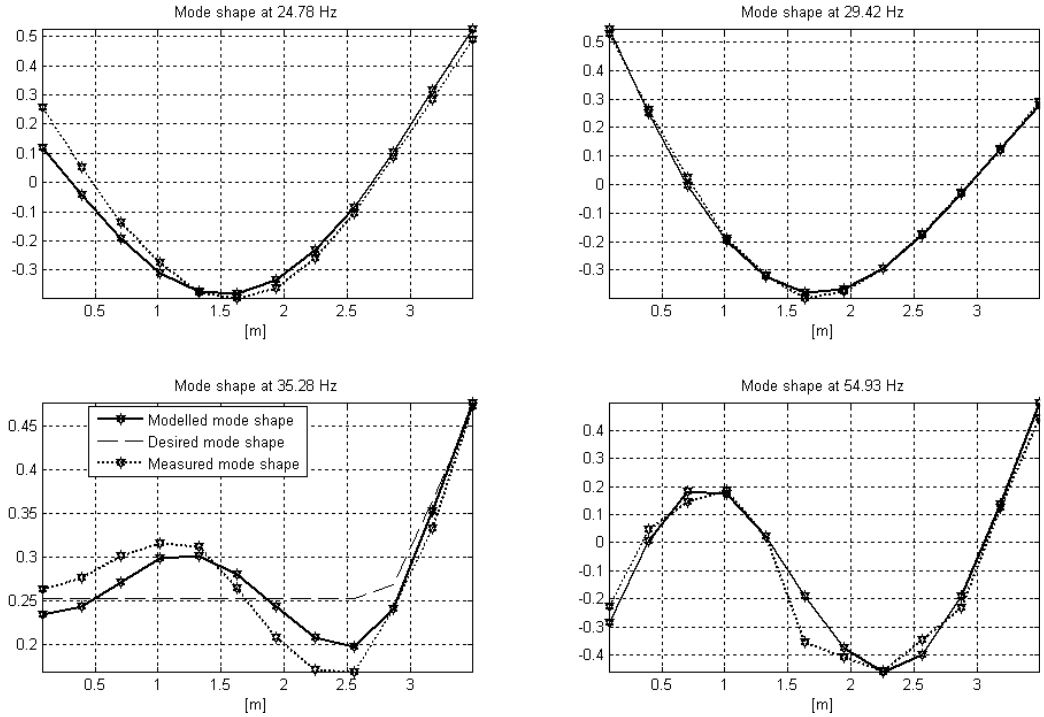

Figure 5.13: Mode shape comparison: modelled and measured mode shapes

Chapter 6. Experimental validation of the method based on the system Frequency Responses

In this chapter the experimental validation of the method proposed in the second Section of Chapter 1 is carried out with reference to a laboratory test-rig.

6.1. Experimental set up

The set up shown in Figure 6.1 has been adopted for the experimental validation of the method proposed in the second section of Chapter 1. It consists of five masses, each one connected to the very rigid test bench by a couple of steel cantilever straight beam springs that provide only bending stiffness. Four additional curved beam springs connect each mass with the contiguous ones. All the beam springs are 50 mm wide. All the other relevant dimensions are shown in the schematic drawing in Figure 6.2, and are nominally equal for all the beams having the same shape.

The modular structure of the test rig allows easy set up extension or reduction, by adding or removing mass-spring subsytems. Each subsystem has been designed in such a way that the lumped masses remain always parallel to the ground during the motion. In fact, the portal frame structure of each subsystem makes the masses move without rotating. Furthermore, the high radius of the curved beam springs allows large amplitude oscillations of the masses without significantly altering the curved beam radius and, hence, the curved beam stiffnesses and linear behavior. All the beams can be modeled as massless lumped springs, since each beam mass and damping are negligible. In addition, the hypothesis of small displacements allows adopting linear spring models.

Therefore, the set up very well represents the undamped 5-dof lumped element system sketched in Figure 6.3.

In this eigenstructure assignment problem, all the lumped masses and grounded springs are modifiable. The eigenstructure of the original system is shown in Table 6.1. It has been

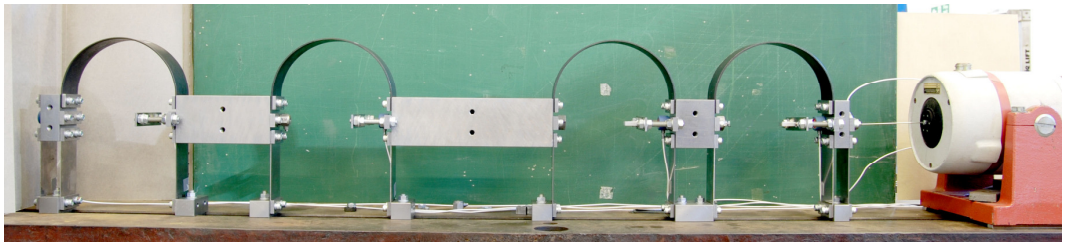

Figure 6.1: Experimental set up

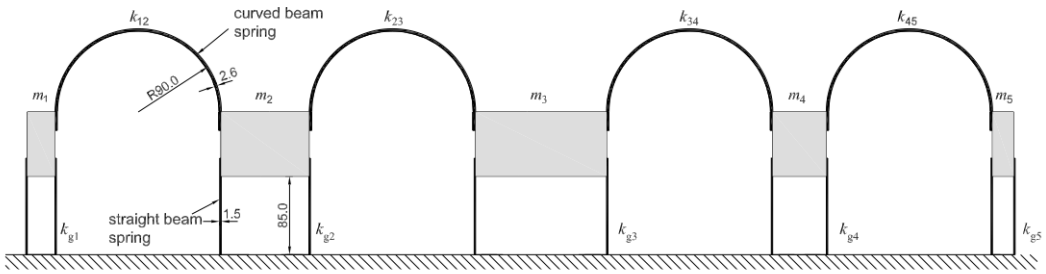

Figure 6.2: Set up significant dimensions [mm]

experimentally identified just for carrying out the comparison with the modified system. The identification has been performed by exciting the system with an electro-dynamic shaker connected to the mass m_5 through a stinger (see Figure 6.1). The shaker employed is a LDS V406, driven by a LDS PA100E power amplifier capable of delivering power up to 147 W to the shaker. The excitation force has been measured by a load cell (PCB 208A02) placed between the mass

m_5 and the stinger. Each mass has been instrumented with a Kistler 8636C50 piezoelectric accelerometer. All the measurements have been recorded by the means of a LMS SCADAS III signal acquisition front-end connected to a PC. The LMS software Test.Lab has been adopted to generate the shaker excitation signal, and to identify the eigenstructure by applying the least squares method in [PEETERS 2004]. The system has been forced with a random excitation over the frequency range 0-100 Hz, which is the interval of interest for the proposed modification task.

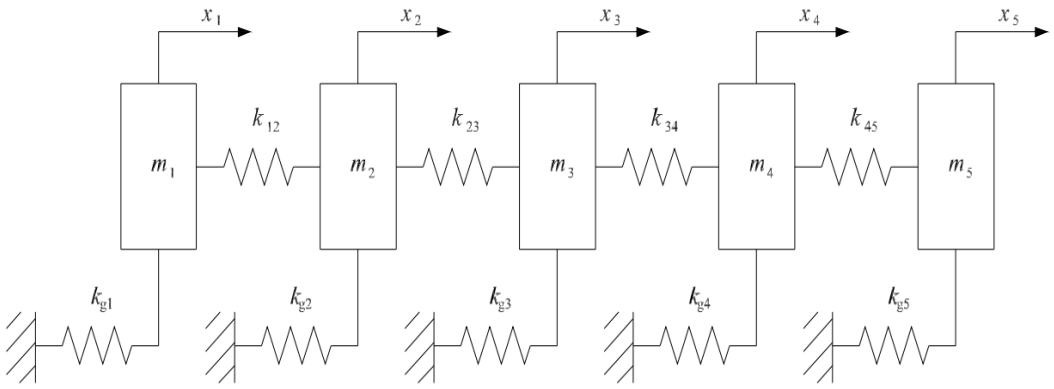

Figure 6.3: Set up model

Table 6.1: Original system eigenstructure

Mode number, *i*	1	2	3	4	5
f_i [Hz]	22.28	32.61	42.94	52.74	64.59
$u_i(1)$	0.391	0.792	0.114	1.000	0.003
$u_i(2)$	0.717	1.000	0.071	-0.249	-0.006
$u_i(3)$	1.000	-0.452	-0.232	0.029	0.038
$u_i(4)$	0.474	-0.404	0.971	-0.011	-0.525
$u_i(5)$	0.233	-0.264	1.000	0.009	1.000

6.2. FRF data acquisition

The application of the method introduced in this paper requires measuring the original system FRFs at the two desired natural frequencies. For this purpose,

a rowing hammer test has been carried out by employing a PCB 086C03 hammer. The measurements of the excitation force as well as of the acceleration of each mass have been acquired through the aforementioned LMS SCADAS III. The software LMS Test.Lab has been adopted to compute the system FRFs. In order to match the hypotheses made in the third section of Chapter 1, the direct use of the rough measured receptances $\mathbf{H}^m(j\omega_h)$ has not been possible. In fact, the unavoidable presence of measurement noise, of structural damping and of nonlinearities introduces complex and non-symmetric terms in the frequency response. Consequently $\mathbf{H}(\omega_h)$ has been calculated from the real and symmetric part of $\mathbf{H}^m(j\omega_h) \in \mathbb{C}^{N\times N}$:

$$\mathbf{H}(\omega_h) = \frac{1}{2}\mathrm{Re}\left(\mathbf{H}^m(j\omega_h) + \mathbf{H}^{m\,\mathrm{T}}(j\omega_h)\right) \tag{6.1}$$

Matrices $\mathbf{H}^m(j\omega_1)$, $\mathbf{H}^m(j\omega_2)$, $\mathbf{H}(\omega_1)$ and $\mathbf{H}(\omega_2)$ are presented in Appendix A.

The norm ratio

$$W_h = \frac{\left\|\mathbf{H}^m(j\omega_h) - \mathbf{H}(\omega_h)\right\|_2}{\left\|\mathbf{H}(\omega_h)\right\|_2} \quad (h=1,2) \tag{6.2}$$

can be taken as a measure of the uncertainty due to the truncated part of the measured receptances. The values attained, (W_1= 0.0295 and W_2=0.0232) prove that the test rig can be correctly modeled as an undamped symmetric system, thus corroborating the hypotheses initially made.

6.3. Design parameter modification

The purpose of the modification is to assign the eigenstructure listed in Table 6.2 and reported in brackets in Table 6.4 ($\omega_h = 2\pi f_h$). Such an eigenstructure is considerably different from that of the original system both in terms of frequencies and mode shapes.

As far as the parameters of the modification problem are concerned, they have been chosen so as to mathematically express both the differing levels of concern about the single eigenpair assignment (which leads to the selection of $\alpha_h, h = 1,2$) and the preferred structural modification strategy (which leads to the selection of $\mathbf{\Omega}_\mathbf{x}$). In detail, it has been set $\alpha_1 = 1$ and $\alpha_2 = 3$, in order to encourage the achievement of the higher frequency mode realization. The regularisation operator has been chosen to penalize the relative modifications of mass m_3 and of stiffnesses k_{g2} and k_{g3}, and to encourage the modifications of masses m_2 and m_4. Specifically it has been set $\mathbf{\Omega}_\mathbf{x} = diag(\mathbf{w} / \|\mathbf{w}\|_2)$, where $\mathbf{w} = \left\{ m_{1,ub}^{-1}, 0.1 m_{2,ub}^{-1}, 100 m_{3,ub}^{-1}, 0.1 m_{4,ub}^{-1}, m_{5,ub}^{-1}, k_{g1,ub}^{-1}, 10 k_{g2,ub}^{-1}, 10 k_{g3,ub}^{-1}, k_{g4,ub}^{-1}, k_{g5,ub}^{-1} \right\}$.

Clearly, a normalization with respect to their upper bound (denoted with the subscript *ub*) has been adopted. The regularisation parameter selected through the L-curve of the unbounded problem is equal to 500.

Table 6.2: Desired eigenstructure

Mode number, *h*	1	2
f_h [Hz]	39.00	55.00
$u_h(1)$	1.00	0
$u_h(2)$	-0.55	0.01
$u_h(3)$	0.2	-0.10
$u_h(4)$	0	0.80
$u_h(5)$	0.05	1.00

Finally, the values in the second and the third columns of Table 6.3 define the lower ($\mathbf{x}_{\min}$) and upper ($\mathbf{x}_{\max}$) bounds of the solution vector **x**. The physical realizability of the modiefied system is ensured by allowing only positive modifications, thus overcoming the lack of knowledge of the values of the original system parameters. The feasible domain is further restricted by adding an upper bound on the total mass modification: $\delta m_1 + \delta m_2 + \delta m_3 + \delta m_4 + \delta m_5 \le \delta m_{\max}$, where $\delta m_{\max} =$ 3 kg. It follows that $\Gamma = \{ \mathbf{x} : \ \mathbf{x}_{\min} \le \mathbf{x} \le \mathbf{x}_{\max} \ \cap \ \{\delta m_1 + \delta m_2 + \delta m_3 + \delta m_4 + \delta m_5 \le \delta m_{\max}\}\}$.

The application of the proposed approach leads to the solution listed in the fourth column of Table 6.3, which is referred to as the computed modifications.

Table 6.3: Modification bounds and values

	Lower bound	Upper bound	Computed modifications	Applied modifications
δm_1 [kg]	0	2	1.375	1.4
δm_2 [kg]	0	2	1.412	1.4
δm_3 [kg]	0	2	0.000	0
δm_4 [kg]	0	2	0.000	0
δm_5 [kg]	0	2	0.053	0
δk_{g1} [kN/m]	0	483	0.000	0
δk_{g2} [kN/m]	0	483	0.359	0
δk_{g3} [kN/m]	0	483	0.000	0
δk_{g4} [kN/m]	0	483	135.837	148.5
δk_{g5} [kN/m]	0	483	52.568	49.5

6.4. Results and discussion

The physical implementation of the modifications causes some approximations of the theoretical solution computed, in order to conform to the actual availability of masses and springs. The values applied are listed in the fifth column of Table 6.3. In particular, the stiffness modifications have been realized

by adding the integer number of standard steel cantilever beams which allows the closest approximation of the theoretical stiffness modification. No investigation of the best integer approximation of the continuous solution has been performed, since it is beyond the scope of this experimental validation. The nominal stiffness of each spring is 49.5 kN/m.

The same procedure and equipment described in Section 6.1 have been adopted for the identification of the modified system eigenstructure. The five modes are listed in Table 6.4, where the two desired modes are also rewritten in brackets in order to improve the readability. The shapes of the third and fourth modes, i.e. the assigned ones, are also shown in dashed line in Figure 6.4 and in Figure 6.5. They match almost perfectly the desired ones (plotted in continuous bold line in the same Figure 6.4 and Figure 6.5), as also shown from the eigenstructure comparison in the last two rows of Table 6.4. Only a small difference in the natural frequency of the first desired mode can be noticed, as a consequence of the applied modification approximations with respect to the theoretical ones.

As a final piece of experimental evidence, the absolute values of the modified system measured frequency responses $\mathbf{H}^{m}_{i,5}(j\omega)$ (i=1,…,5) are shown in solid lines in Figure 6.5, where they are compared with those of the original system (dotted lines). The vertical solid lines highlight the two frequencies of the assigned modes of the modified system.

Table 6.4: Modified mode shapes and eigenstructure comparison

Modified system mode number, i	1	2	**3**	**4**	5
f_i [Hz]	21.96	29.89	**39.67** (39.00)	**54.98** (55.00)	74.15
$u_i(1)$	0.674	1.000	**1.000** (1.000)	**-0.003** (0.000)	-0.001
$u_i(2)$	1.000	0.705	**-0.498** (-0.550)	**0.014** (0.010)	0.003
$u_i(3)$	0.894	-0.900	**0.130** (0.200)	**-0.089** (-0.100)	-0.039
$u_i(4)$	0.205	-0.274	**0.026** (0.000)	**0.793** (0.800)	0.670
$u_i(5)$	0.074	-0.123	**0.118** (0.050)	**1.000** (1.000)	-1.000
Desired mode number, h			**1**	**2**	
$\|f_h-f_i\|$ [Hz]	-	-	**0.67**	**0.02**	-
$\cos(u_i,u_h)$	-	-	**0.9954**	**1.000**	-

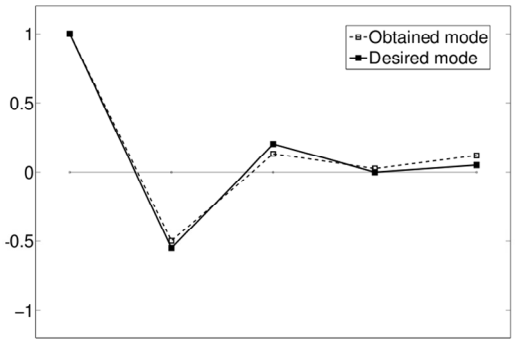

Figure 6.4: Lower frequency mode shapes

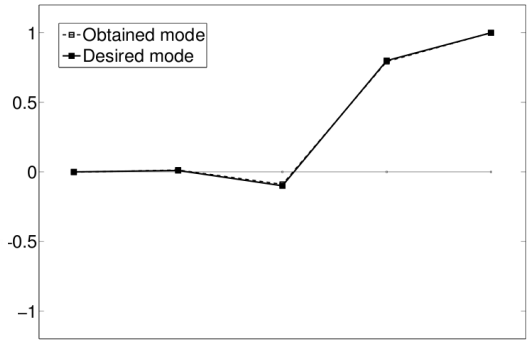

Figure 6.5: Higher frequency mode shapes

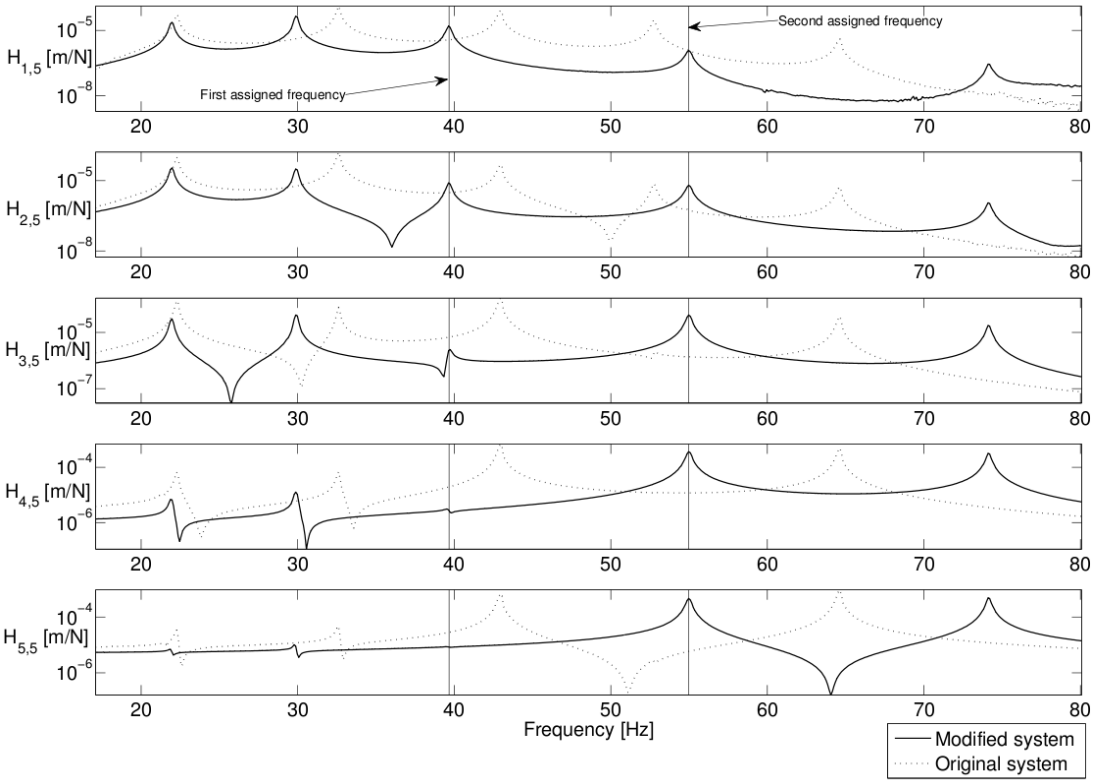

Figure 6.6: System FRFs and assigned natural frequencies

Chapter 7. Experimental validation of the method allowing for discrete modifications

In this chapter the experimental validation of the method proposed in the fourth section of Chapter 1 is carried out with reference to the same laboratory test-rig described in Chapter 6. A description of the experimental set up is firstly given in the first section. Then, the application of the method is described in the second section, where the rules adopted for the branching and bounding phases are given and the results of the method application on the system model are described. Finally, in third section, the effects of the calculated modifications on the experimental set up are described: the measurement chain is illustrated and a comparison between the desired and the obtained eigenstructure is proposed.

7.1. Experimental set up

The set up shown in Figure 7.1 has been adopted for the experimental validation of the method proposed in the third section of Chapter 1. It consists of five masses, each one connected to the very rigid test bench by a couple of steel cantilever straight beam springs that provide only bending stiffness. Four additional curved beam springs connect each mass with the contiguous ones. All the beam springs are 50 mm wide. All the other relevant dimensions are shown in the schematic drawing in Figure 7.2, and are nominally equal for all the beams having the same shape.

The modular structure of the test rig allows easy set up extension or reduction, by adding or removing mass-spring subsytems. Each subsystem has been designed in such a way that the lumped masses remain always parallel to the

ground during the motion. In fact, the portal frame structure of each subsystem makes the masses move without rotating. Furthermore, the high radius of the curved beam springs allows large amplitude oscillations of the masses without significantly altering the curved beam radius and, hence, the curved beam stiffnesses and linear behavior. All the beams can be modeled as massless lumped springs, since each beam mass and damping are negligible. In addition, the hypothesis of small displacements allows adopting linear spring models. Therefore, the set up is very well represented by the undamped 5-dof lumped element system sketched in Figure 7.3.

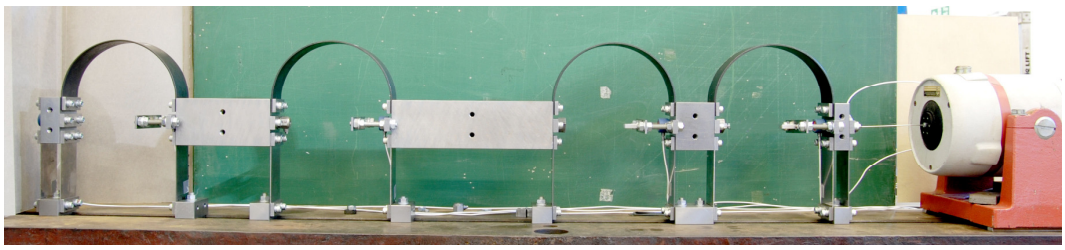

Figure 7.1: Experimental set up

The original system parameters are listed in Table 7.1, where the same stiffness value k_g has been assumed for all the ground springs k_{gi}, i = 1..5. The eigenstructure of the original system has been computed on the basis of the system nominal model, and is shown in Table 7.2.

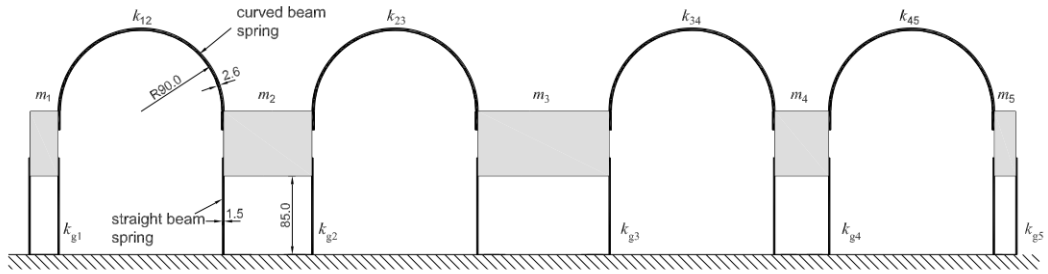

Figure 7.2: Set up significant dimensions [mm]

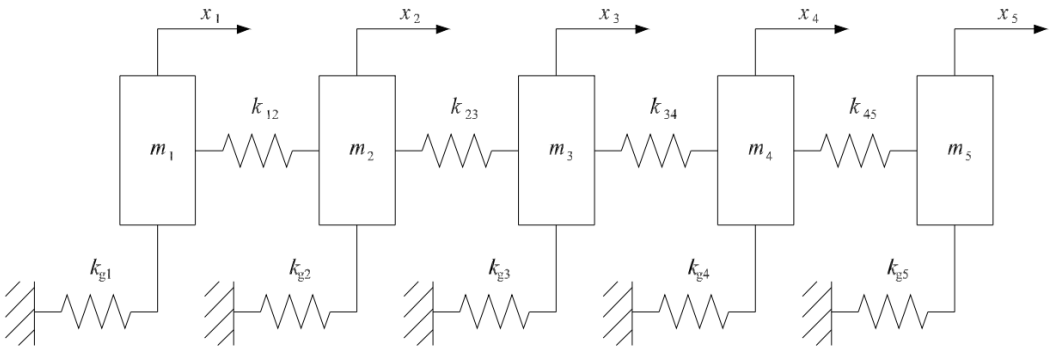

Figure 7.3: Lumped parameter model of the set up

Table 7.1: Original system parameters

	Applied modifications
m_1 [kg]	1.727
m_2 [kg]	5.123
m_3 [kg]	8.214
m_4 [kg]	2.609
m_5 [kg]	1.339
k_g [kN/m]	94.26
k_{12} [kN/m]	75.14
k_{23} [kN/m]	67.74
k_{34} [kN/m]	75.47
k_{45} [kN/m]	83.40

Table 7.2: Original system eigenstructure

Mode number, i	1	2	3	4	5
f_i [Hz]	21.87	32.13	42.48	52.44	64.36
$u_i(1)$	0.111	0.269	0.048	-0.702	0.002
$u_i(2)$	0.201	0.354	0.030	0.169	-0.003
$u_i(3)$	0.294	-0.150	-0.109	-0.018	0.024
$u_i(4)$	0.141	-0.125	0.474	0.006	-0.351
$u_i(5)$	0.077	-0.085	0.480	0.014	0.709

7.2. Application of the method and simulated tests

7.2.1 Definition of the B&B rules

As it has been pointed out in the fourth section of Chapter 1, the rule adopted for the selection of branching variables may have a meaningful effect on the overall computational efficiency of a branch and bound algorithm. In this work, three different variable selection strategies have been selected and tested:

1. Most Fractional Integer Variable. This strategy suggests selecting as the branching variable the farthest from the respectively nearest integer value. This heuristic strategy is aimed at attaining the largest degradation of the objective function when the branching is performed, in order to fathom a high number of nodes at an early stage.
2. Lowest-Index-First. The branching variable is the one with the lower index among those which have not an integer value. The variable are usually indexed coherently with the problem definition.
3. Highest-Index-First. Contrary to the previous approach, the branching variable is the one with the higher index among those not displaying an integer value.

As far as the selection of the branching nodes is concerned, the strategy adopted suggests selecting the node with the lowest bound on the objective function. The chief advantage of this approach is that, for a given problem, any branching operation performed under this strategy must also be performed under any other strategy [LI 2006].

Other heuristic techniques have been proposed in literature for reducing the number of problems to be solved by adopting the so-called pseudo costs,

which are estimations of the importance of the integer variables and of the local behaviour of the function to be minimised [LI 2006].

In each bounding phase, finally, the lower bound on the optimum of the discrete function has been set equal to the optimum of the continuous relaxation of the respective problem. Since no analytical solution exists for such a continuous relaxation (the non linear constrained problem), at each node the NLP subproblems have been solved numerically by applying the reflective Newton methods discussed in [COLEMANN 1990] and in [COLEMANN 1996]. Such a technique is suitable for large scale problems and ensures quadratic convergence to the unique solution.

The Branch and Bound algorithm has been implemented using Matlab on a PC running Microsoft Windows XP Professional. The PC has 2 GB RAM and a 2 GHz Intel Centrino Processor.

7.2.2 Lumped parameter modification

The purpose of the modification is to assign the eigenstructure listed in Table 7.3 ($\omega_h = 2\pi f_h$). Such an eigenstructure is considerably different from that of the original system both in terms of frequencies and mode shapes. In this eigenstructure assignment problem, all the lumped masses and grounded springs are modifiable. The discretisation values have been set equal to 0.18 kg and 47.13 kN/m respectively for the mass and the stiffness modifications. Such chosen values allow conforming the discretisation adopted in the method to the parameters of the mass modules and springs actually available.

As far as the parameters of the modification problem are concerned, they have been chosen so as to mathematically express both the equal levels of concern about the single eigenpair assignment (which leads to the selection of $\alpha_h, h = 1,2$) and the preferred structural modification strategy (which leads to the selection of $\mathbf{\Omega}_\mathbf{x}$). In detail, it has been set $\alpha_1 = \alpha_2 = 1$, and the regularisation operator has been chosen to equally weigh the relative parameter modifications with respect to the respective discretisation step. Specifically it has been set $\mathbf{\Omega}_\mathbf{x} = diag(\mathbf{w} / \|\mathbf{w}\|_2)$, where $\mathbf{w} = \{1,1,1,1,1,1,1,1,1,1\}$. The regularisation parameter selected through the L-curve of the unbounded problem is equal to 0.1.

Table 7.3: Desired eigenstructure

Mode number, *h*	1	2
f_h [Hz]	50.00	60.00
$u_h(1)$	-0.55	0.0025
$u_h(2)$	0.2	-0.005
$u_h(3)$	-0.03	0.03
$u_h(4)$	0.015	-0.375
$u_h(5)$	0.025	0.525

Finally, the values in the second and the third columns of Table 7.4 define the lower ($\mathbf{x}_{\min}$) and upper ($\mathbf{x}_{\max}$) bounds of the solution vector **x**.

The application of the proposed approach leads to the solution listed in the fifth column of Table 7.4, which is referred to as optimal discrete. It is noteworthy that the optimal discrete modifications cannot be obtained by simply rounding the optimal continuous solution (listed in the fourth column of Table 7.4) to the nearest integer.

Table 7.4: Discrete modification bounds and values

χ	Lower bound	Upper bound	Optimal continuous	Optimal discrete
z_{m1}	0	6	6	4
z_{m2}	0	6	0.613	0
z_{m3}	0	6	5.455	5
z_{m4}	0	6	0.200	4
z_{m5}	0	6	6	2
z_{kg1}	0	3	1.663	1
z_{kg2}	0	3	1.294	1
z_{kg3}	0	3	3.000	3
z_{kg4}	0	3	0	2
z_{kg5}	0	3	2.206	0

The eigenstructure of the systems obtained by applying the modifications in Table 7.4 are collected in Table 7.5.

A set of indexes is useful to understand the performances of the modifications proposed:

- the difference between the desired and the attained natural frequency of each assigned mode, shown in the second last row of Table 7.5.
- the cosine between the desired eigenvector and the attained one of each assigned mode, shown in the forth last row of Table 7.5, and the respective angle, shown in the third last row of Table 7.5.
- the value of the function to be minimised $f(\chi)$, shown in the last row of Table 7.5.

It is apparent that the proposed method provides a discrete solution whose effectiveness is comparable with that of the continuous solution. In fact the value of function f at the discrete optimum, though higher than at the continuous optimum, is much lower than the original system one. As a consequence, both the frequency mismatches and the cosines are only slightly better for the system

modified according to optimal continuous solution which, however, is impossible to put into operation with the adopted parameter discretisation.

Table 7.5: Simulated systems: Modified mode shapes and eigenstructure comparison

	Original		*Optimal continuous*		*Optimal discrete*	
	4^{th} *Mode*	5^{th} *Mode*	4^{th} *Mode*	5^{th} *Mode*	4^{th} *Mode*	5^{th} *Mode*
x_1	-0.7016	0.0019	-0.5326	0.0025	0.5690	0.0034
x_2	0.1691	-0.0029	0.1931	-0.0050	-0.1978	-0.0057
x_3	-0.0181	0.02416	-0.0267	0.0302	0.0258	0.0332
x_4	0.0055	-0.3513	0.0125	-0.3665	-0.0023	-0.3921
x_5	0.0144	0.7089	0.0230	0.5127	-0.0239	0.5302
f [Hz]	52.44	64.36	49.99	60.00	50.23	59.74
cosine	0.9929	0.9870	0.9999	0.9999	0.9996	0.9998
angle [°]	6.79	9.22	0.33	0.09	1.56	0.97
Δf [Hz]	2.44	4.36	0.00	0.00	0.23	0.26
$f(\chi)$	2.4*e9*		5.36*e6*		33.6*e6*	

As far as the computational effort is concerned, it is clear from the number of investigated discrete solutions, listed in the second column of Table 7.6, that the Branch and Bound technique allows effectively computing the optimal solution. In fact, with reference to the total solution enumeration, the Branch and Bound partial enumeration leads to the optimal solution with a much lower number of investigated solutions. Also, as could be expected, the rule adopted in the selection of the branching variable plays an important role: in this case, branching the variable with the highest fractional part reduces the number of investigated solutions by more than half.

Table 7.6: Computational efficiency comparison

Scheme adopted	*Number of investigated discrete solutions*
Total enumeration	17210368
BB Lowest Index First	621
BB Highest Index First	393
BB Most Fractional Integer Variable	263

7.3. Experimental validation

The physical implementation of the discrete modifications is intrinsically straightforward, since no approximation of the theoretical solution computed is required in order to conform to the actual availability of masses and springs.

The eigenstructure of the modified system has been experimentally identified. The measured data have been produced by exciting the system with an electro-dynamic shaker connected to the mass m_5 through a stinger (see Figure 7.1). The shaker employed is a LDS V406, driven by a LDS PA100E power amplifier capable of delivering power up to 147 W to the shaker. The excitation force has been measured by a load cell (PCB 208A02) placed between the mass m_5 and the stinger. Each mass has been instrumented with a Kistler 8636C50 piezoelectric accelerometer. All the measurements have been recorded through a LMS SCADAS III signal acquisition front-end connected to a PC. The LMS software Test.Lab has been adopted to generate the shaker excitation signal, and to identify the eigenstructure by applying the least squares method in [PEETERS 2004]. The system has been forced with a random excitation over the frequency range 0-100 Hz, which is the frequency interval of interest for the proposed modification task.

The five modes are listed in Table 7.7, where the two desired modes are also rewritten in brackets in order to improve the readability. The shapes of the fourth and fifth modes, i.e. the assigned ones, are also shown in solid line in Figure 7.4 and in Figure 7.5. They match almost perfectly the desired ones (plotted in dashed line in the same Figure 7.4 and Figure 7.5), as shown also in the eigenstructure comparison in the last two rows of Table 7.7. Only a small

difference in the natural frequency of the first desired mode can be noticed, as a consequence of the unavoidable model approximations.

As a final piece of experimental evidence, the absolute values of the modified system measured frequency responses $\mathbf{H}^{m}_{i,5}(j\omega)$ (i=1,…,5) are shown in solid lines in Figure 7.5, where they are compared with those of the original system (dotted lines). The vertical solid lines highlight the two frequencies of the assigned modes of the modified system.

Table 7.7: Experimental set up: Modified mode shapes and eigenstructure comparison

Modified system mode number, i	1	2	3	**4**	**5**
f_i [Hz]	28.90	36.19	43.60	**50.43** (50.00)	**60.45** (60.00)
$u_i(1)$	0.520	0.849	0.121	**1.000** (1.000)	**0.008** (0.005)
$u_i(2)$	0.950	1.000	0.058	**-0.361** (-0.364)	**-0.013** (-0.010)
$u_i(3)$	1.000	-0.577	-0.191	**0.055** (0.055)	**0.067** (0.057)
$u_i(4)$	0.397	-0.436	0.642	**-0.012** (0.027)	**-0.740** (-0.714)
$u_i(5)$	0.247	-0.378	1.000	**-0.019** (0.046)	**1.000** (1.000)
Desired mode number, h				**1**	**2**
$\lvert f_h - f_i \rvert$ [Hz]	-	-	-	**0.43**	**0.45**
$\cos(u_i, u_h)$	-	-	-	**0.9996**	**0.9998**

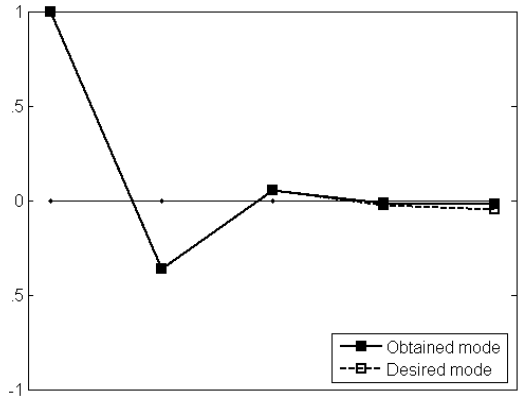

Figure 7.4: Lower frequency mode shapes

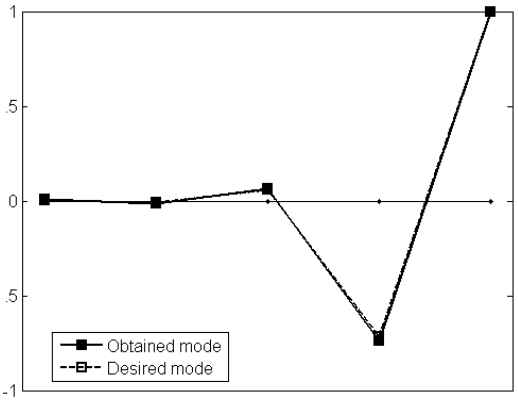

Figure 7.5: Higher frequency mode shapes

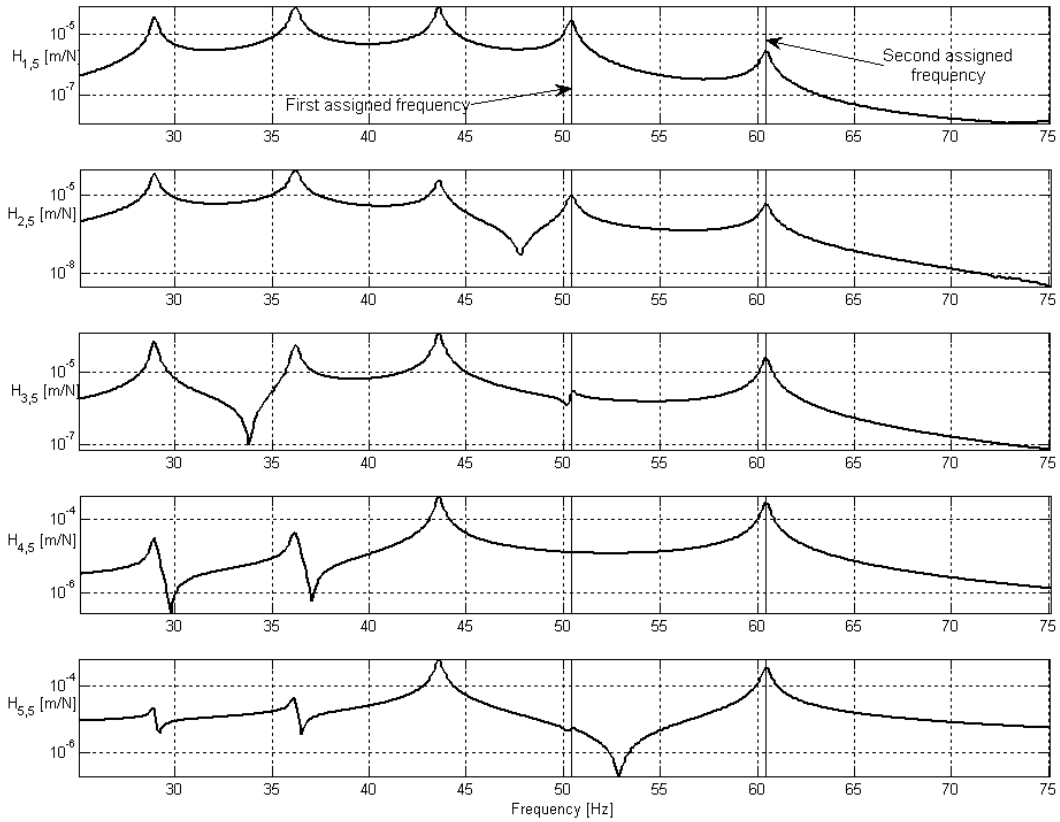

Figure 7.6: System FRFs and assigned natural frequencies

Conclusions

In this Thesis the research on structural modification approaches to modal design optimisation is presented. State-of-the-art methods in the field of inverse structural modification allow computing effective structural modifications. However, they lack flexibility both in the formulation and in the solution of the problems and solutions are not ensured to be feasible. Original formulations based on convex constrained optimisation are proposed and validated for the optimal inverse structural modification of multi-body vibrating systems. The approaches developed aim to compute the optimal inertial and stiffness parameter modifications for attaining a desired eigenstructure. Such approaches are particularly suitable when a small number of mode shapes at specific natural frequencies need to be imposed in the system dynamics. The modification parameters include those affecting both the inertial and the elastic properties of the system and do not need to impose diagonal or tridiagonal matrices.

A strength of the proposed approaches is that they allow finding an optimal solution for any number of dofs and of design parameters. Therefore, such approaches are suitable for the optimisation of high order systems. The adopted formulations allow including constraints on both the single design parameters and on linear combinations of such parameters.

Additionally, the introduction of a regularisation term penalizing large modifications, ensures obtaining physically and technically feasible solutions and therefore enlarges the practical applications where it can be successfully employed. Through the suggested regularisation it is also possible to translate differing levels of concern about the modifications to be adopted (e.g. to penalize

the modifications of some parameters), and hence to bias the solution towards preferable modifications

In this Thesis, three different approaches are presented for calculating realizable mass and stiffness modifications of undamped systems. These approaches differ for the system model employed and for the mathematical frame of solution. In particular, the first approach is based on the spatial model and employs the system mass and stiffness matrices, while the second relies on the sole system frequency responses. Such approaches consist in formulating continuous optimisation problems. On the contrary, in the third approach the modification problem has been cast as a mixed-integer non-linear optimisation problem, in order to reflect discretisation constraints on modification parameters. The aforementioned convexity of the problem ensures computing global optima with all the approaches provided.

The theory developed has been applied to test cases involving lumped-parameter systems and distributed parameter systems. Comparative evaluations have been carried out with reference to state-of-the-art methods. Not only do the results achieved prove the effectiveness of the methods but they also highlight their computational efficiency. Given the good results in the numerical simulations, experimental activity has been carried out in order to validate the approaches on real structures

Experimental evidence for the effectiveness of the proposed approaches have also been provided. The approach employing the system spatial model has been used to design a vibrating device of industrial relevance on the basis of the desired dynamic behavior expressed by means of a vibration mode. Also, an

eigenstructure assignment on a laboratory set up has been considered for the approach based on the sole FRF data. Furthermore, the same laboratory set up has been used to validate the approach allowing for discrete modification. The experimental results are very satisfactory, in the sense that the modifications are easily computed and the desired eigenstructure is achieved.

List of publications

The major outcomes of this research may be found in the following references:

1. Richiedei D., Trevisani A., Zanardo G., "Inverse eigenvalue problem for optimal structural modification of multibody systems under single harmonic excitation", *Proceedings of the ECCOMAS Thematic Conference on Multibody Dynamics*, 2009 Warzawa (Poland).
2. Caracciolo R., Richiedei D., Trevisani A., Zanardo G., "Structural modification of vibrating systems: an approach based on a constrained inverse eigenvalue problem", *Proceedings of the AIMETA Conference*, 2009 Ancona (Italy).
3. Caracciolo R., Ouyang H., Richiedei D., Trevisani A., Zanardo G., "Eigenstructure Optimization of Undamped Vibrating Systems: a Constrained Mixed-Integer Programming Approach", *ECCOMAS Thematic Conference on Multibody Dynamics,* 2011, Brussels (Belgium) (submitted for possible publication).
4. Richiedei D., Trevisani A., Zanardo G., "A Constrained Convex Approach to Modal Design Optimization of Vibrating Systems" (submitted to the *ASME Journal of Mechanical Design* in July 2010 for possible publication).
5. Ouyang H., Richiedei D., Trevisani A., Zanardo G. "Eigenstructure Assignment In Undamped Vibrating Systems: A Convex-Constrained Modification Method Based On Receptances" (submitted to *Mechanical Systems and Signal Processing* in November 2010 for possible publication).

References

[AHMADIAN 1998] H. Ahmadian, J. E. Mottershead, M. I. Friswell, "Regularisation methods for finite element model updating," *Mechanical Systems and Signal Processing*, 12 (1), 47-64 (1998).

[BALDWIN 1985] J.F. Baldwin, S.G. Hutton, "Natural modes of modified structures," *AIAA Journal*, 23, 1737–1743 (1985).

[BOYD 2004] S. Boyd, L. Vandenberghe, *Convex Optimization*, Cambridge University Press, 2004.

[BRAUN 2001] S.G. Braun, Y.M. Ram, "Modal modification of vibrating systems: some problems and their solutions," *Mechanical Systems and Signal Processing*, 15, 101-119 (2001).

[BUCHER 1993] I. Bucher, S. Braun, "The structural modification inverse problem: an exact solution," *Mechanical Systems and Signal Processing*, 7, 217-238 (1993).

[BUCHER 1997] I. Bucher, S. Braun, "Left eigenvectors: extraction from measurements and physical interpretation," *ASME Journal of Applied Mechanics*, 64, 97-104 (1997).

[CALVETTI 2004] D. Calvetti, L. Reichel, A. Shuibi, "L-curve and curvature bounds for Tikhonov regularization," *Numerical Algorithms*, 35, 301-314 (2004).

[CALVETTI 2005] D. Calvetti, L. Reichel, "Tikhonov regularization with a solution constraint," *SIAM Journal of Scientific Computing*, 26, 224-239 (2005).

[CHOI 2007] H. G. Choi, A. N. Thite, D. J. Thompson, "Comparison of methods for parameter selection in Tikhonov regularization with application to inverse force determination," *Journal of Sound and Vibration*, 304, 894-917 (2007).

[COLEMANN 1990] T. Colemann, L. F. Hulbert, "A globally and superlinearly convergent algorithm for convex quadratic programs with simple bounds," *Computer Science Technical Reports Cornell University*, (1990).

http://techreports.library.cornell.edu:8081/Dienst/UI/1.0/Display/cul.cs/TR90-1092

[COLEMANN 1996] T. Colemann, Y. Li, "A Reflective Newton Method for minimizing a quadratic function subject to bounds on some of the variables," *SIAM Journal on Optimization*, 6:4, 1040-1058 (1996).

[DEMEULENAERE 2006] B. Demeulenaere, E. Aertbelien, M. Verschuure, J. Swevers, and J. De Schutter, "Ultimate Limits for Counterweight Balancing of Crank-Rocker Four-Bar Linkages," *ASME Journal of Mechanical Design*, 128, 1272–1284 (2006).

[EWINS 1994] D.J. Ewins, *Modal testing: theory and practice*, Research Studies Press LTD, Letchworth, Hertfordshire, England, 1984.

[FARAHANI 2004A] K. Farahani, H. Bahai, "An inverse strategy for relocation of eigenfrequencies in structural design. Part I: first order approximate solutions," *Journal of Sound and Vibration*, 274, 481-505 (2004).

[FARAHANI 2004B] K. Farahani, H. Bahai, "An inverse strategy for relocation of eigenfrequencies in structural design. Part II: second order approximate solutions," Journal of Sound and Vibration, 274, 507-528 (2004).

[GLADWELL 2004] G. M. L. Gladwell, *Inverse Problems in Vibration*. Kluwer Academic Publishers (2004).

[GOLUB] G. H. Golub, and C. F. Van Loan, *Matrix Computations*, Johns Hopkins University Press, Baltimore and London (1996).

[GRANT 2008] M. Grant, and S. Boyd, "Graph implementations for non smooth convex programs," *Recent Advances in Learning and Control (a tribute to M. Vidyasagar),* V. Blondel, S. Boyd, and H. Kimura, editors, 95-110, Lecture Notes in Control and Information Sciences, Springer. http://stanford.edu/~boyd/graph_dcp.html(2008)

[GRANT 2010] M. Grant, S. Boyd, CVX: Matlab software for disciplined convex programming, version 1.21. http://cvxr.com/cvx. (2010).

[GUPTA 1985] O. K. Gupta, A. Ravindran, "Branch and bound experiments in convex nonlinear integer programming," Management Science, 31, 1533-1546 (1985).

[HANSEN 2000] P.C. Hansen. "The L-curve and its use in the numerical treatment of inverse problems," *Computational Inverse Problems in Electrocardiology*, 4**,** Advances in Computational Bioengineering, 119–142 (2000).

[HANSEN 2002] P. C Hansen, "Deconvolution and regularization with toepliz matrices," *Numerical Algorithms*, 29, 323-378 (2002).

[HE 2001] J. He. Structural Modification. *Philosophical Transactions: Mathematical, Physical and Engineering Sciences*, 359 (1778), Experimental Modal Analysis, 187-204 (2001).

[HOLDER 2004] D. Holder, *EIT: Methods, History and Applications*. Taylor and Francis, (2004)

[KYPRIANOU 2004] A. Kyprianou, J. E. Mottershead, and H. Ouyang, "Assignment of natural frequencies by an added mass and one or more springs," *Mechanical Systems and Signal Processing*, 18, 263-289 (2004).

[KYPRIANOU 2005] A. Kyprianou, J.E. Mottershead, H. Ouyang, "Structural modification. Part 2: assignment of natural frequencies and antiresonances by an added beam," *Journal of Sound and Vibration,* 284, 267-281 (2005).

[LAND 1960] A. H. Land, A. G. Doig, "An automatic method of solving discrete programming problems," Econometrica, 28:497-520 (1960).

[LI 1999] T. Li, J. He, "Local structural modification using mass and stiffness changes," *Engineering Structures*, 21, 1028-1037 (1999).

[LI 2006] D. Li, X. Sun, *Nonlinear Integer Programming*, International Series in Operations Research & Management Science, 2006.

[LIANGSHENG 2003] W. Liangsheng, "Direct method of inverse eigenvalue problems for structure redesign," *ASME Journal of Mechanical Design*, 125, 845-847 (2003).

[MEIROVITCH 1980] L. Meirovitch, *Computational Methods in Structural Dynamics.*

[MOTTERSHEAD 1999] J. E. Mottershead, G. Lallement, "Vibration Nodes, and the Cancellation of Poles and Zeros by Unit-Rank Modifications to Structures", *Journal of Sound and Vibration*, 222, 833-851 (1999).

[MOTTERSHEAD 2000] J. E. Mottershead, T. Li, J. He, "Pole–zero cancellation in structures: repeated roots", Journal of Sound and Vibration, 231, 219-231, (2000).

[MOTTERSHEAD 2001] J. E. Mottershead, "Structural modification for the assignment of zeros using measured receptances," *ASME Journal of Applied Mechanics*, 68, 791-798 (2001).

[MOTTERSHEAD 2005] J. E. Mottershead, A. Kyprianou and H. Ouyang, "Structural modification. Part 1: rotational receptances," *Journal of Sound and Vibration*, 284, 249-265 (2005).

[MOTTERSHEAD 2006] J. E. Mottershead, Y. M. Ram. "Inverse eigenvalue problems in vibration absorption: Passive modification and active control," *Mechanical Systems and Signal Processing*, 20, 5–44 (2006).

[OUYANG 2009] H. Ouyang, "Prediction and assignment of latent roots of damped asymmetric systems by structural modifications," *Mechanical Systems and Signal Processing,* 23, 1920-1930 (2009).

[PARK 2000] Y. H. Park, and Y. Park, "Structural modification based on measured frequency response functions: an exact eigenproperties reallocation," *Journal of Sound and Vibration*, 237, 411-426 (2000).

[PEETERS 2004] B. Peeters, G. Lowet, H. V. der Auweraer, J. Leuridan, "A new procedure for modal parameter estimation," *Sound and Vibration,* 24-28 (2004).

[RAM 1991] Y. M. Ram, and S.G. Braun, "An inverse problem associated with modification of incomplete dynamic systems," *ASME Journal of Applied Mechanics*, 58, 233-237 (1991).

[RAM 1996] Y. M. Ram, S. Elhay. "The theory of a multi-degree-of-freedom dynamic absorber," *Journal of Sound and Vibration*. 195 (4), 607–615 (1996).

[RAM 2009] Y. M. Ram, "Optimal mass distribution in vibrating systems," *Mechanical Systems and Signal Processing*, 23, 2130-2140 (2009).

[RAYLEIGH 1945] J. W. S. Rayleigh, *Theory of Sound, 2nd edn*. New York, Dover, (1945).

[SIVAN 1996] D. D. Sivan, Y. M. Ram. "Mass and stiffness modifications to achieve desired natural frequencies", *Communications in numerical methods in engineering*, 12, 531-542 (1996).

[SIVAN 1997] D. D. Sivan, Y. M: Ram, "Optimal construction of a mass-spring system with prescribed modal and spectral data," *Journal of Sound and Vibration*, 201(3), 323-334 (1997).

[SIVAN 1999] D. D. SIVAN, Y. M. RAM, "Physical modifications to vibratory systems with assigned eigendata", *ASME Journal of Applied Mechanics,* 66, 427–432 (1999).

[VAN DEN BERG 2004] S. Van Den Berg, P. Mohanty, and D. J. Rixen, "Investigating the causes of non-uniform cookie flow in vibratory conveyors: part 1," *Experimental Techniques*, 28, 46-49 (2004).

[WANG 2004] D. Wang, J. S. Jiang, W. H. Zhang, "Optimization of support positions to maximize the fundamental frequency of structures," *International Journal For Numerical Methods In Engineering*, 61, 1584–1602 (2004).

[WANG 2006] D. Wang, M. I. Friswell, Y. Lei, "Maximizing the natural frequency of a beam with an intermediate elastic support," *Journal of Sound and Vibration*, 291, 1229–1238 (2006).